

# AdS/CFT and condensed matter

## Reviews:

[arXiv:0907.0008](https://arxiv.org/abs/0907.0008)

[arXiv:0901.4103](https://arxiv.org/abs/0901.4103)

[arXiv:0810.3005](https://arxiv.org/abs/0810.3005) (with Markus Mueller)

Talk online: [sachdev.physics.harvard.edu](http://sachdev.physics.harvard.edu)



Lars Fritz, Harvard  
Victor Galitski, Maryland  
Max Metlitski, Harvard  
Eun Gook Moon, Harvard  
Markus Mueller, Trieste  
Yang Qi, Harvard  
Joerg Schmalian, Iowa  
Cenke Xu, Harvard

Frederik Denef, Harvard  
Sean Hartnoll, Harvard  
Christopher Herzog, Princeton  
Pavel Kovtun, Victoria  
Dam Son, Washington



## Outline

# A. “Relativistic” field theories of quantum phase transitions

1. Coupled dimer antiferromagnets
2. Triangular lattice antiferromagnets
3. Graphene
4. AdS/CFT and quantum critical transport

## Outline

# B. Finite density quantum matter

## 1. Graphene

*Fermi surfaces and Fermi liquids*

## 2. Quantum phase transitions of Fermi liquids

*Pomeranchuk instability and spin density waves;  
Fermi surfaces and “non-Fermi liquids”*

## 3. AdS<sub>2</sub> theory

## 4. Cuprate superconductivity

# Outline

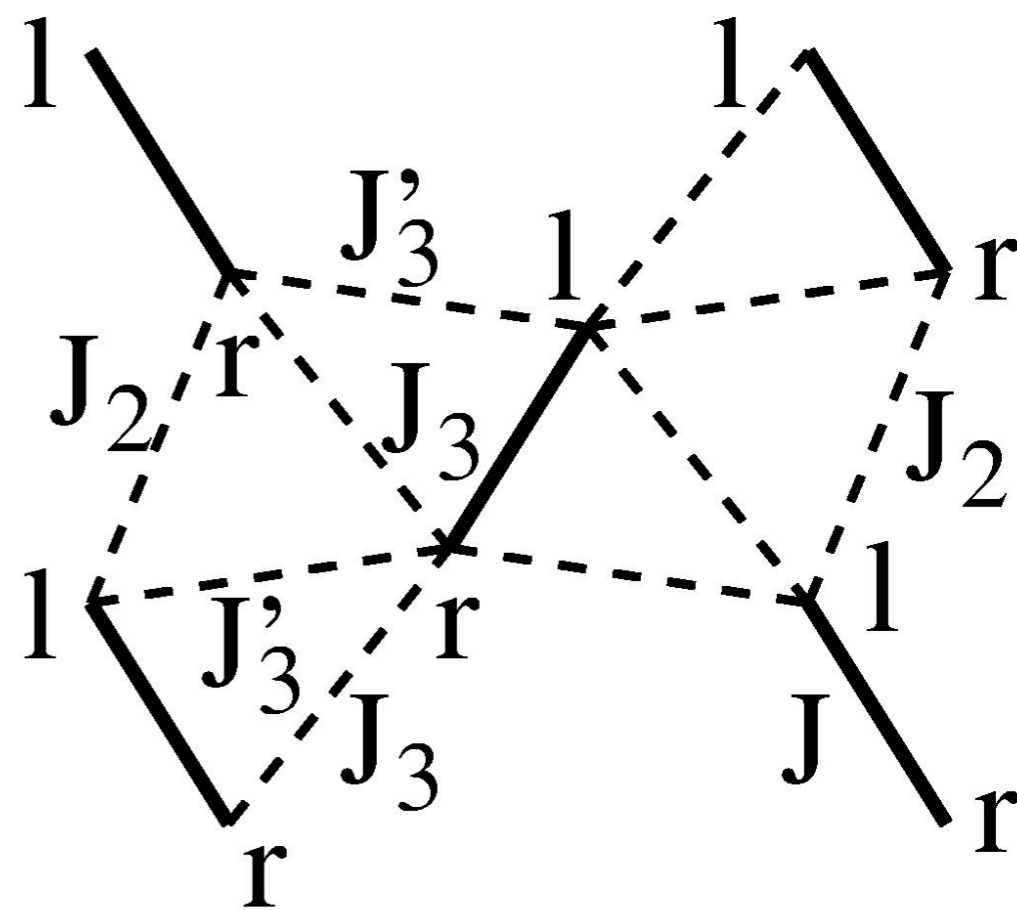
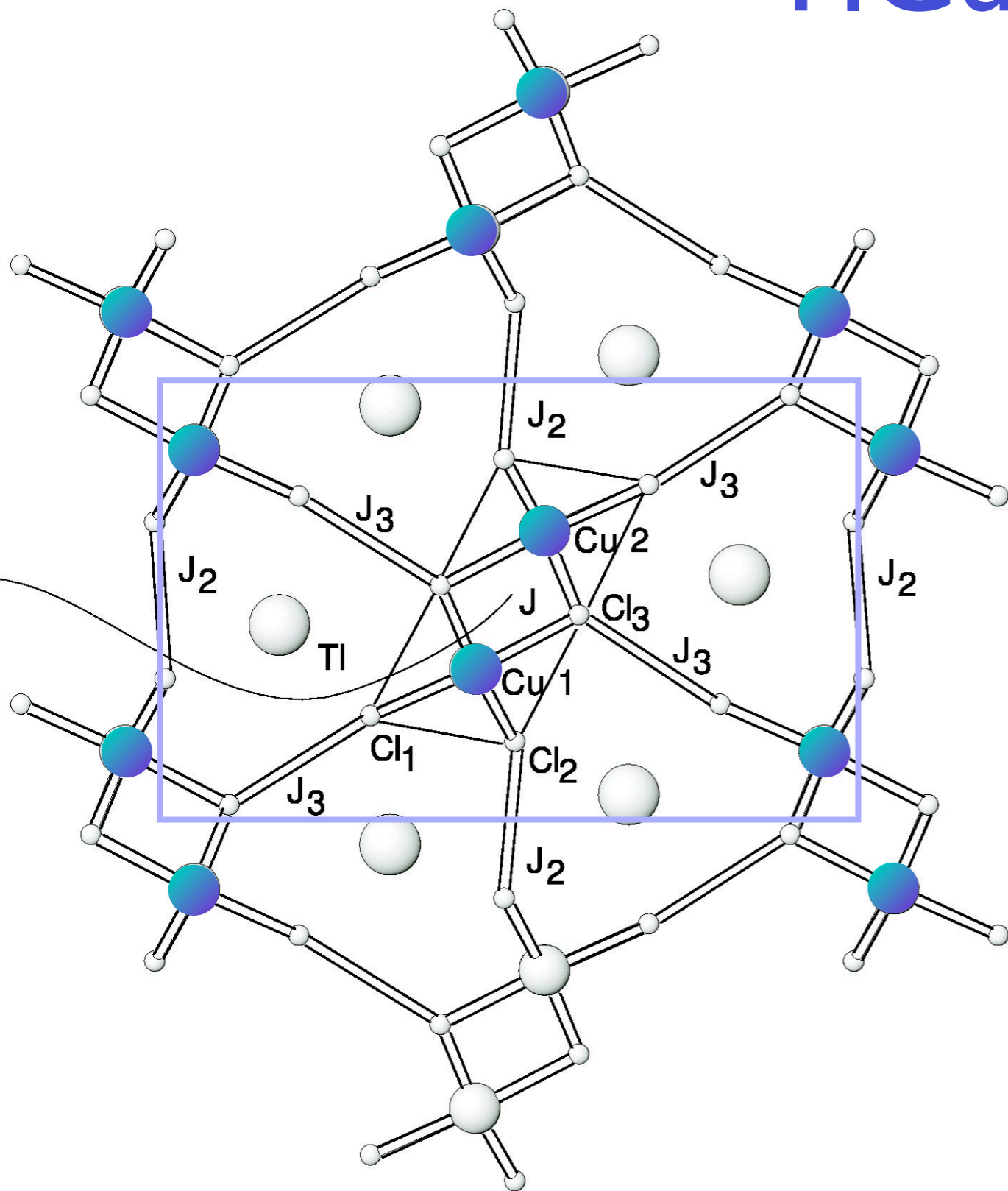
A. “Relativistic” field theories  
of quantum phase transitions

## Outline

# A. “Relativistic” field theories of quantum phase transitions

1. Coupled dimer antiferromagnets
2. Triangular lattice antiferromagnets
3. Graphene
4. AdS/CFT and quantum critical transport

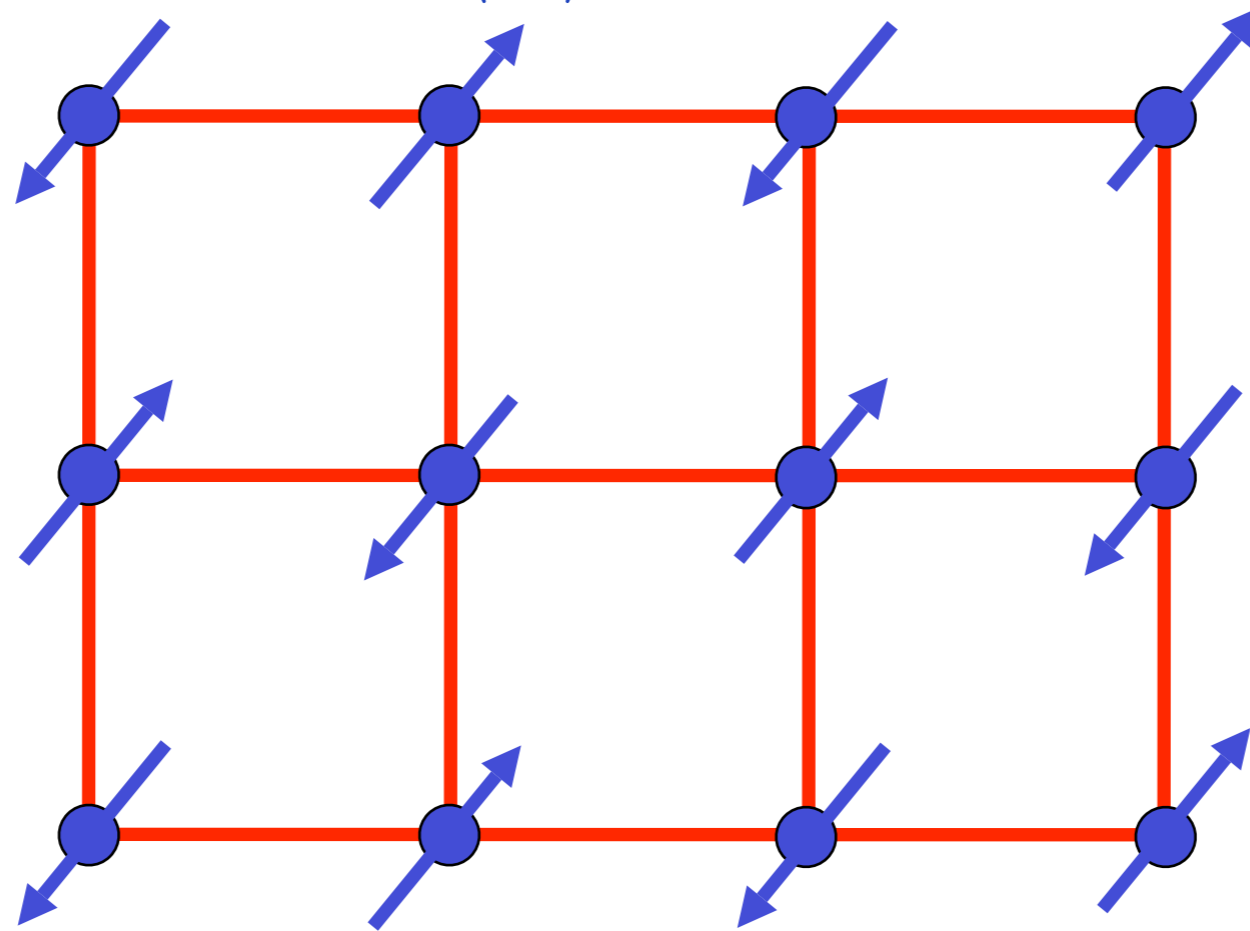
# TlCuCl<sub>3</sub>





# Square lattice antiferromagnet

$$H = \sum_{\langle ij \rangle} J_{ij} \vec{S}_i \cdot \vec{S}_j$$



Ground state has long-range Néel order

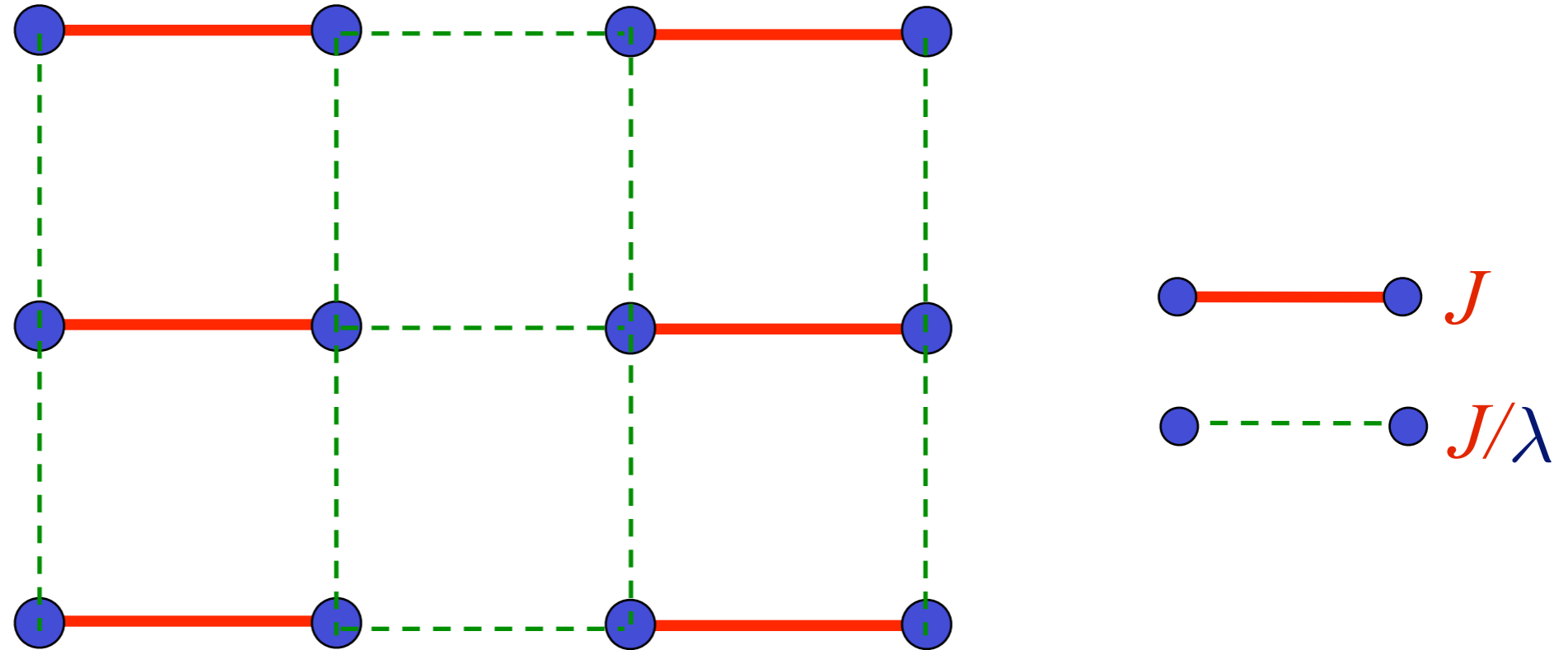
Order parameter is a single vector field  $\vec{\varphi} = \eta_i \vec{S}_i$

$\eta_i = \pm 1$  on two sublattices

$\langle \vec{\varphi} \rangle \neq 0$  in Néel state.

# Square lattice antiferromagnet

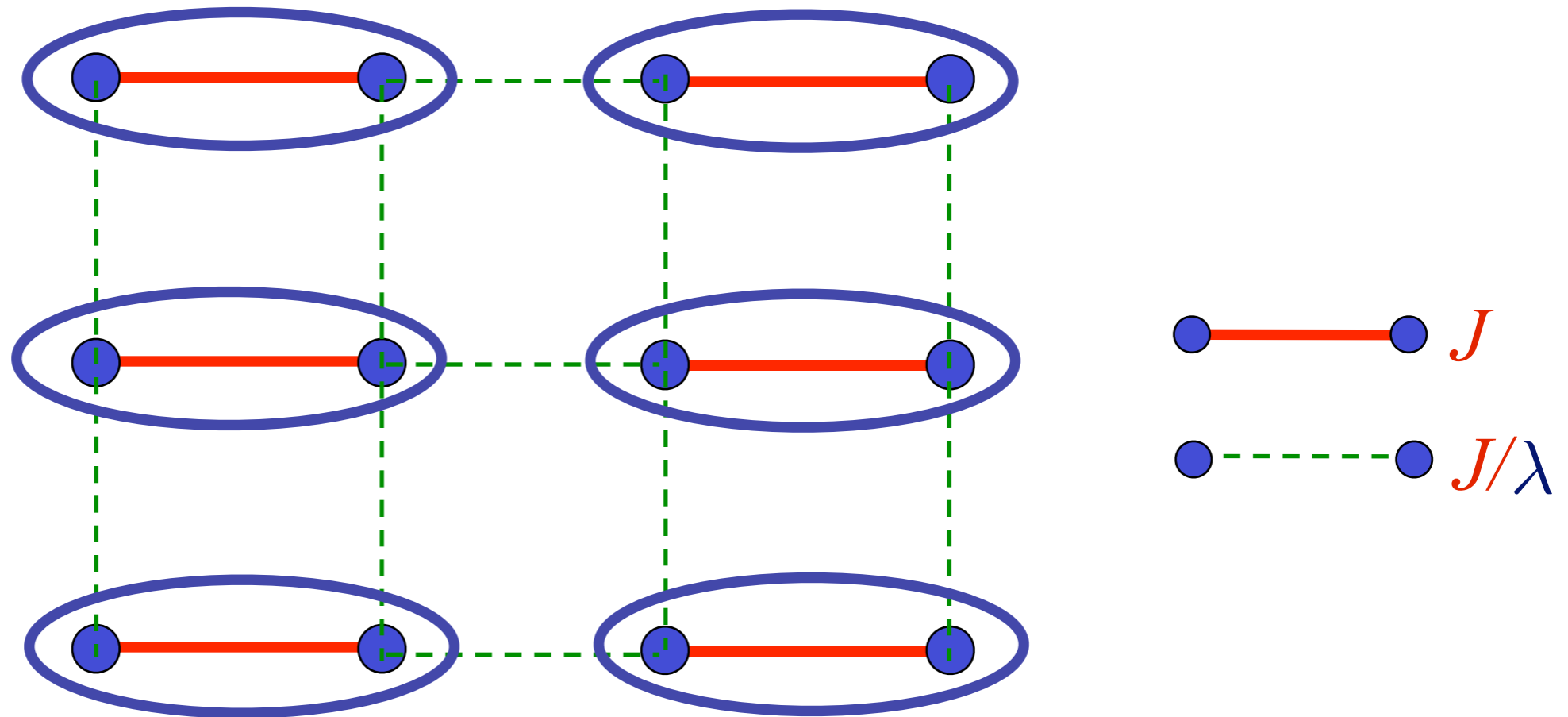
$$H = \sum_{\langle ij \rangle} J_{ij} \vec{S}_i \cdot \vec{S}_j$$



Weaken some bonds to induce spin entanglement in a new quantum phase

# Square lattice antiferromagnet

$$H = \sum_{\langle ij \rangle} J_{ij} \vec{S}_i \cdot \vec{S}_j$$

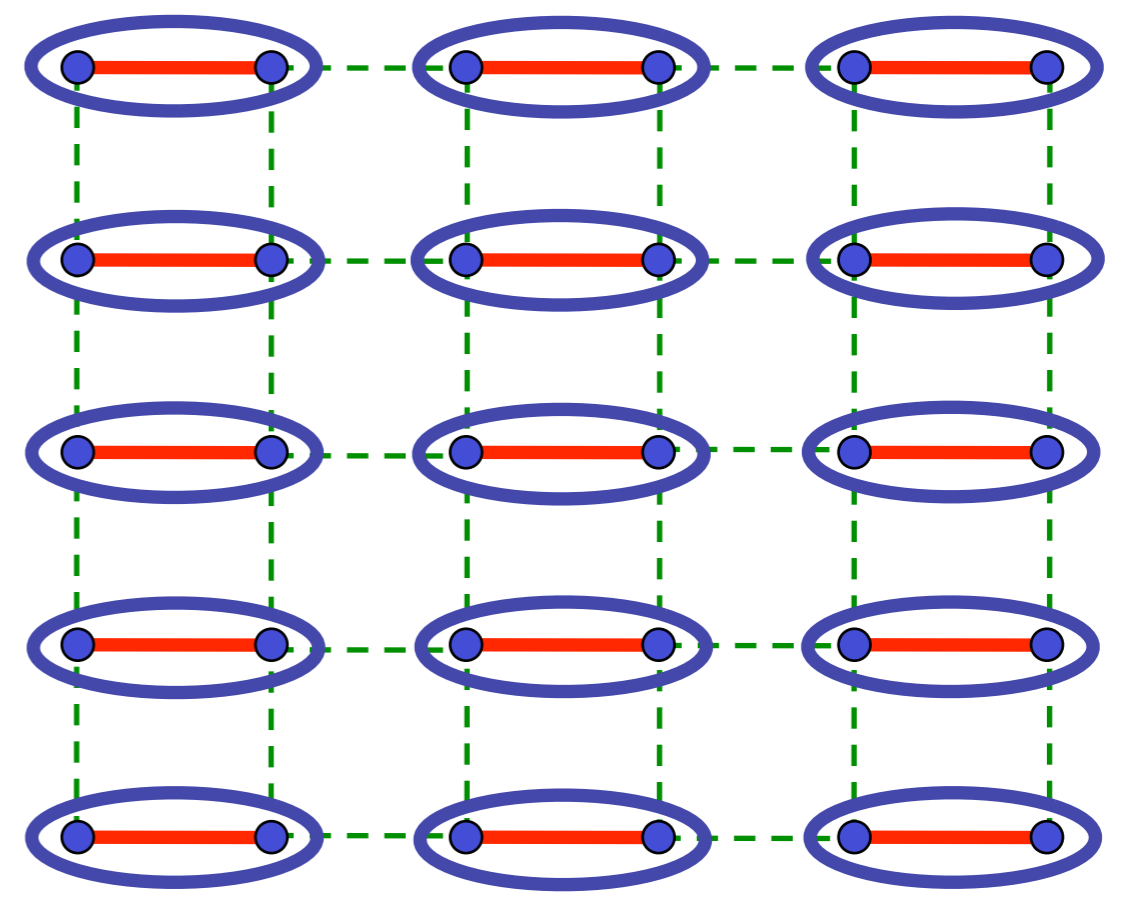
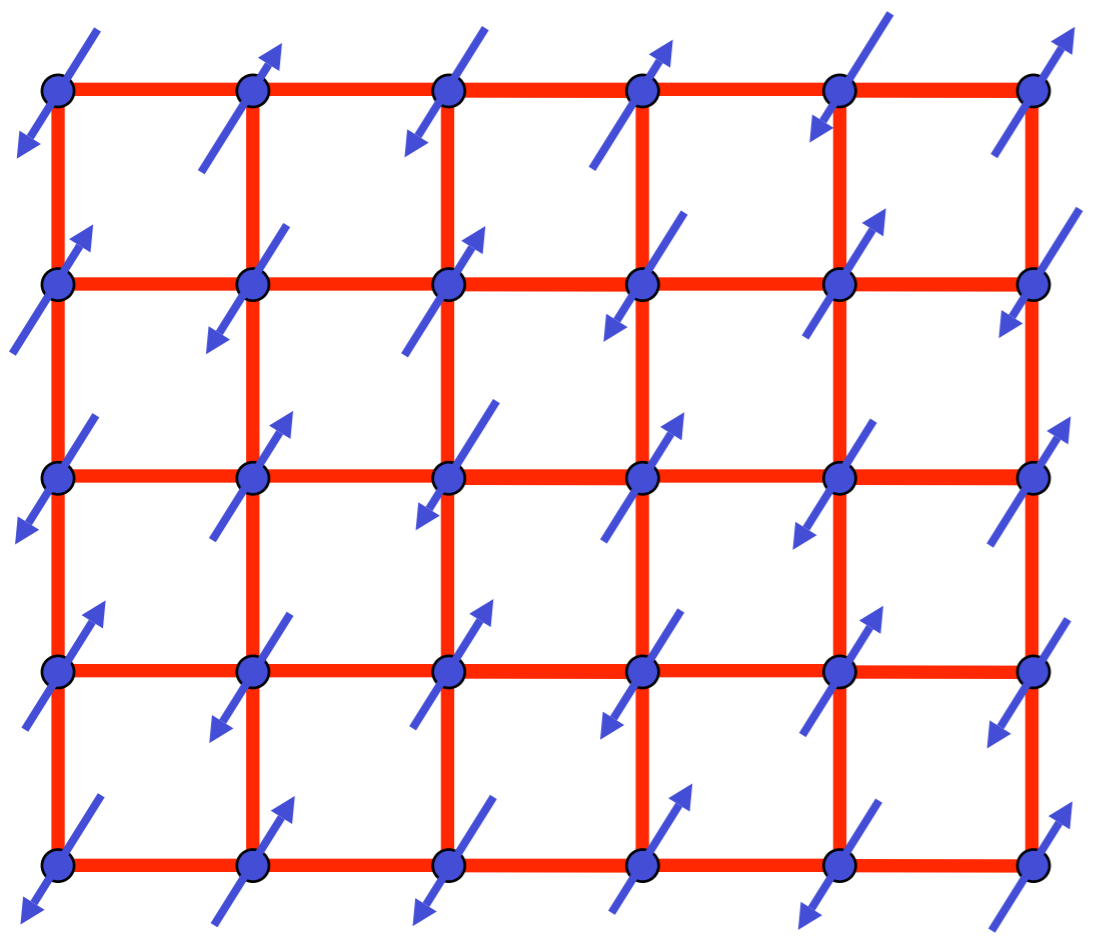


Ground state is a “quantum paramagnet”  
with spins locked in valence bond singlets

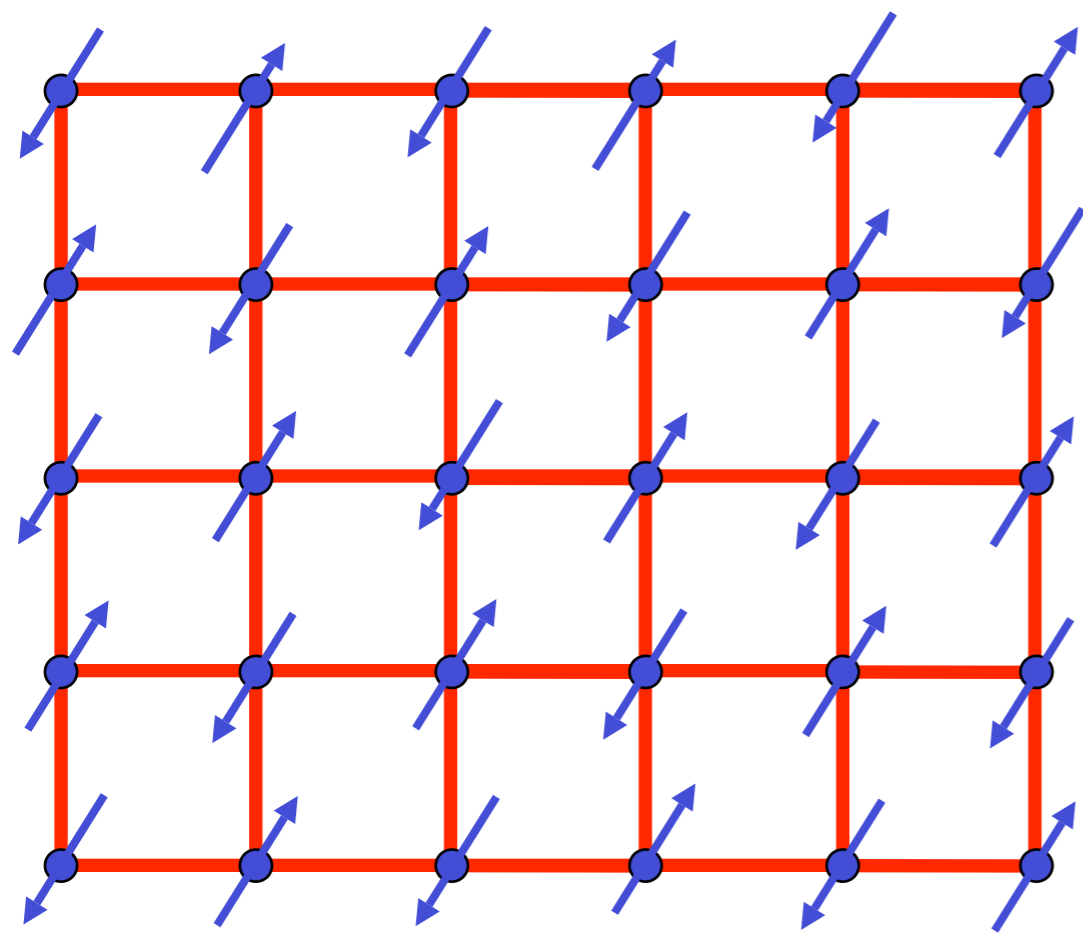
$$\text{[Diagram of a valence bond singlet]} = \frac{1}{\sqrt{2}} \left( |\uparrow\downarrow\rangle - |\downarrow\uparrow\rangle \right)$$



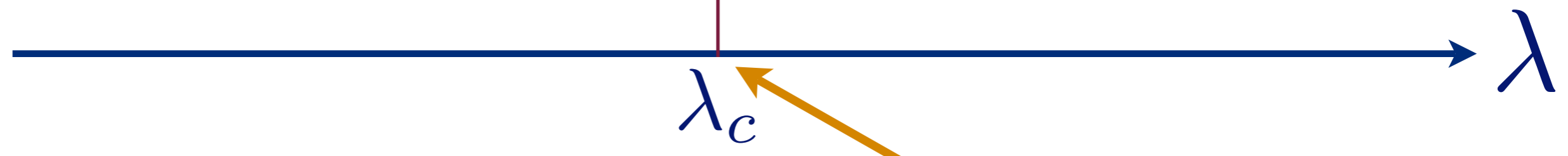
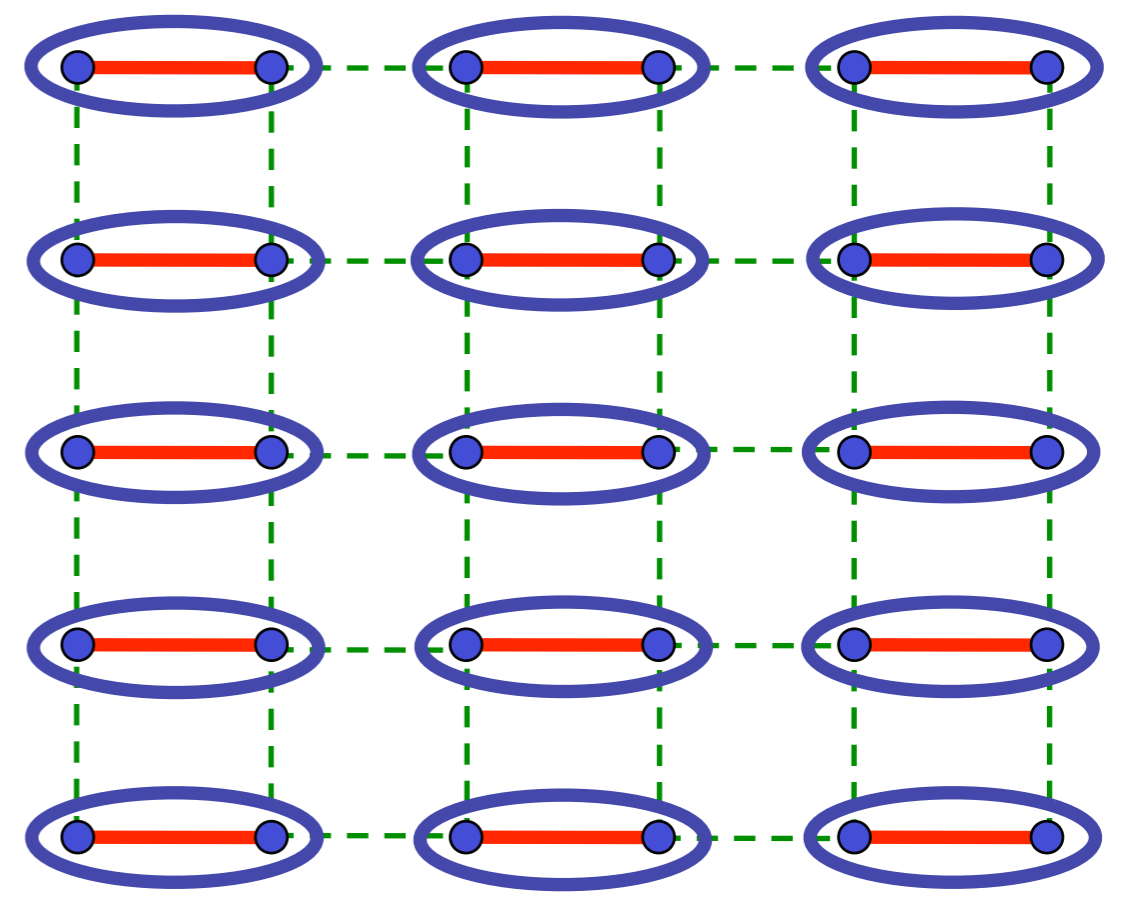
$$= \frac{1}{\sqrt{2}} (|\uparrow\downarrow\rangle - |\downarrow\uparrow\rangle)$$



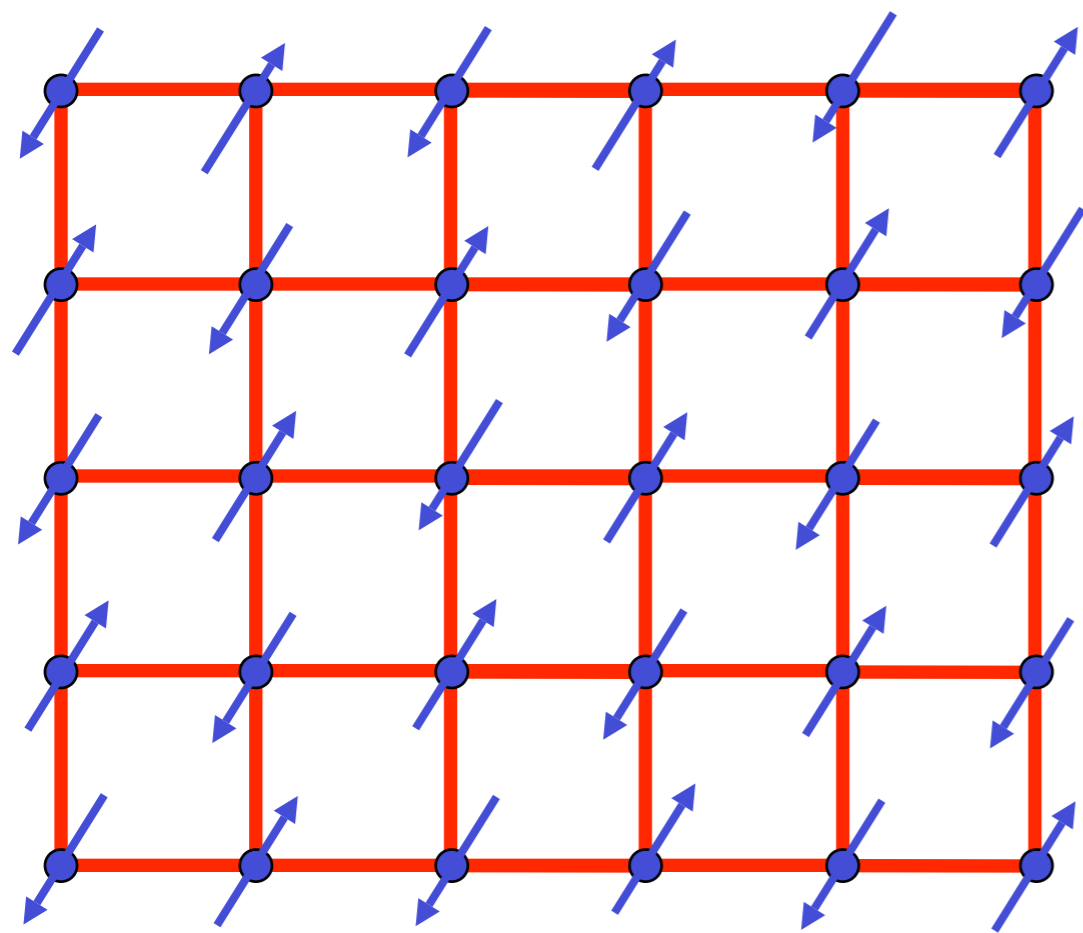
← Pressure in  $\text{TlCuCl}_3$



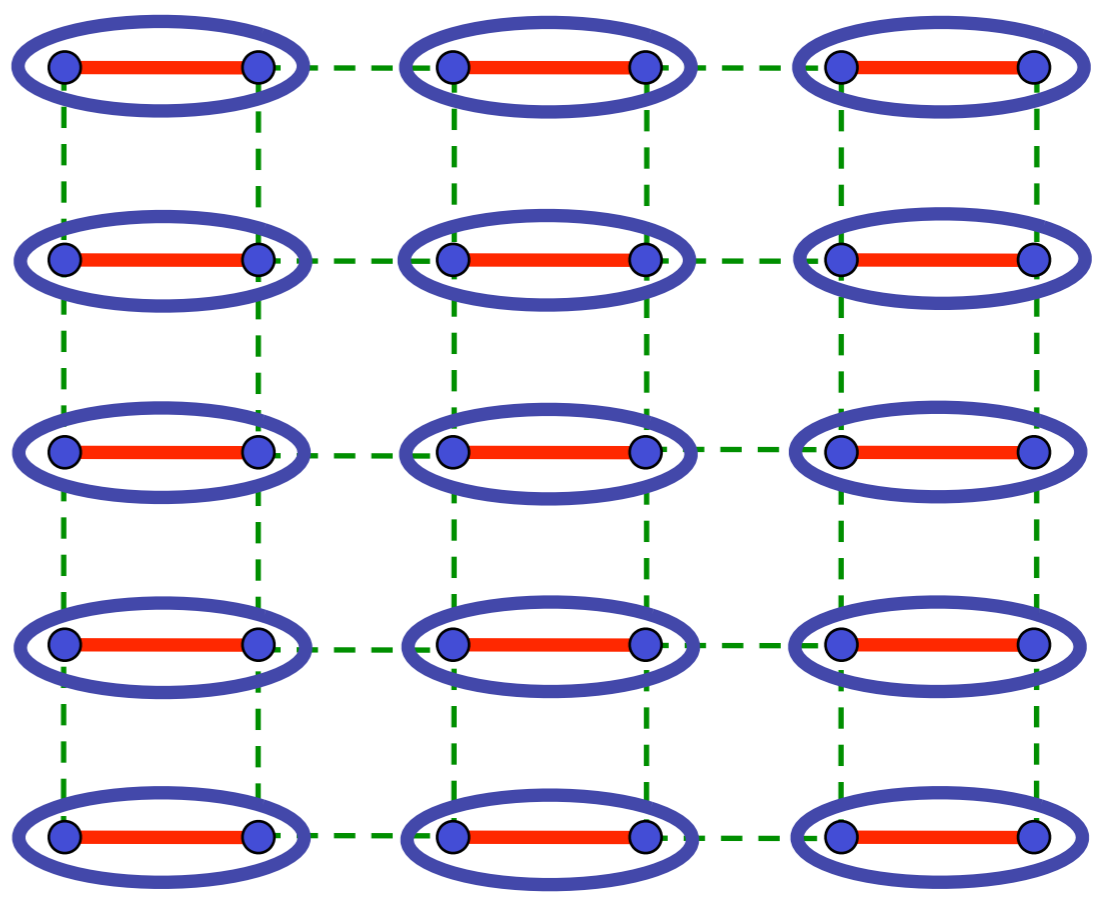
$$= \frac{1}{\sqrt{2}} (|\uparrow\downarrow\rangle - |\downarrow\uparrow\rangle)$$



Quantum critical point with non-local entanglement in spin wavefunction



$$= \frac{1}{\sqrt{2}} (|\uparrow\downarrow\rangle - |\downarrow\uparrow\rangle)$$

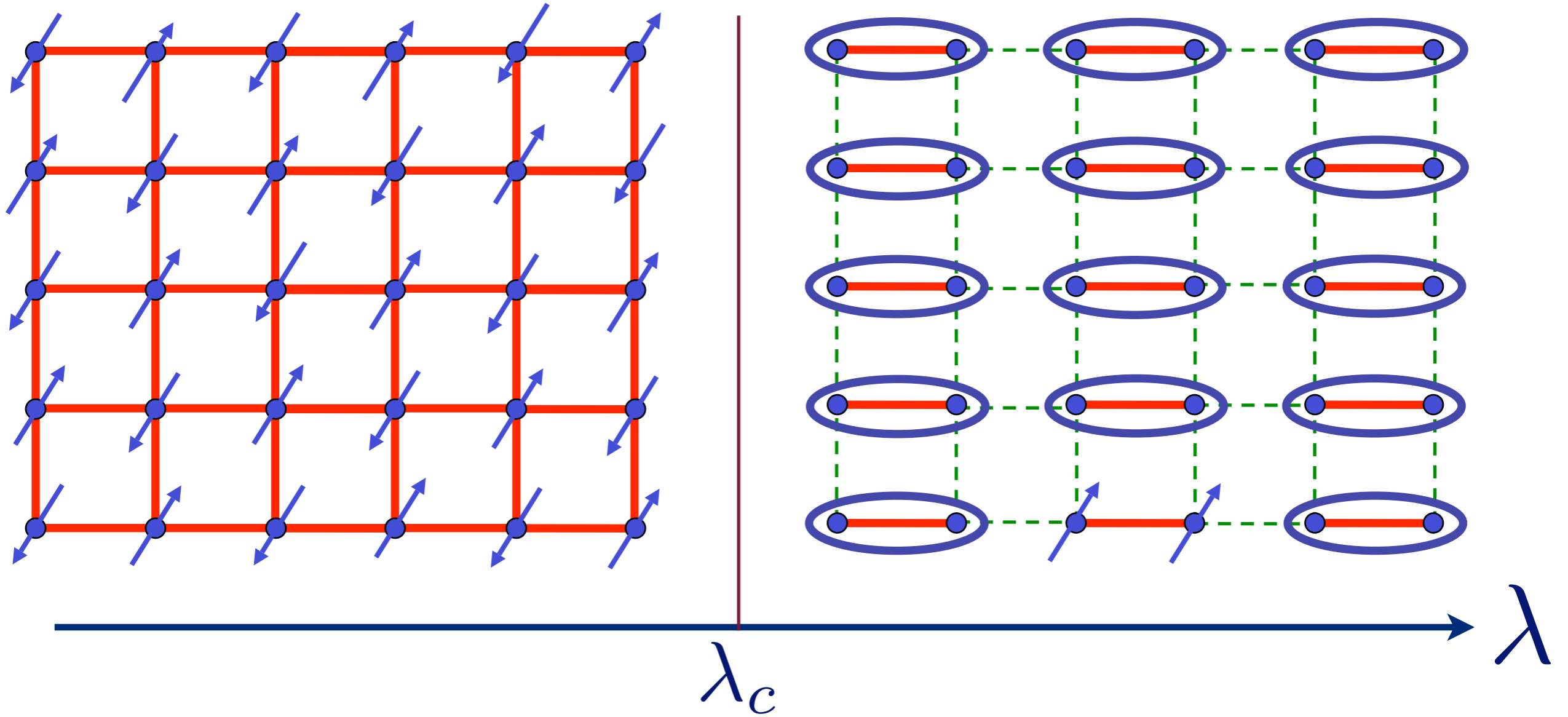


$O(3)$  order parameter  $\vec{\varphi}$

CFT3

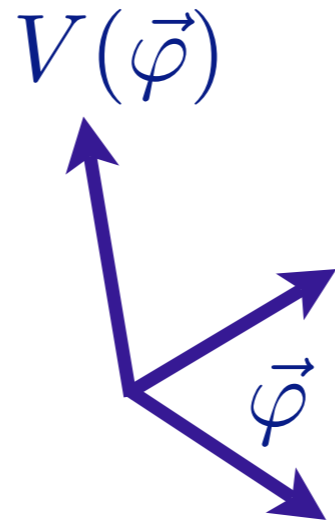
$$\mathcal{S} = \int d^2r d\tau \left[ (\partial_\tau \vec{\varphi})^2 + c^2 (\nabla_r \vec{\varphi})^2 + (\lambda - \lambda_c) \vec{\varphi}^2 + u (\vec{\varphi}^2)^2 \right]$$

# Excitation spectrum in the paramagnetic phase



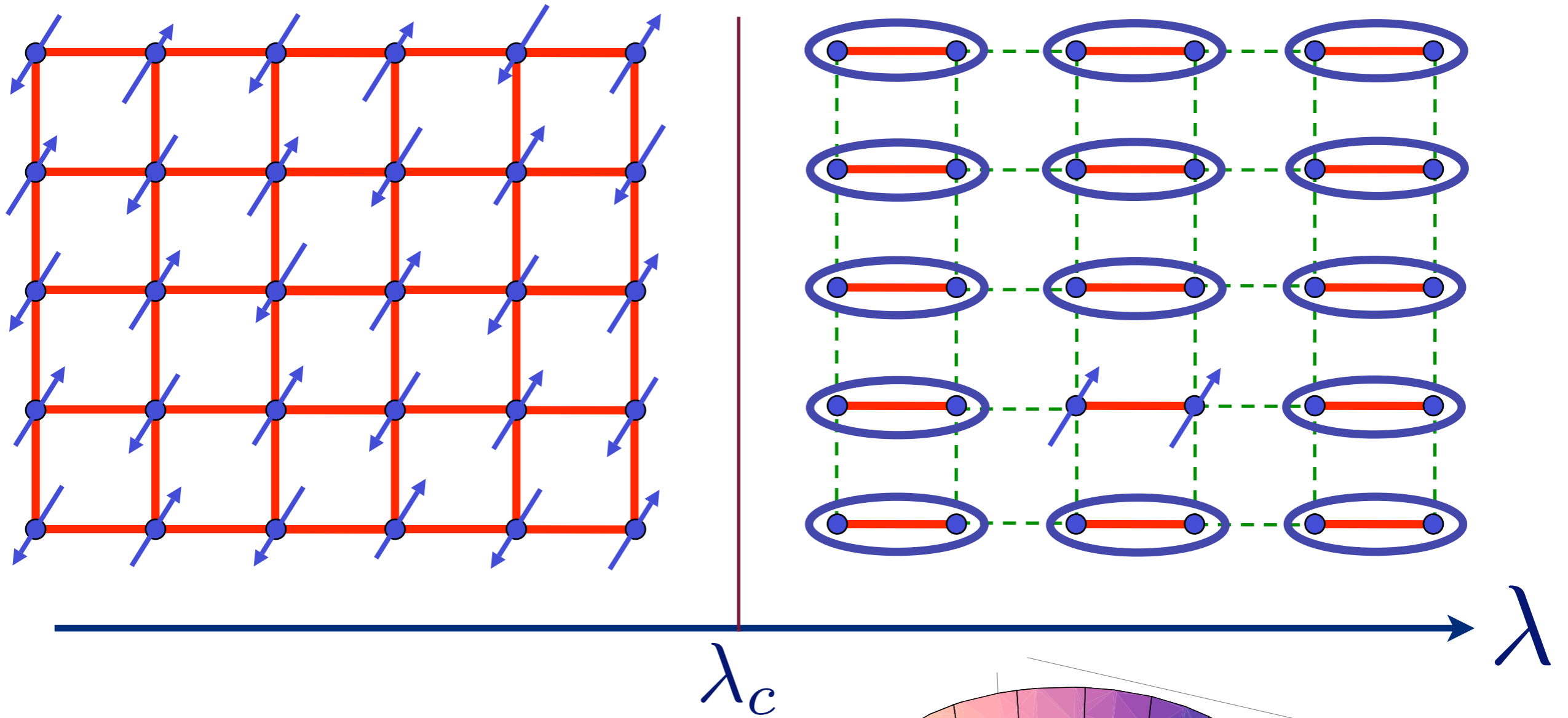
$$V(\vec{\varphi}) = (\lambda - \lambda_c) \vec{\varphi}^2 + u (\vec{\varphi}^2)^2$$

$$\lambda > \lambda_c$$



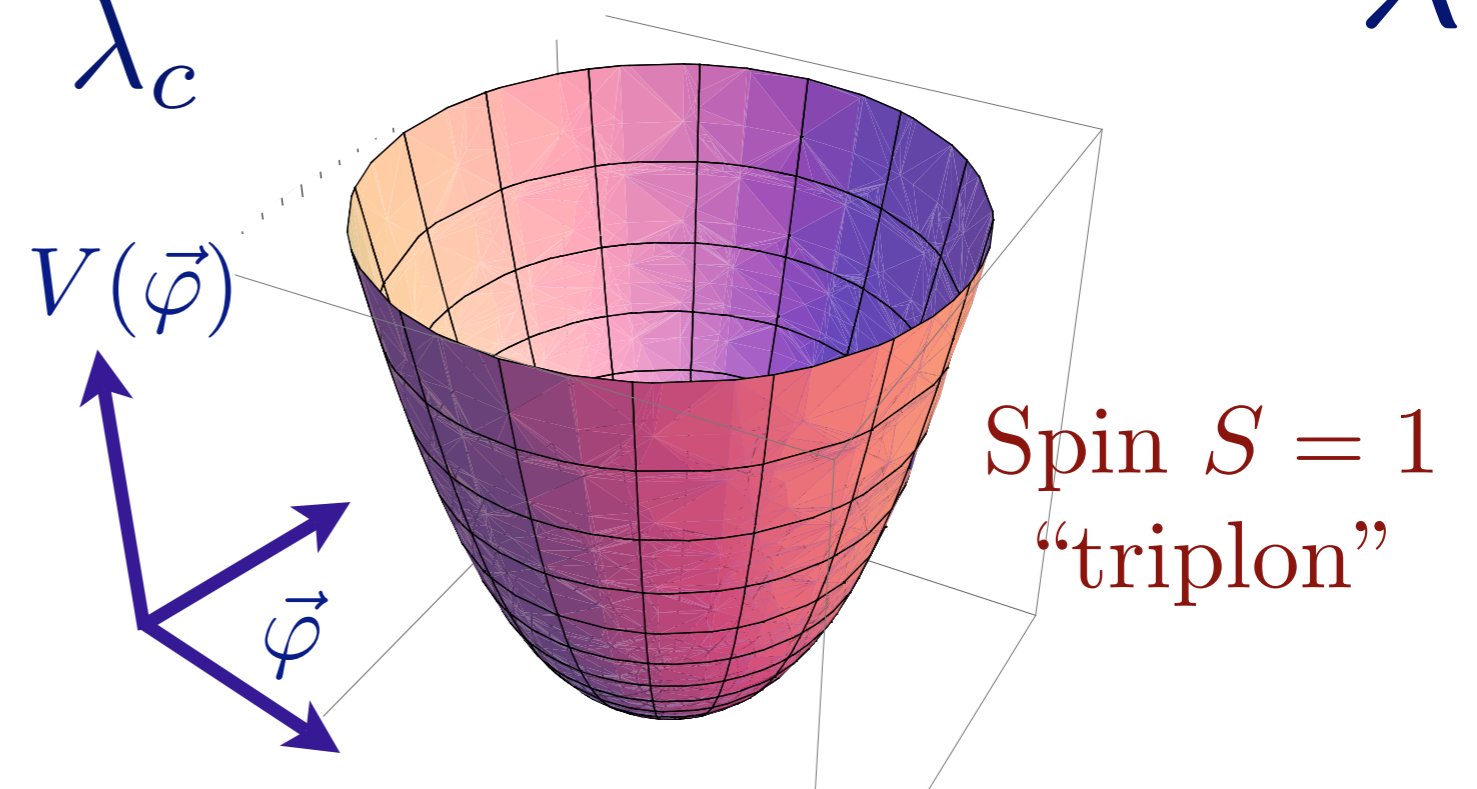
Spin  $S = 1$   
“triplon”

# Excitation spectrum in the paramagnetic phase

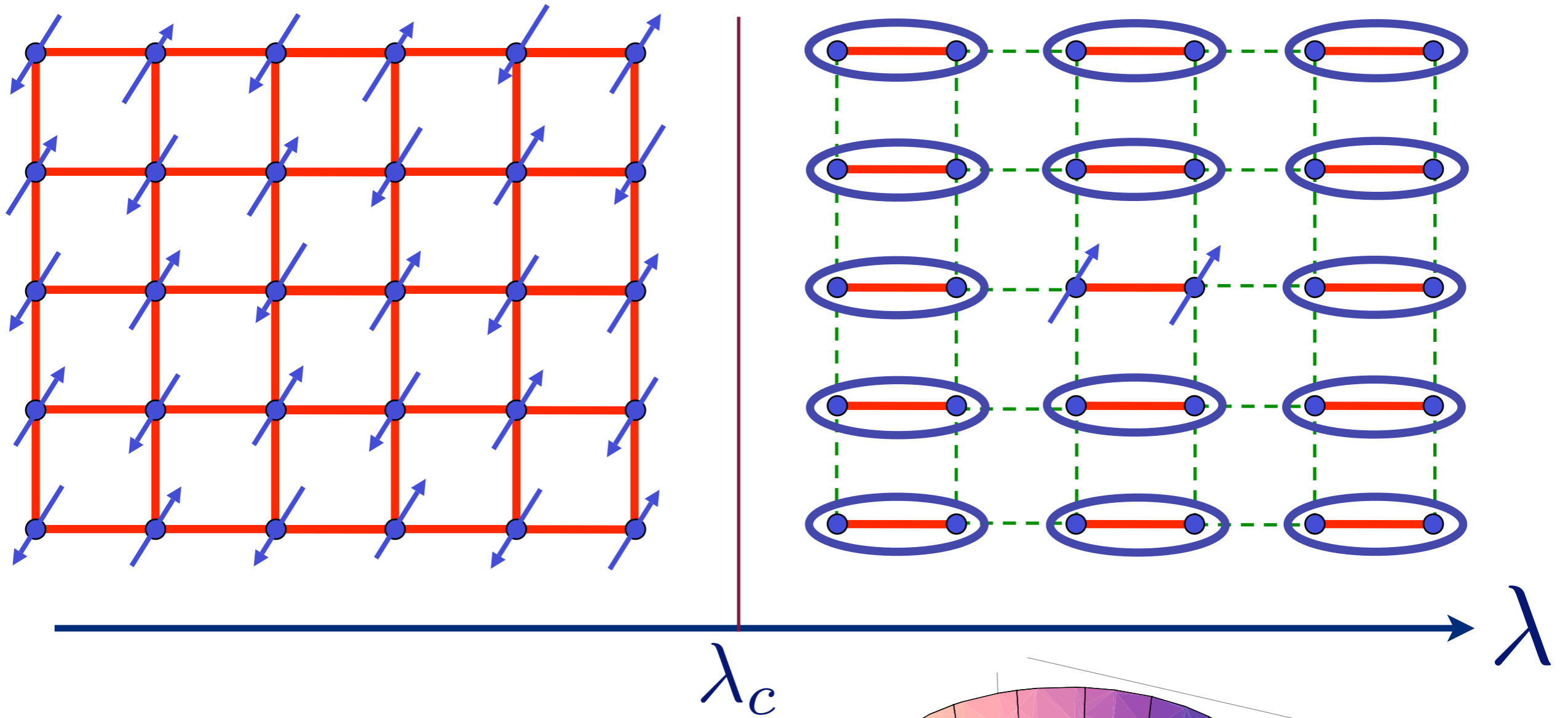


$$V(\vec{\varphi}) = (\lambda - \lambda_c) \vec{\varphi}^2 + u (\vec{\varphi}^2)^2$$

$\lambda > \lambda_c$

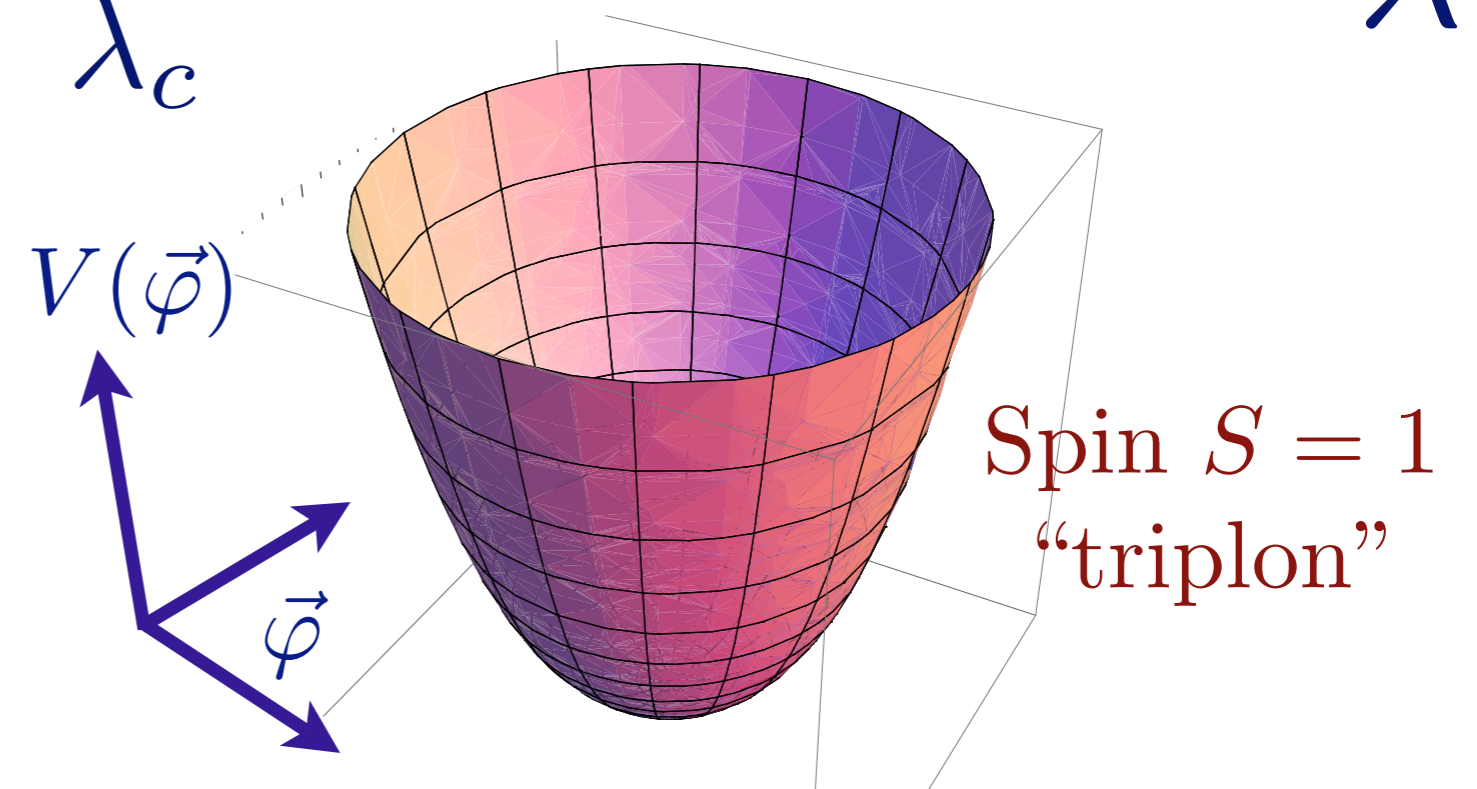


# Excitation spectrum in the paramagnetic phase

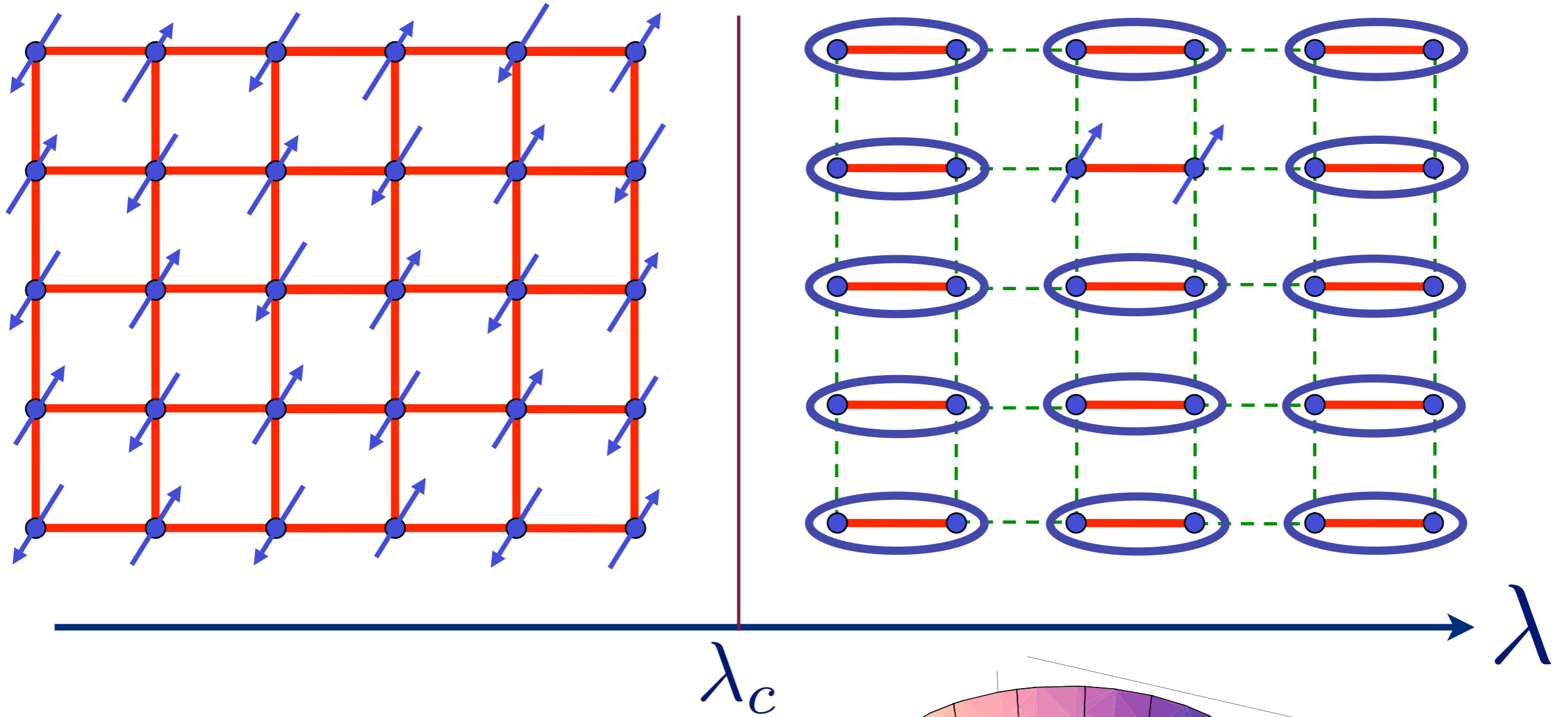


$$V(\vec{\varphi}) = (\lambda - \lambda_c) \vec{\varphi}^2 + u (\vec{\varphi}^2)^2$$

$\lambda > \lambda_c$

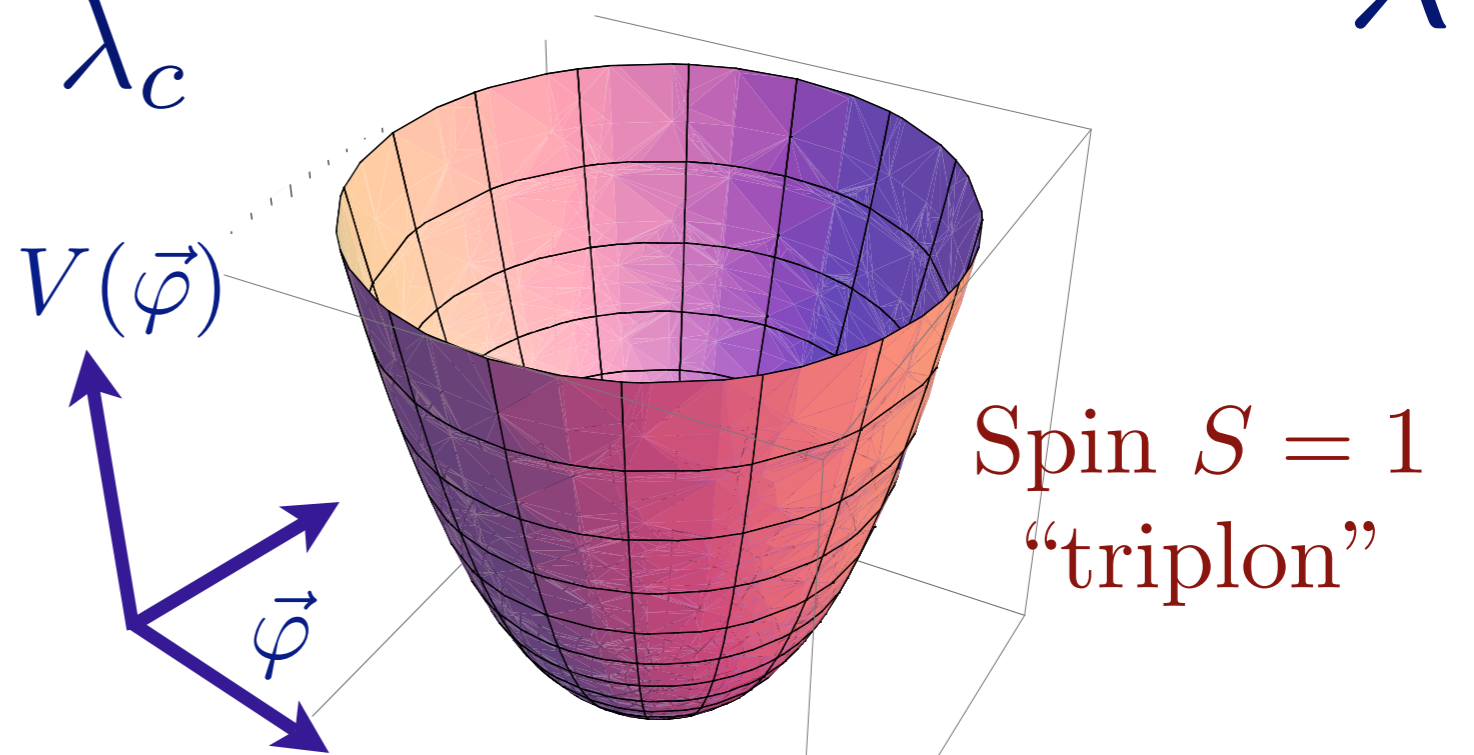


# Excitation spectrum in the paramagnetic phase

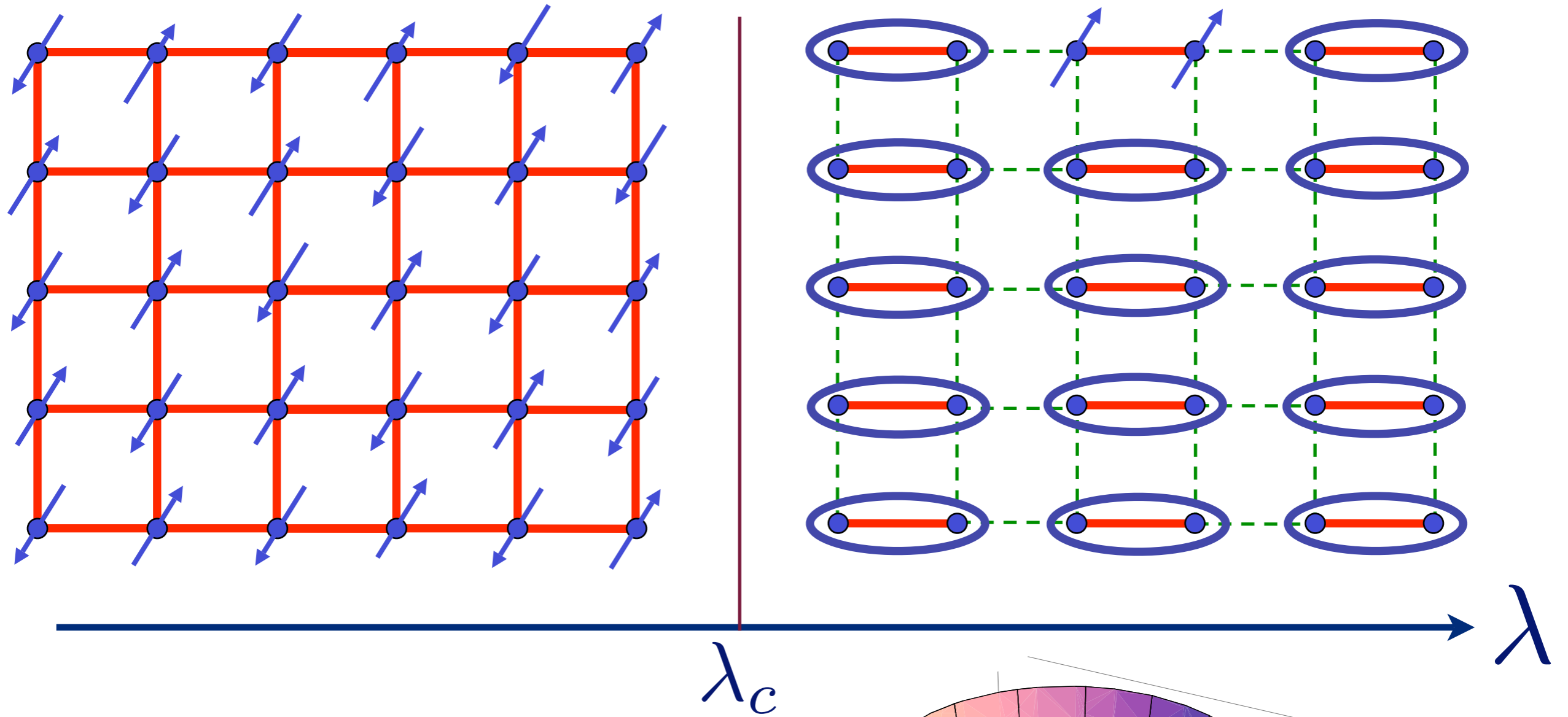


$$V(\vec{\varphi}) = (\lambda - \lambda_c) \vec{\varphi}^2 + u (\vec{\varphi}^2)^2$$

$$\lambda > \lambda_c$$

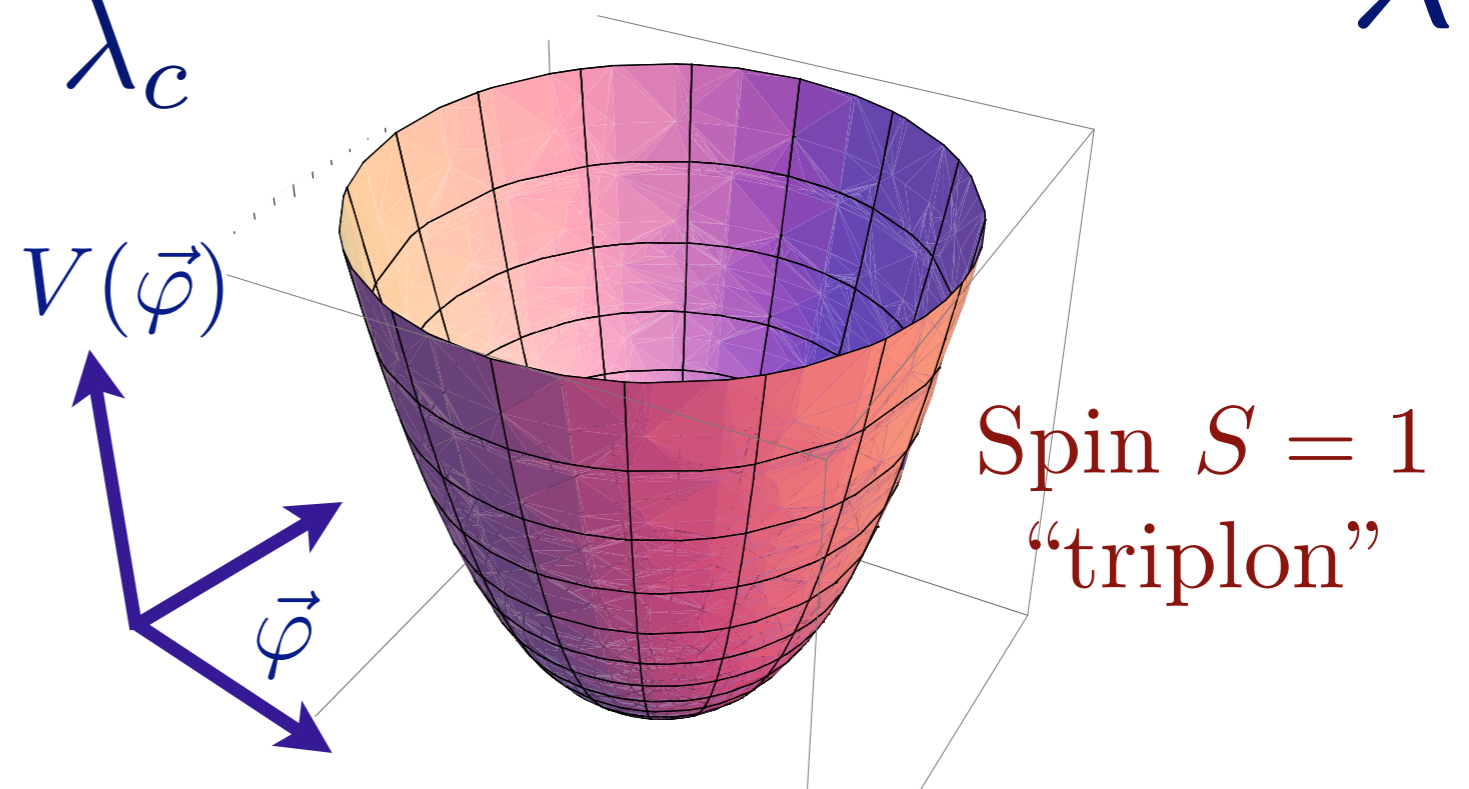


# Excitation spectrum in the paramagnetic phase



$$V(\vec{\varphi}) = (\lambda - \lambda_c) \vec{\varphi}^2 + u (\vec{\varphi}^2)^2$$

$\lambda > \lambda_c$



# TlCuCl<sub>3</sub> at ambient pressure

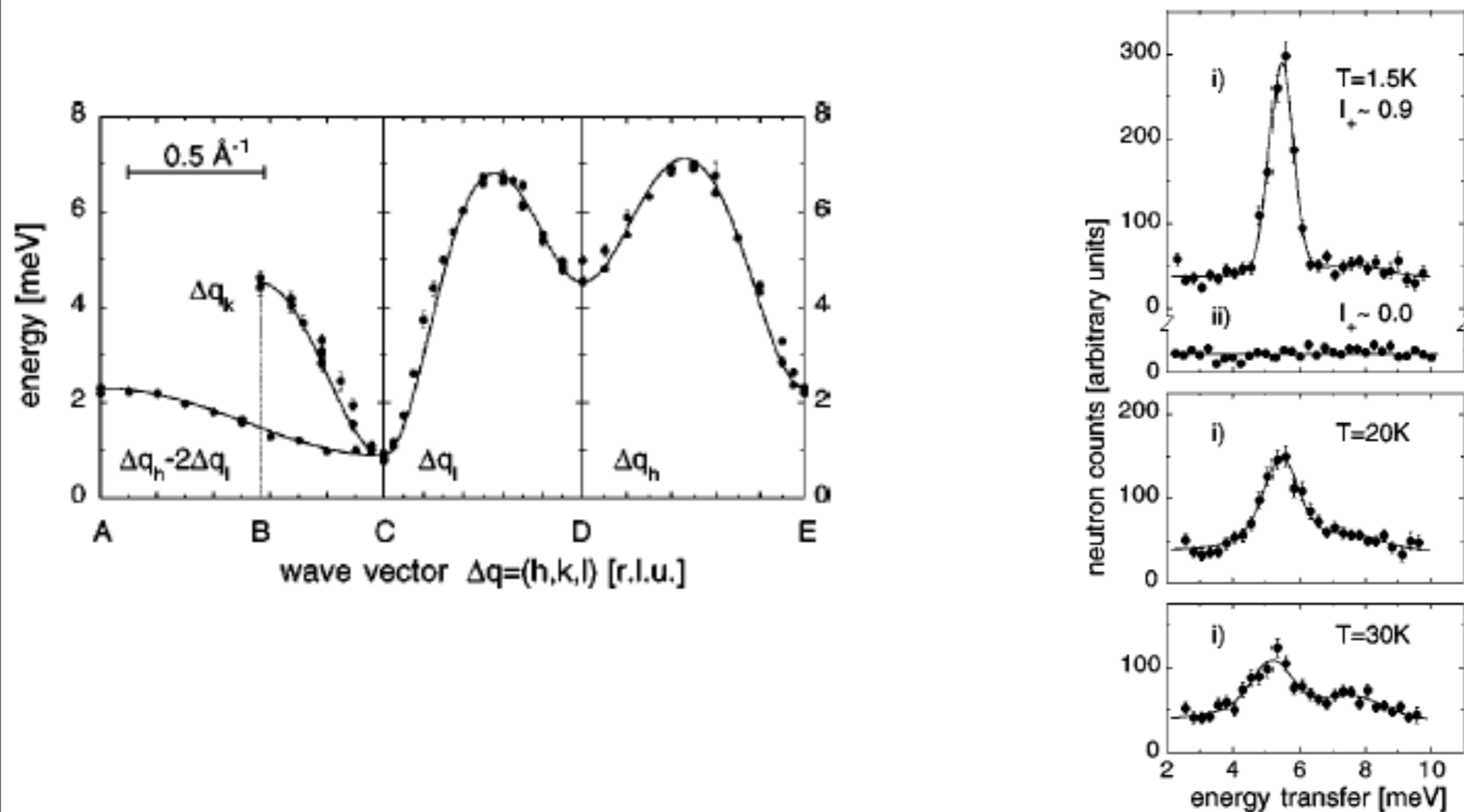
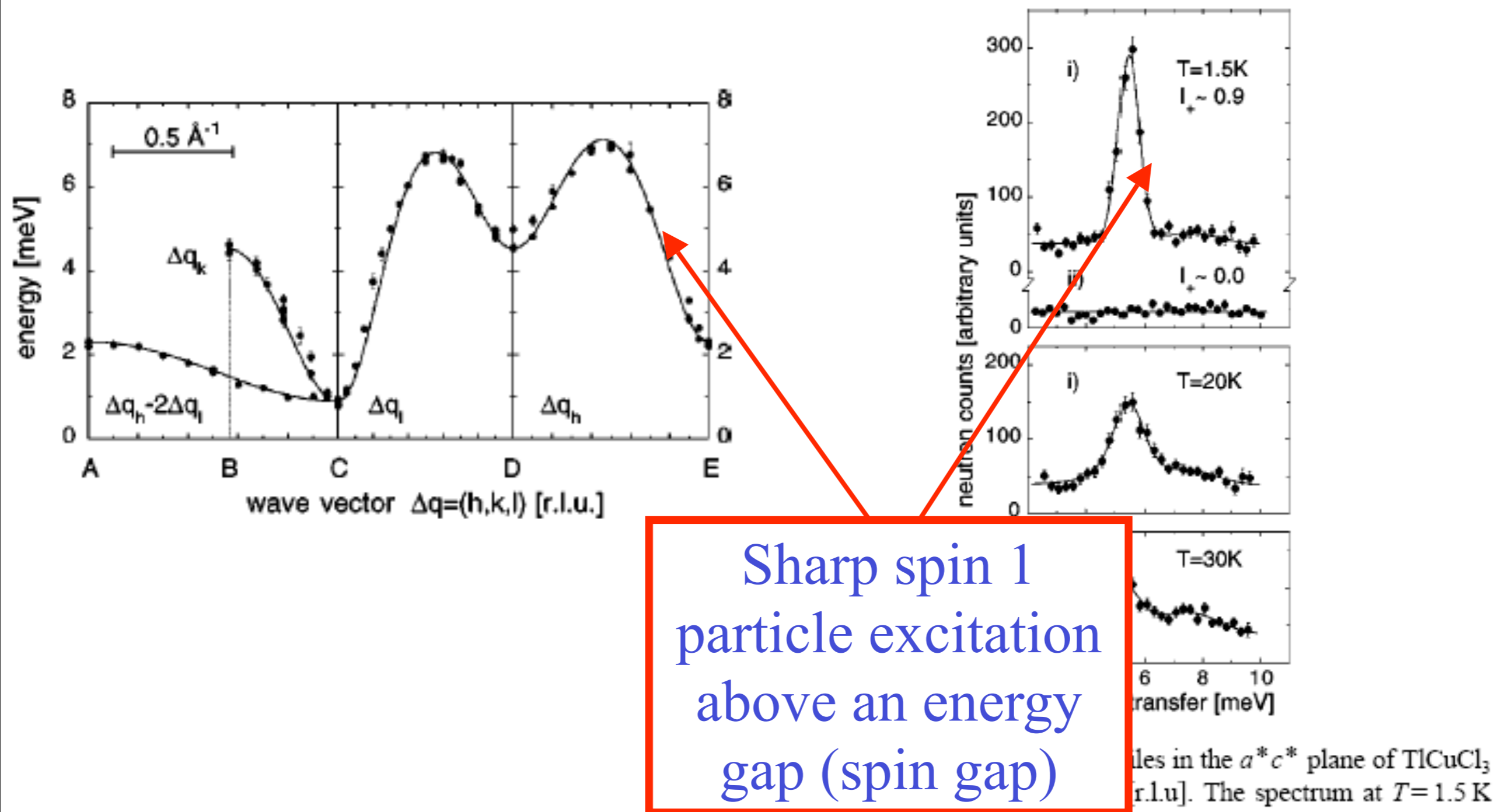


FIG. 1. Measured neutron profiles in the  $a^*c^*$  plane of TlCuCl<sub>3</sub> for  $i = (1.35, 0, 0)$ ,  $ii = (0, 0, 3.15)$  [r.l.u.]. The spectrum at  $T = 1.5 \text{ K}$

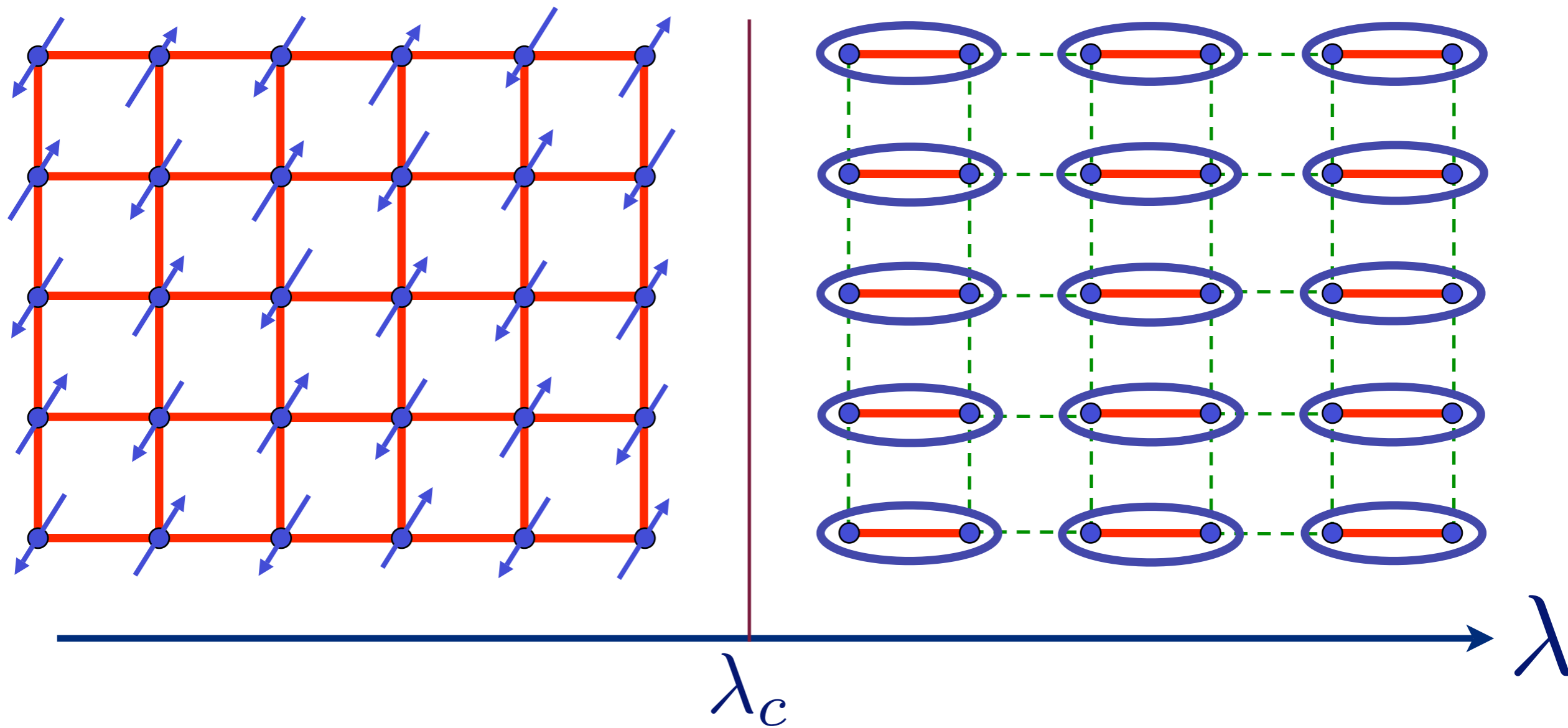
N. Cavadini, G. Heigold, W. Henggeler, A. Furrer, H.-U. Güdel, K. Krämer and H. Mutka, *Phys. Rev. B* 63 172414 (2001).

# TlCuCl<sub>3</sub> at ambient pressure

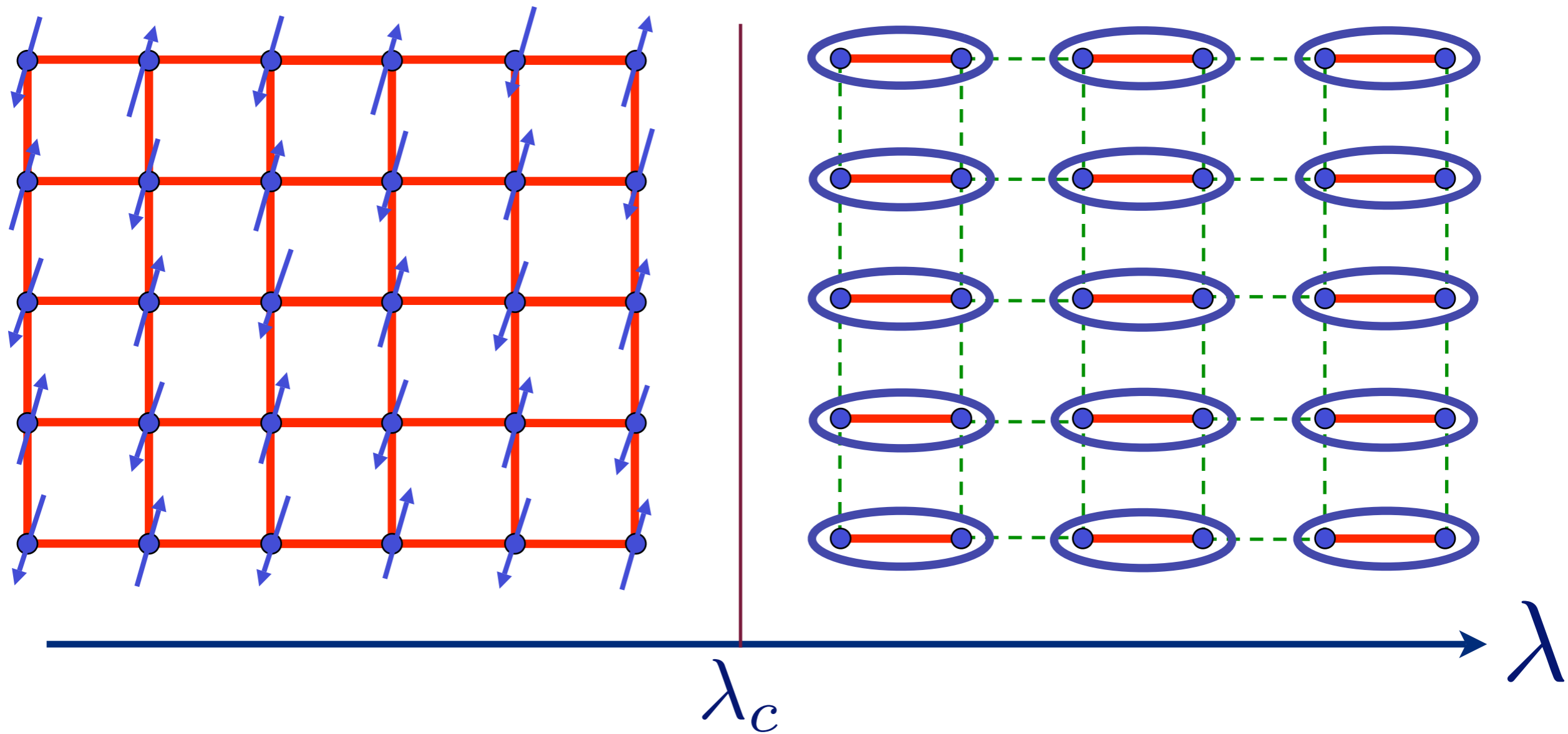


N. Cavadini, G. Heigold, W. Henggeler, A. Furrer, H.-U. Güdel, K. Krämer  
and H. Mutka, *Phys. Rev. B* 63 172414 (2001).

# Excitation spectrum in the Néel phase

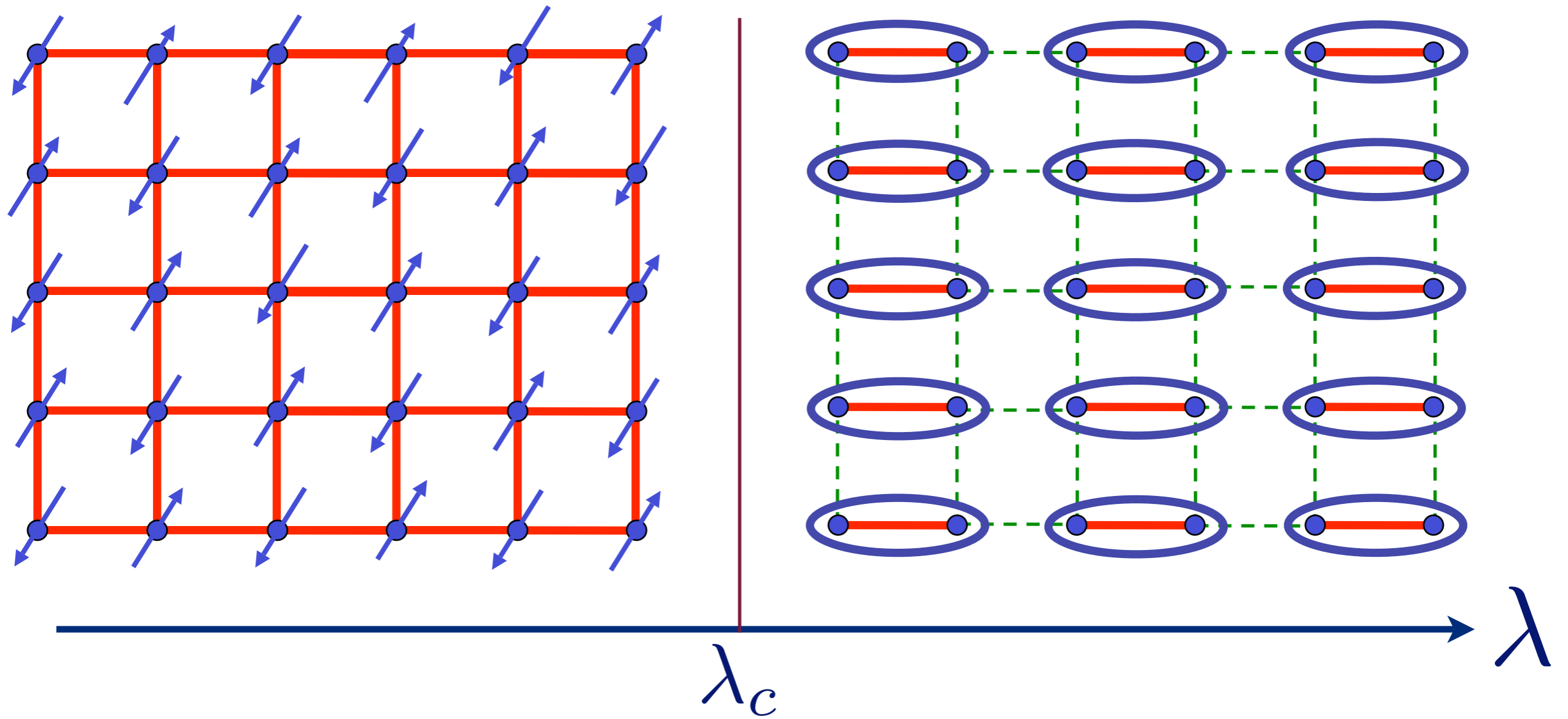


# Excitation spectrum in the Néel phase



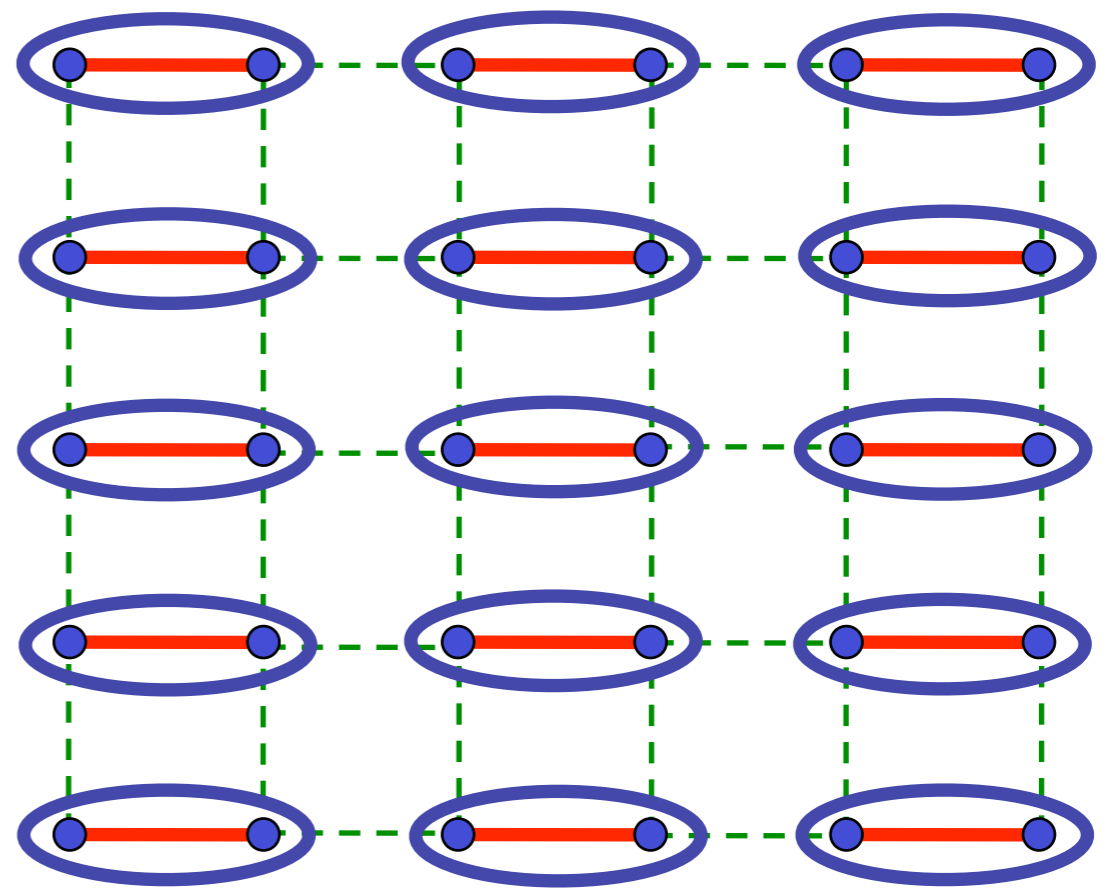
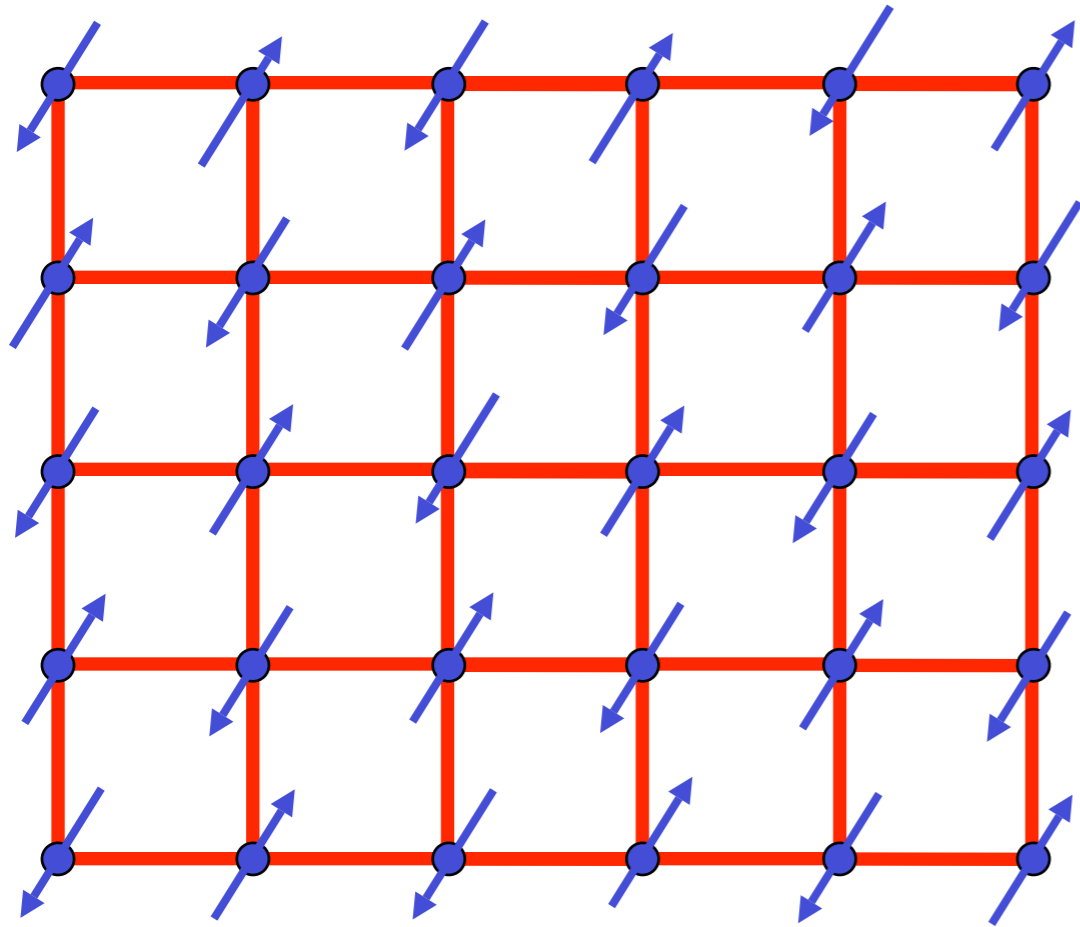
Spin waves

# Excitation spectrum in the Néel phase



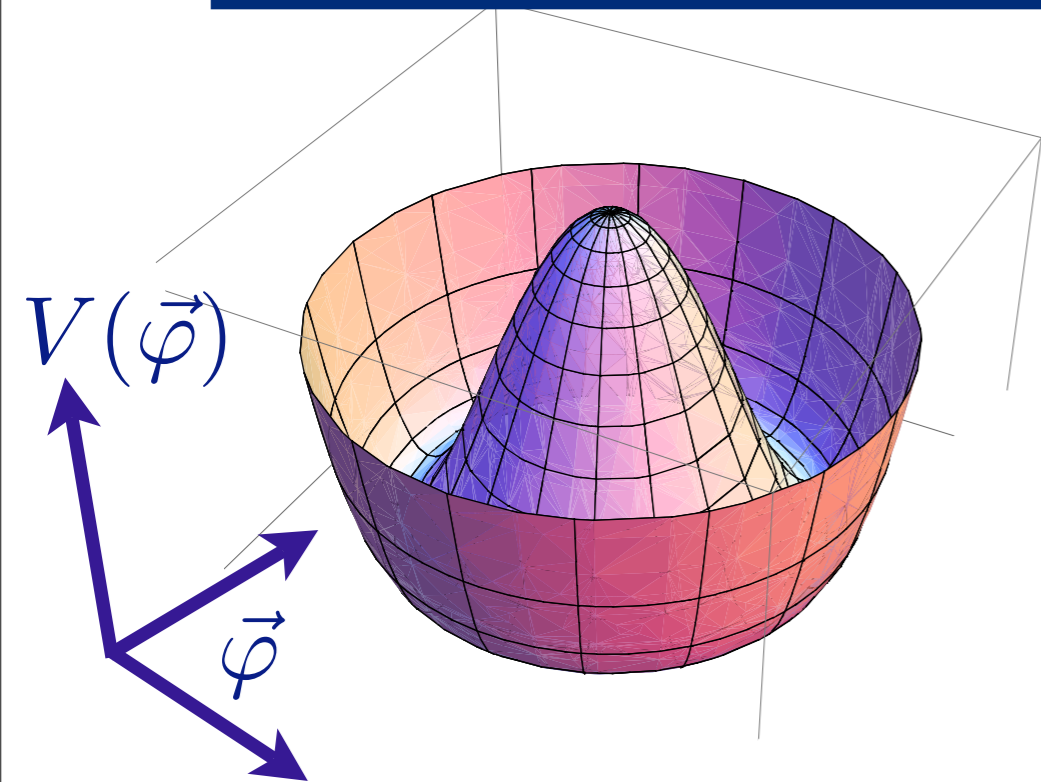
Spin waves

# Excitation spectrum in the Néel phase

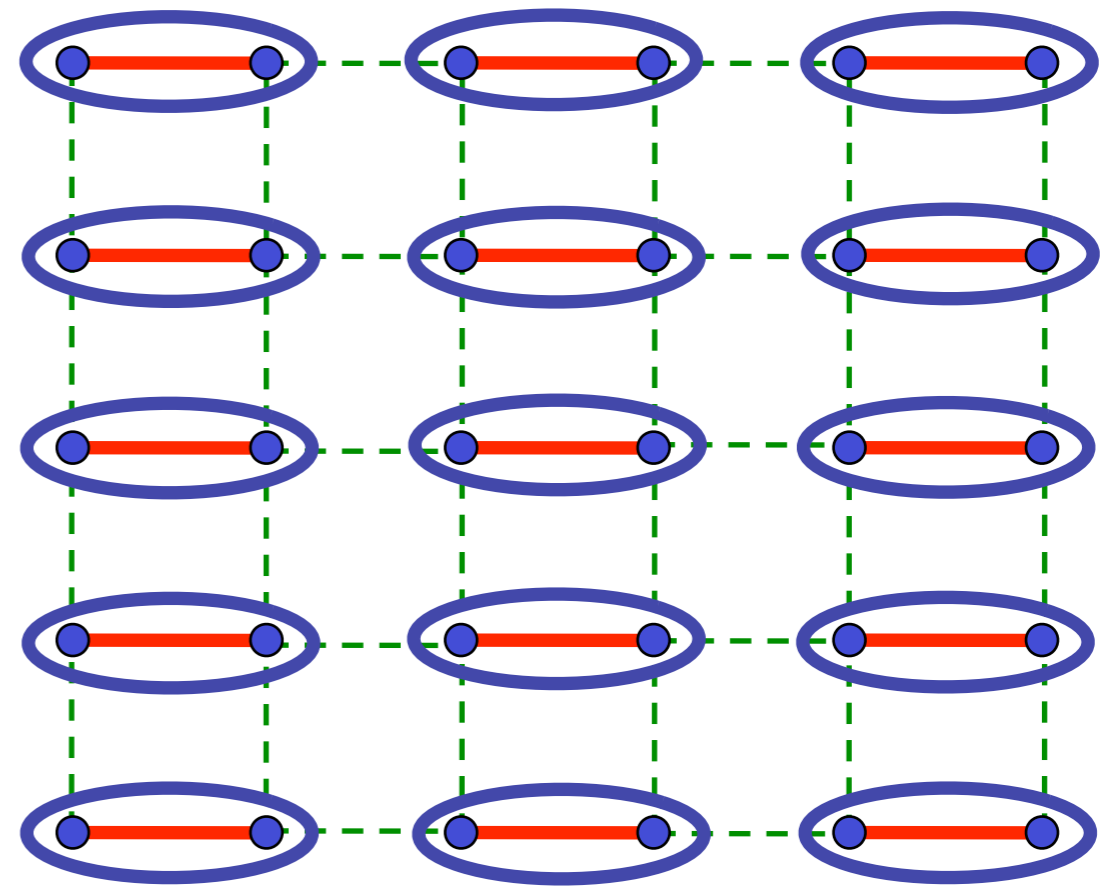
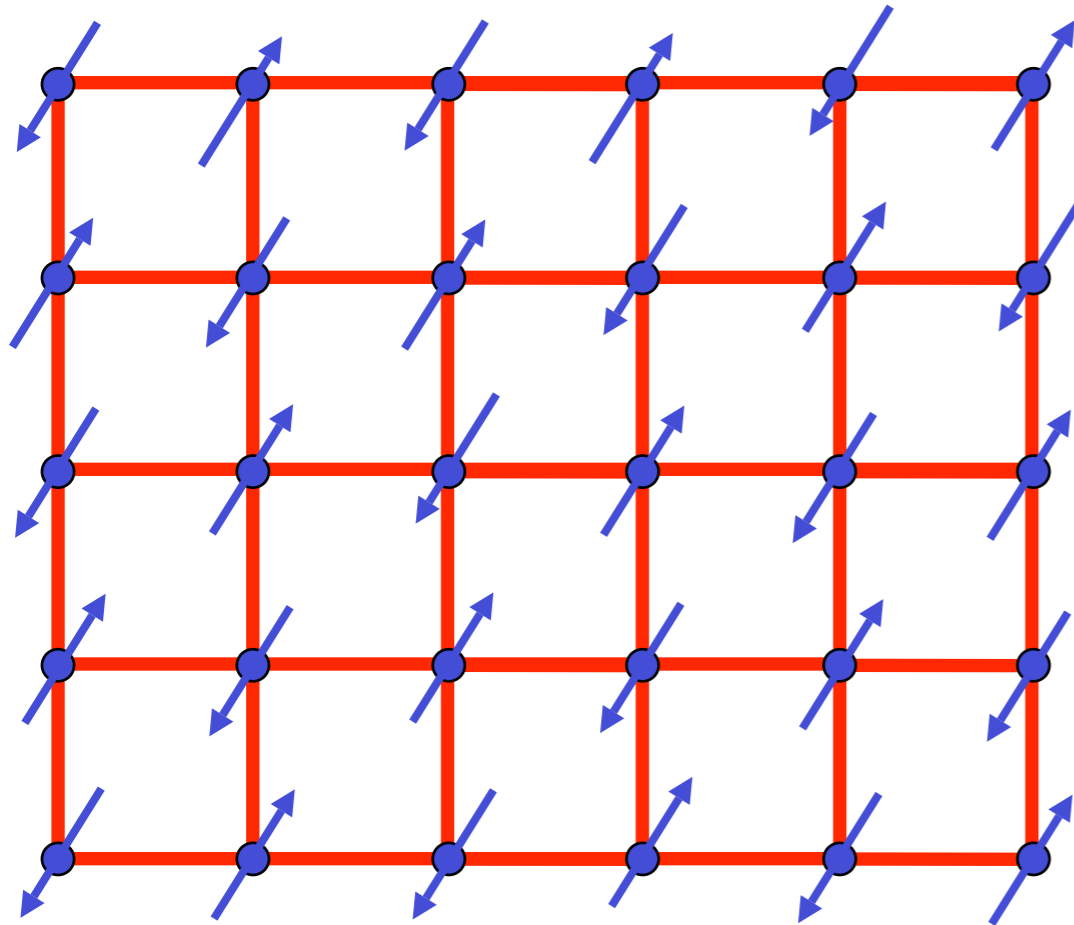


$$V(\vec{\varphi}) = (\lambda - \lambda_c)\vec{\varphi}^2 + u(\vec{\varphi}^2)^2$$

$$\lambda < \lambda_c$$

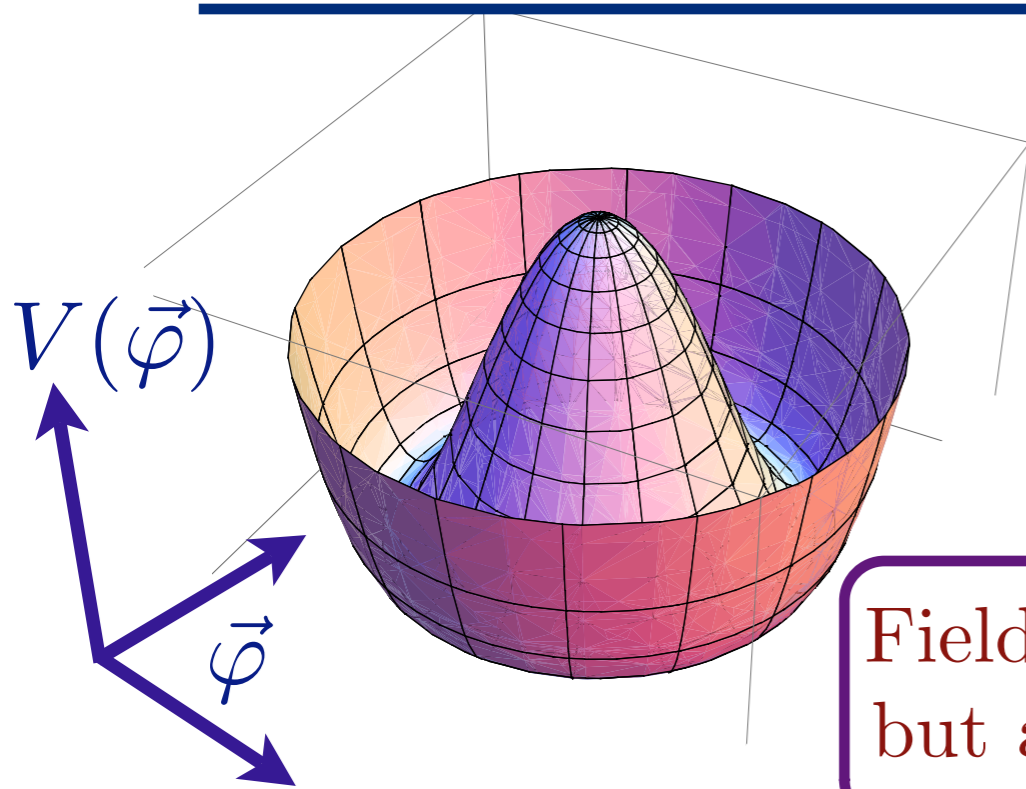


# Excitation spectrum in the Néel phase

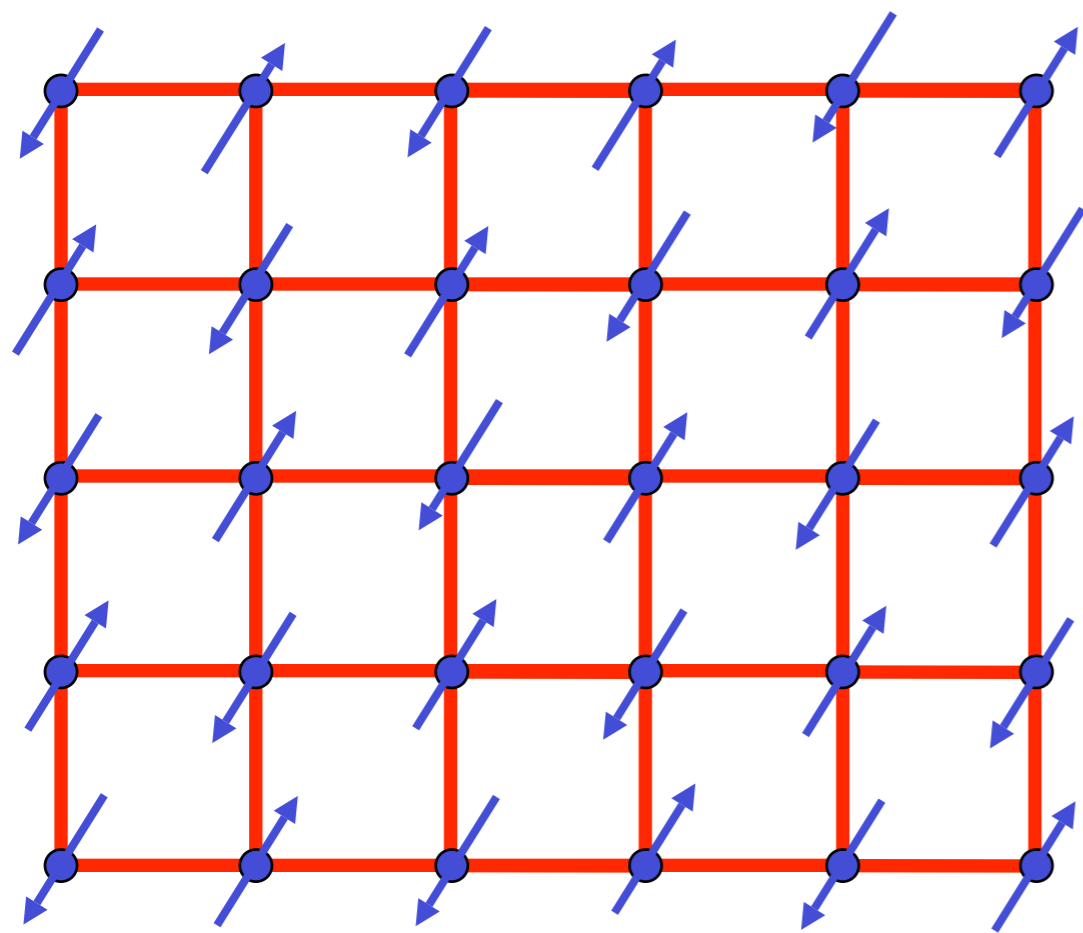


$$V(\vec{\varphi}) = (\lambda - \lambda_c)\vec{\varphi}^2 + u(\vec{\varphi}^2)^2$$

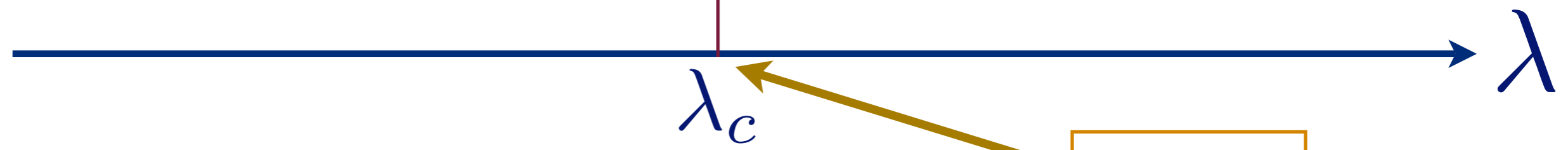
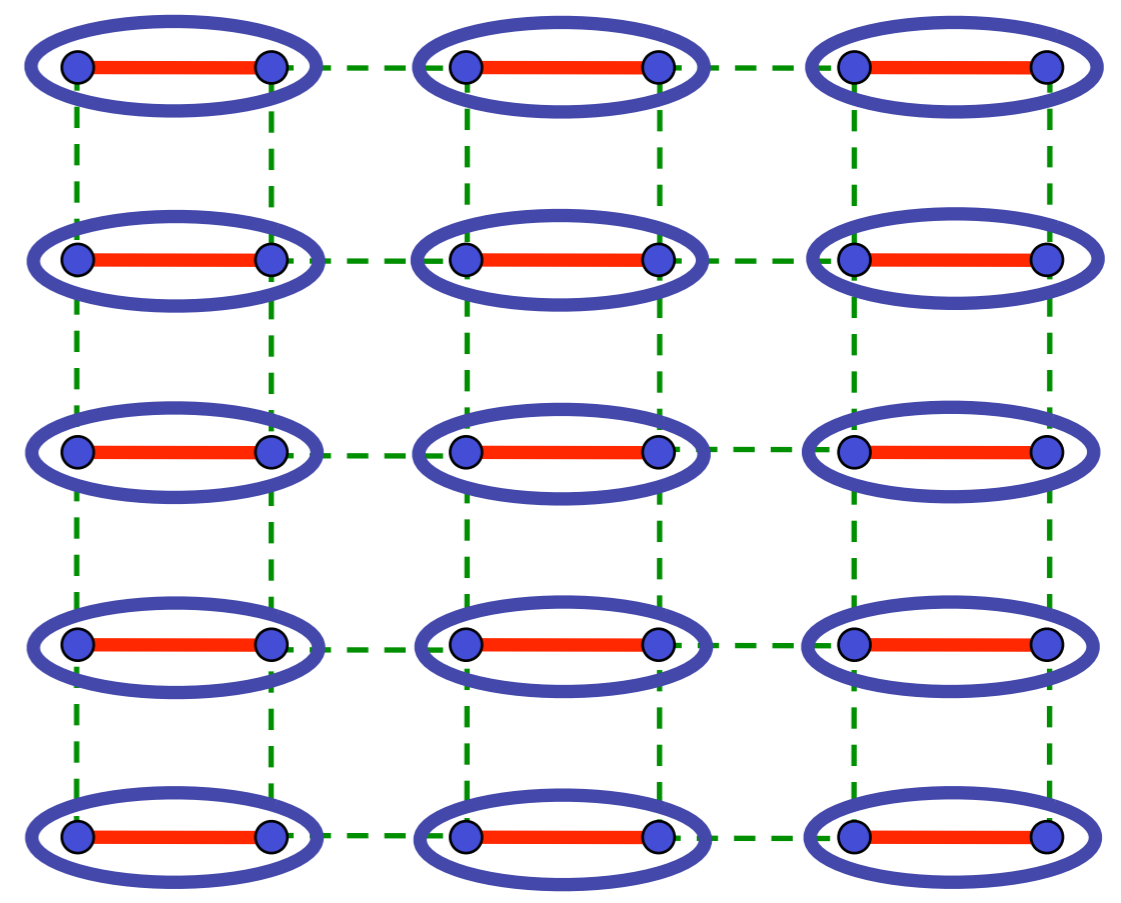
$$\lambda < \lambda_c$$



Field theory yields spin waves (“Goldstone” modes) but also an additional longitudinal “Higgs” particle



$$= \frac{1}{\sqrt{2}} (|\uparrow\downarrow\rangle - |\downarrow\uparrow\rangle)$$



$O(3)$  order parameter  $\vec{\varphi}$

CFT3

$$\mathcal{S} = \int d^2r d\tau \left[ (\partial_\tau \vec{\varphi})^2 + c^2 (\nabla_r \vec{\varphi})^2 + (\lambda - \lambda_c) \vec{\varphi}^2 + u (\vec{\varphi}^2)^2 \right]$$

# Quantum Monte Carlo - critical exponents

Table IV: Fit results for the critical exponents  $\nu$ ,  $\beta/\nu$ , and  $\eta$ . We summarize results including a variation of the critical point within its error bar. For the ladder model (top group of values) fit results and quality of fits are also given at the previous best estimate of  $\alpha_c$ . The bottom group are results for the plaquette model. Numbers in [...] brackets denote the  $\chi^2/\text{d.o.f.}$  For comparison relevant reference values for the 3D  $O(3)$  universality class are given in the last line.

$\alpha_c$	$\nu^a$	$\beta/\nu^b$	$\eta^c$
1.9096 $-\sigma$	0.712(4) [1.8]	0.516(2) [0.5]	0.026(2) [0.2]
1.9096	0.711(4) [1.8]	0.518(2) [1.1]	0.029(5) [0.8]
1.9096 $+\sigma$	0.710(4) [1.8]	0.519(3) [2.5]	0.032(7) [1.4]
1.9107 <sup>d</sup>	0.709(3) [1.7]	0.525(8) [15.3]	0.051(10) [12]
1.8230 $-\sigma$	0.708(4) [0.99]	0.515(2) [0.84]	0.025(4) [0.15]
1.8230	0.706(4) [1.04]	0.516(2) [0.40]	0.028(3) [0.31]
1.8230 $+\sigma$	0.706(4) [1.10]	0.517(2) [1.6]	0.031(5) [0.80]
Ref. 49	0.7112(5)	0.518(1)	0.0375(5)

<sup>a</sup> $L > 12$ .

<sup>b</sup> $L > 16$ .

<sup>c</sup> $L > 20$ .

<sup>d</sup>Previous best estimate of Ref. 19.

S. Wenzel and W. Janke, arXiv:0808.1418

M. Troyer, M. Imada, and K. Ueda, *J. Phys. Soc. Japan* (1997)

# Quantum Monte Carlo - critical exponents

Table IV: Fit results for the critical exponents  $\nu$ ,  $\beta/\nu$ , and  $\eta$ . We summarize results including a variation of the critical point within its error bar. For the ladder model (top group of values) fit results and quality of fits are also given at the previous best estimate of  $\alpha_c$ . The bottom group are results for the plaquette model. Numbers in [...] brackets denote the  $\chi^2/\text{d.o.f.}$  For comparison relevant reference values for the 3D  $O(3)$  universality class are given in the last line.

$\alpha_c$	$\nu^a$	$\beta/\nu^b$	$\eta^c$
1.9096 $-\sigma$	0.712(4) [1.8]	0.516(2) [0.5]	0.026(2) [0.2]
1.9096	0.711(4) [1.8]	0.518(2) [1.1]	0.029(5) [0.8]
1.9096 $+\sigma$	0.710(4) [1.8]	0.519(3) [2.5]	0.032(7) [1.4]
1.9107 <sup>d</sup>	0.709(3) [1.7]	0.525(8) [15.3]	0.051(10) [12]
1.8230 $-\sigma$	0.708(4) [0.99]	0.515(2) [0.84]	0.025(4) [0.15]
1.8230	0.706(4) [1.04]	0.516(2) [0.40]	0.028(3) [0.31]
1.8230 $+\sigma$	0.706(4) [1.10]	0.517(2) [1.6]	0.031(5) [0.80]
Ref. 49	0.7112(5)	0.518(1)	0.0375(5)

<sup>a</sup> $L > 12$ .

<sup>b</sup> $L > 16$ .

<sup>c</sup> $L > 20$ .

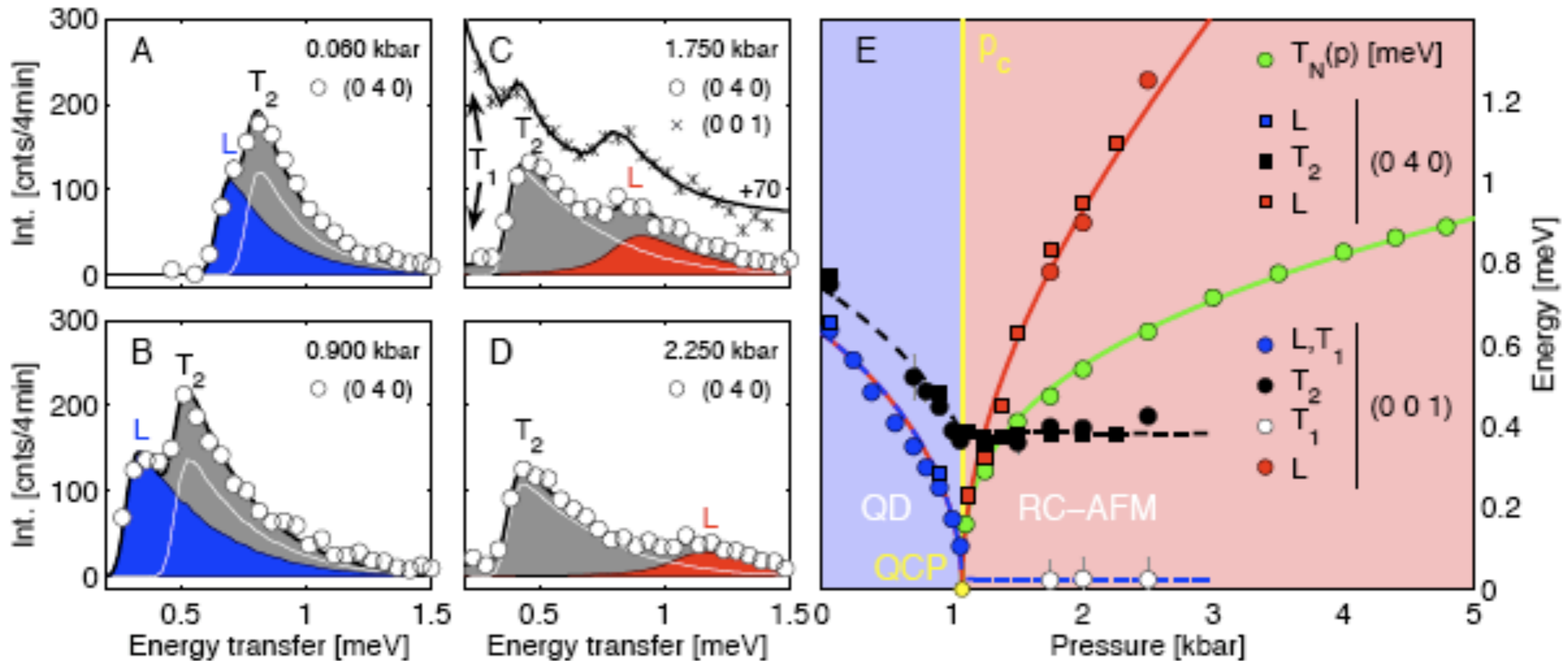
<sup>d</sup>Previous best estimate of Ref. 19.

Field-theoretic  
RG of CFT3  
E.Vicari *et al.*

S. Wenzel and W. Janke, arXiv:0808.1418

M. Troyer, M. Imada, and K. Ueda, *J. Phys. Soc. Japan* (1997)

# TiCuCl<sub>3</sub> with varying pressure



Observation of 3 → 2 low energy modes,  
emergence of new Higgs particle in the Néel phase,  
and vanishing of Néel temperature at the quantum critical point

Christian Ruegg, Bruce Normand, Masashige Matsumoto, Albert Furrer, Desmond McMorrow, Karl Kramer, Hans-Ulrich Gudel, Severian Gvasaliya, Hannu Mutka, and Martin Boehm, *Phys. Rev. Lett.* **100**, 205701 (2008)

# Prediction of quantum field theory

Potential for  $\vec{\varphi}$  fluctuations:  $V(\vec{\varphi}) = (\lambda - \lambda_c)\vec{\varphi}^2 + u (\vec{\varphi}^2)^2$

Paramagnetic phase,  $\lambda > \lambda_c$

Expand about  $\vec{\varphi} = 0$ :

$$V(\vec{\varphi}) \approx (\lambda - \lambda_c)\vec{\varphi}^2$$

Yields 3 particles with energy gap  $\sim \sqrt{(\lambda - \lambda_c)}$

Néel phase,  $\lambda < \lambda_c$

Expand  $\vec{\varphi} = (0, 0, \sqrt{(\lambda_c - \lambda)/(2u)}) + \vec{\varphi}_1$ :

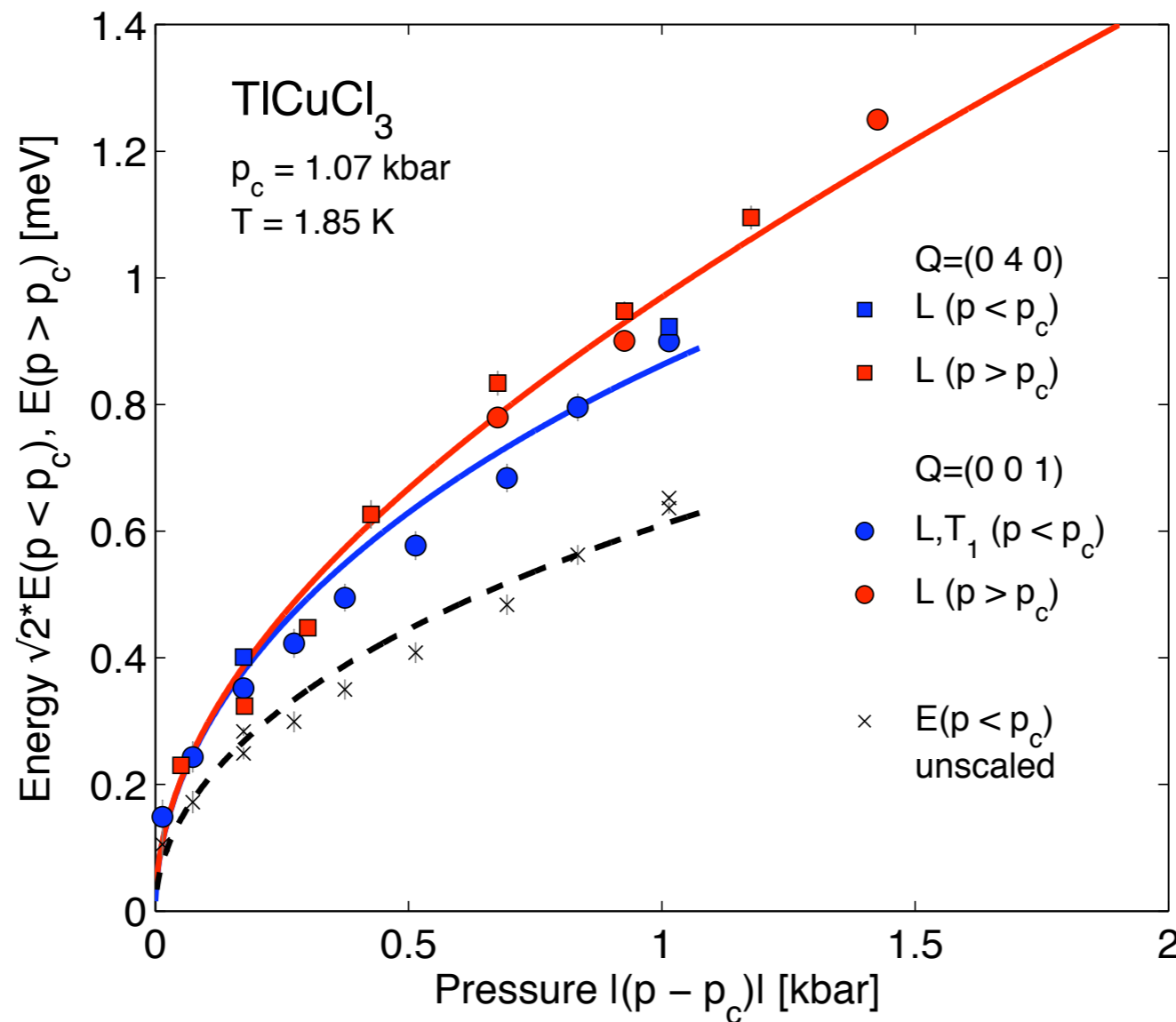
$$V(\vec{\varphi}) \approx 2(\lambda_c - \lambda)\varphi_{1z}^2$$

Yields 2 gapless spin waves and one Higgs particle with energy gap  $\sim \sqrt{2(\lambda_c - \lambda)}$

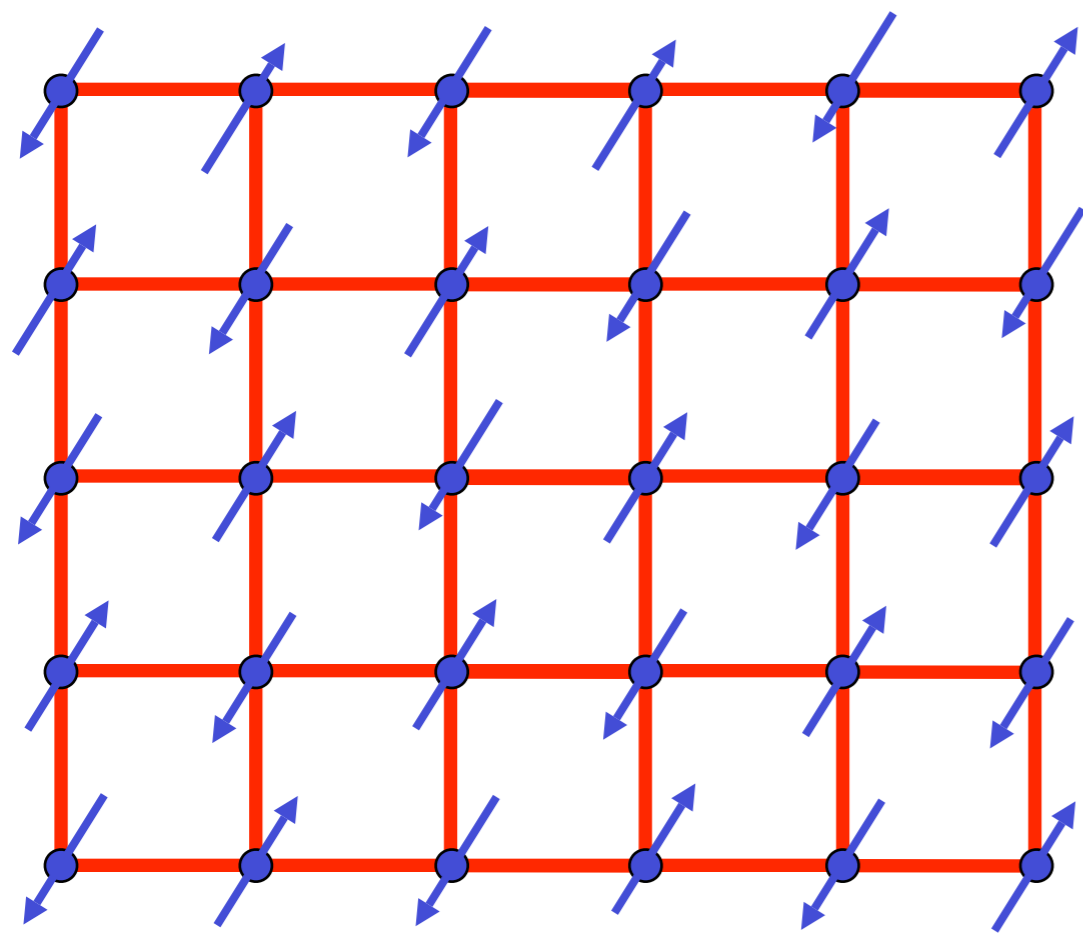
# Prediction of quantum field theory

$$\frac{\text{Energy of "Higgs" particle}}{\text{Energy of triplon}} = \sqrt{2}$$

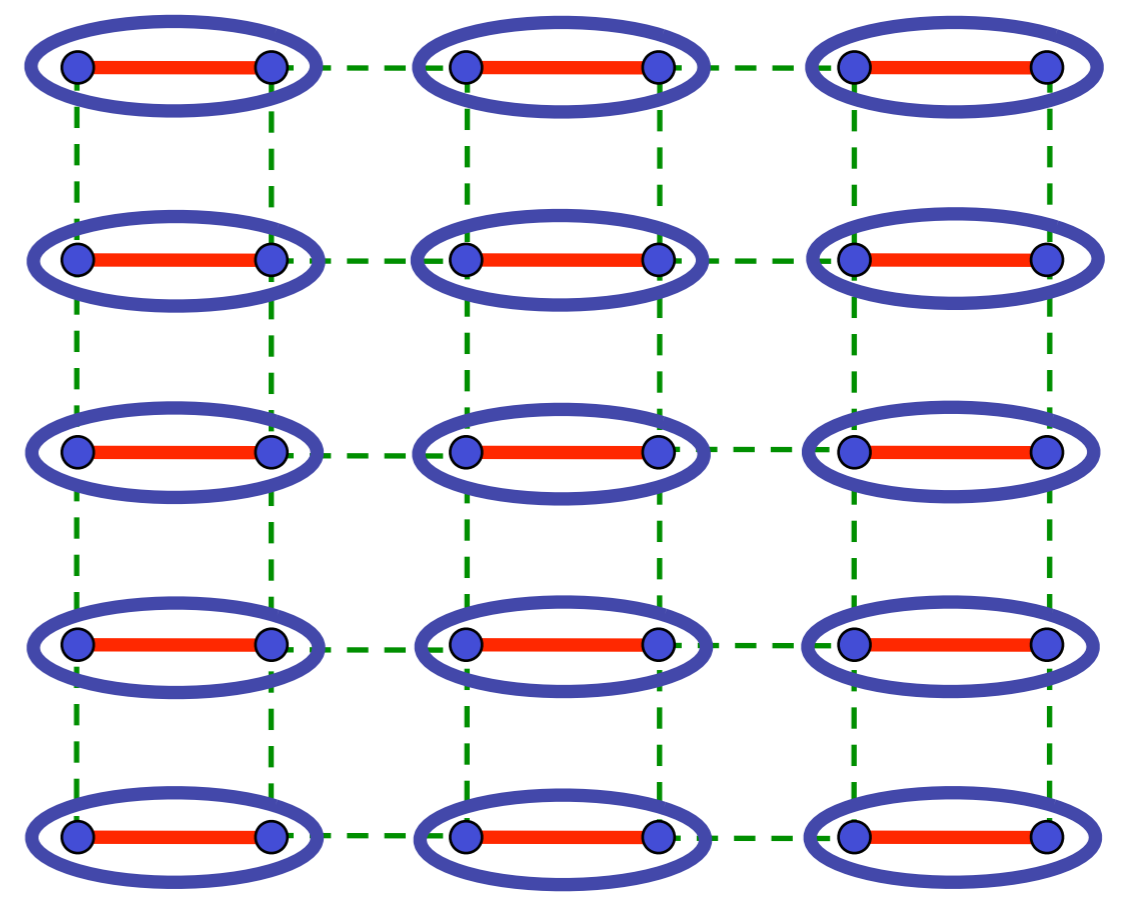
$$V(\vec{\varphi}) = (\lambda - \lambda_c)\vec{\varphi}^2 + u(\vec{\varphi}^2)^2$$



Christian Ruegg, Bruce Normand, Masashige Matsumoto, Albert Furrer, Desmond McMorrow, Karl Kramer, Hans-Ulrich Gudel, Severian Gvasaliya, Hannu Mutka, and Martin Boehm, *Phys. Rev. Lett.* **100**, 205701 (2008)



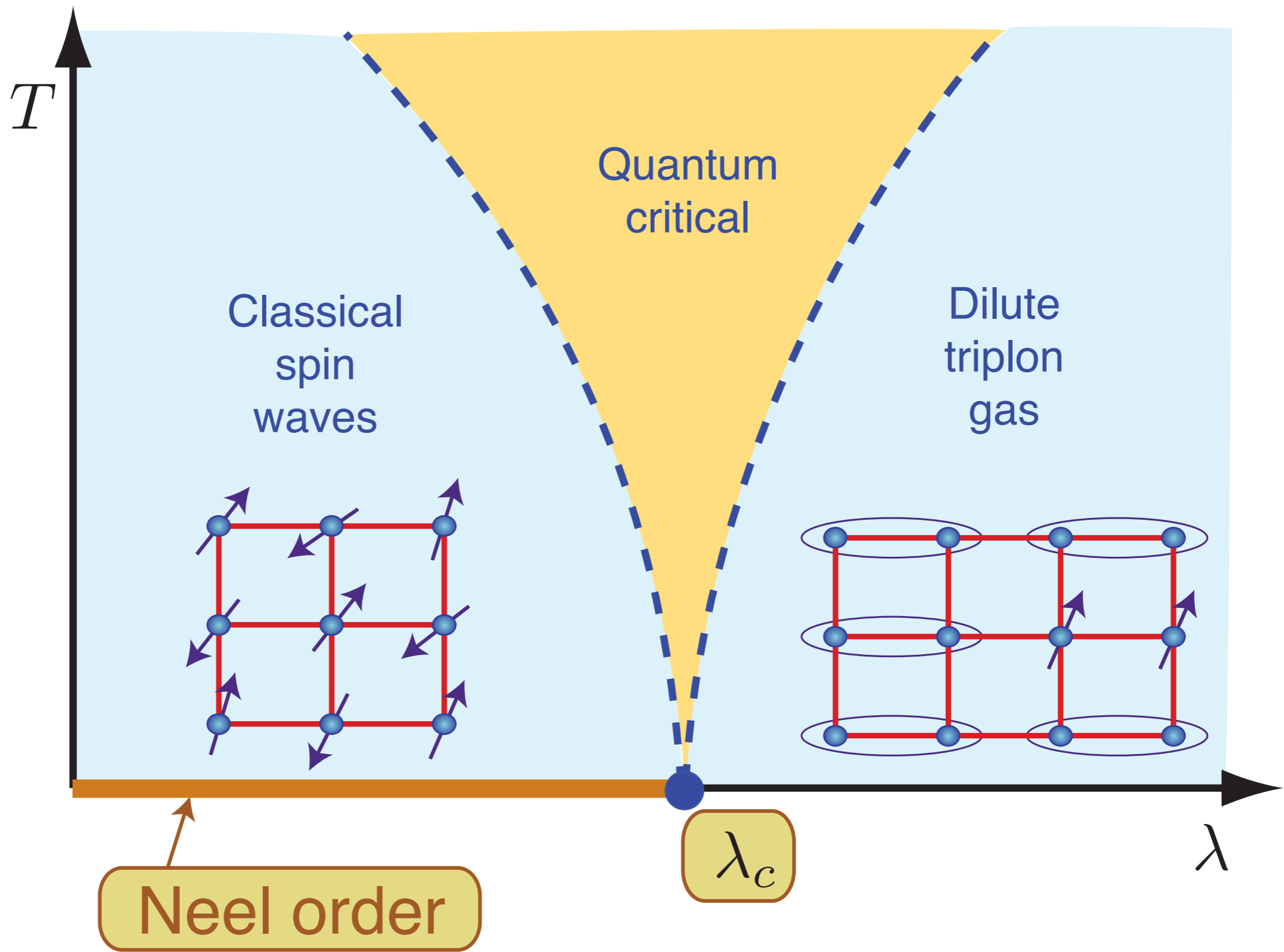
$$= \frac{1}{\sqrt{2}} (|\uparrow\downarrow\rangle - |\downarrow\uparrow\rangle)$$



$O(3)$  order parameter  $\vec{\varphi}$

CFT3

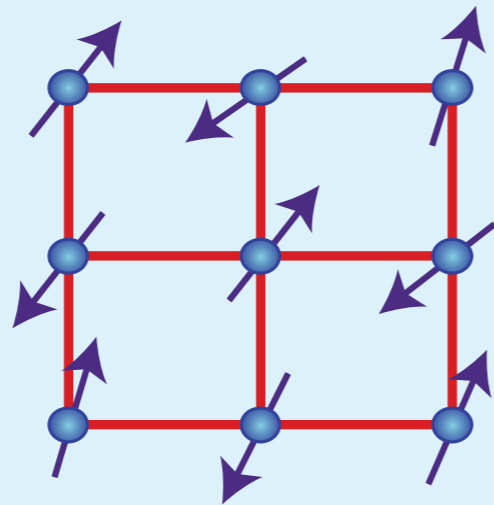
$$\mathcal{S} = \int d^2r d\tau \left[ (\partial_\tau \varphi)^2 + c^2 (\nabla_r \vec{\varphi})^2 + s \vec{\varphi}^2 + u (\vec{\varphi}^2)^2 \right]$$



# Classical dynamics of spin waves

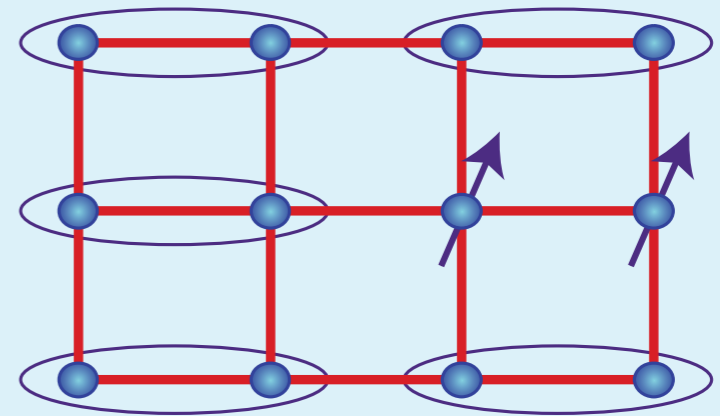
$T$

Classical spin waves



Quantum critical

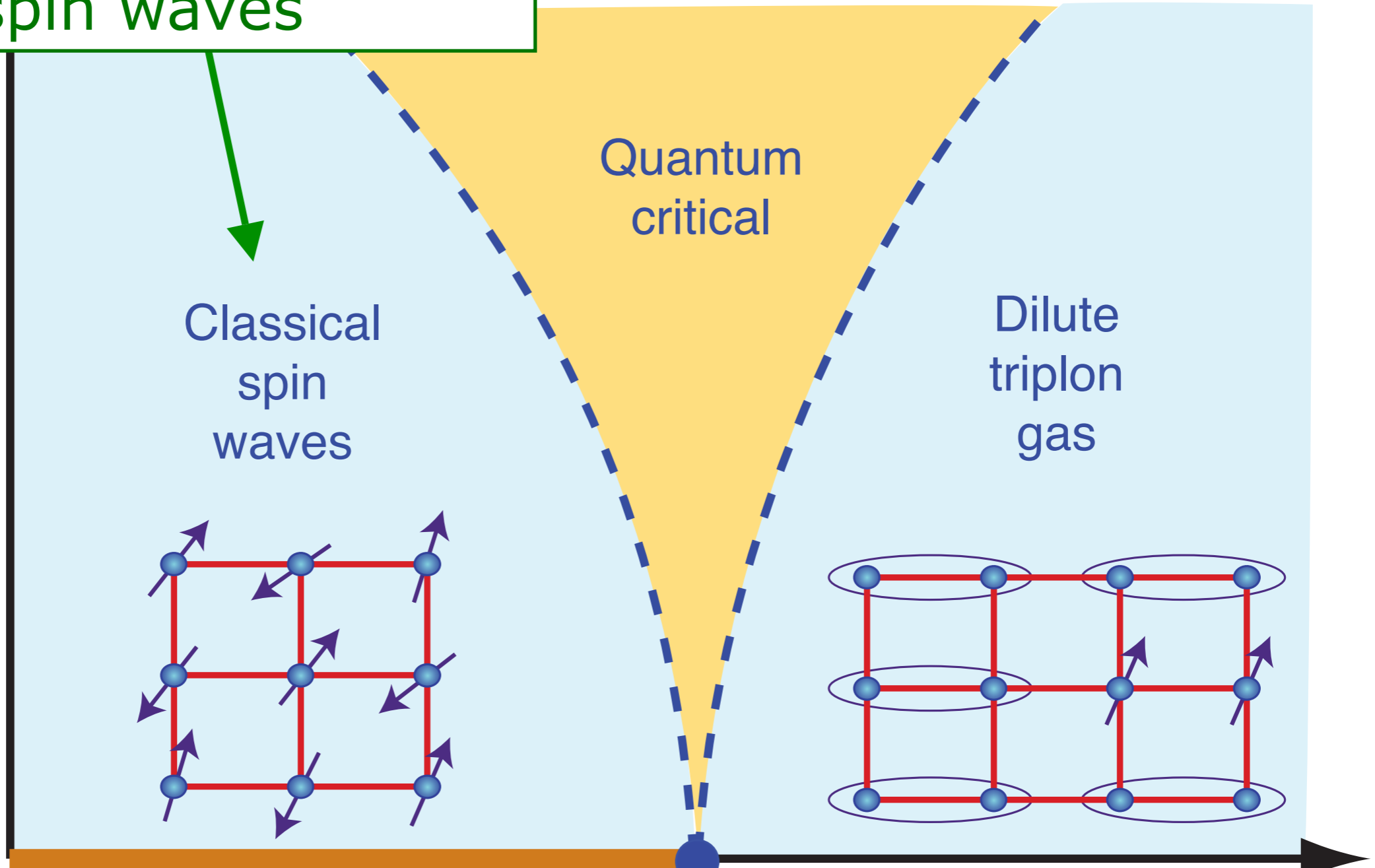
Dilute triplon gas

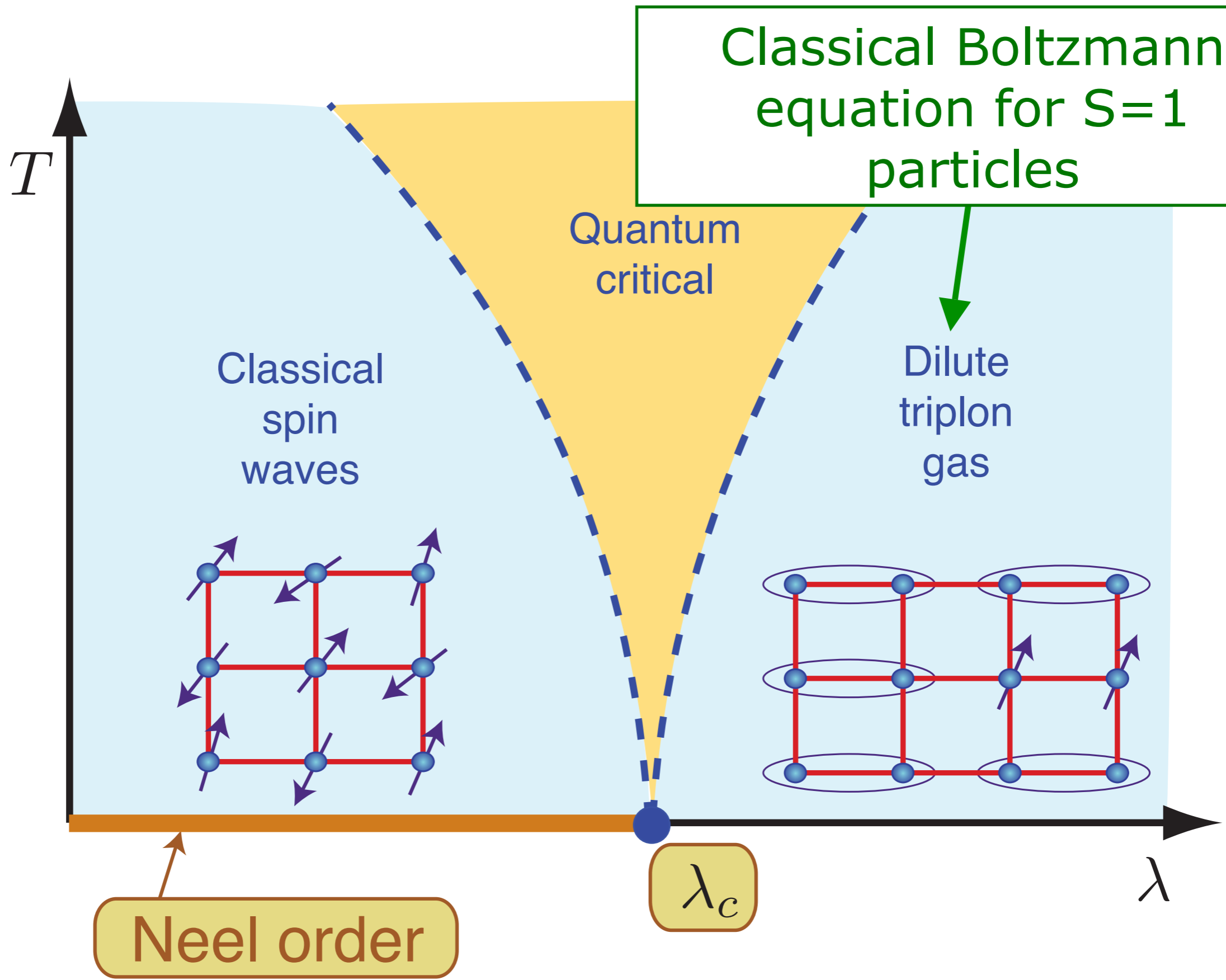


Neel order

$\lambda_c$

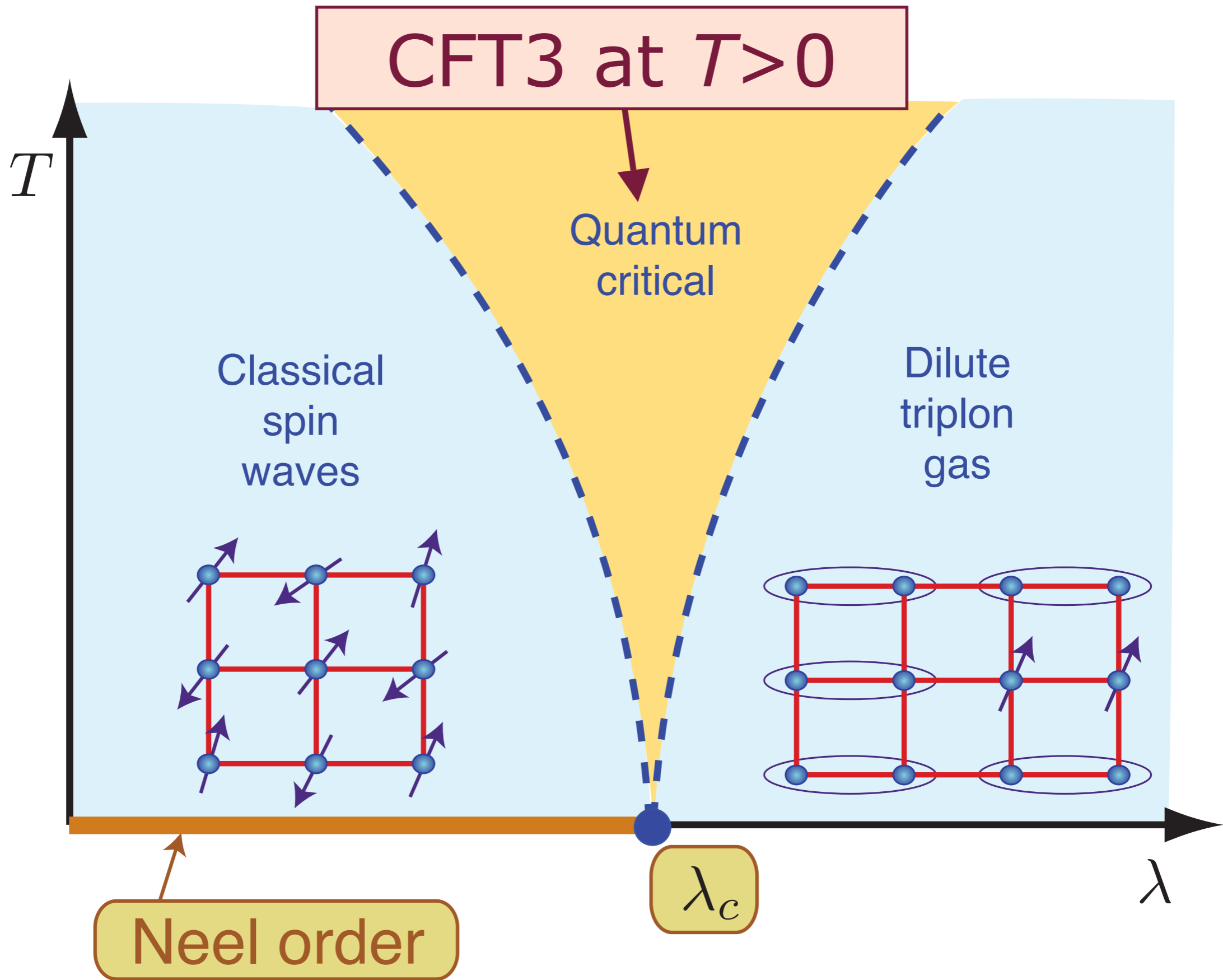
$\lambda$





Neel order

$\lambda_c$



## Outline

# A. “Relativistic” field theories of quantum phase transitions

1. Coupled dimer antiferromagnets
2. Triangular lattice antiferromagnets
3. Graphene
4. AdS/CFT and quantum critical transport

## Outline

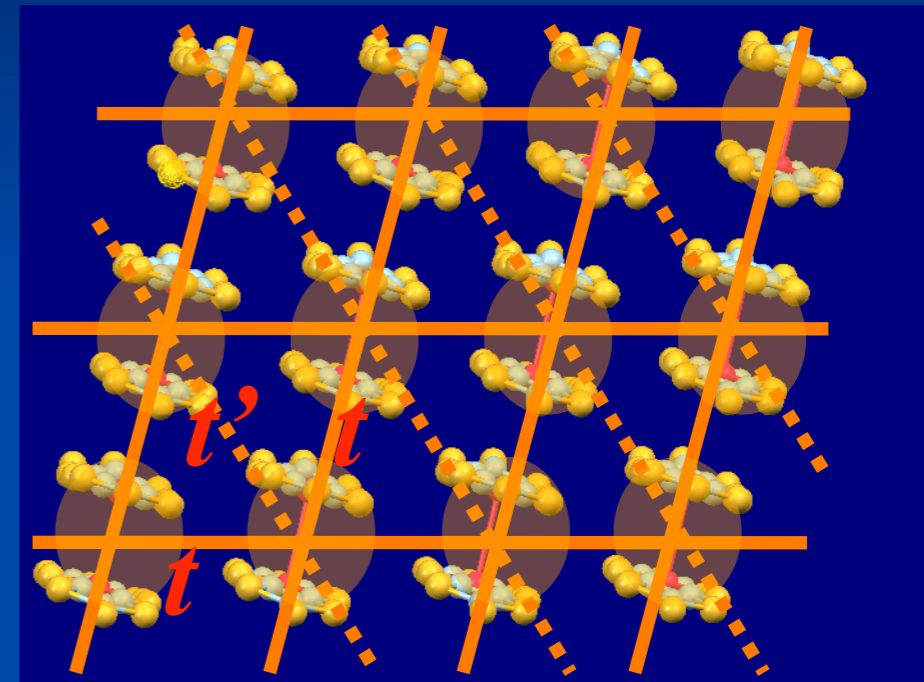
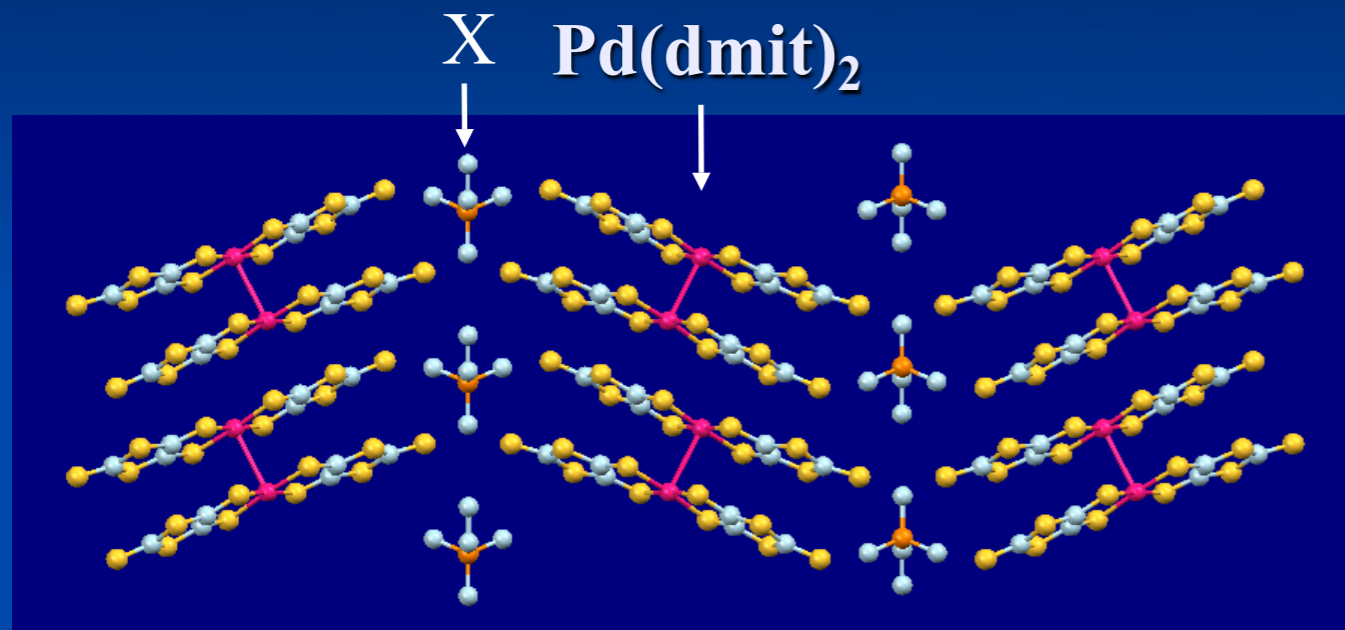
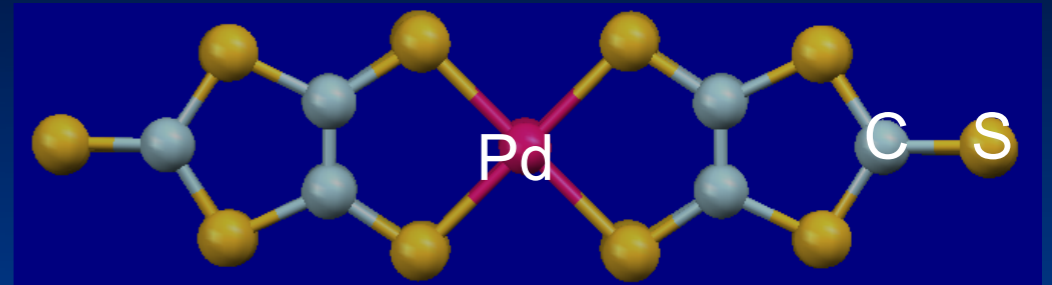
# A. “Relativistic” field theories of quantum phase transitions

1. Coupled dimer antiferromagnets

2. Triangular lattice antiferromagnets

3. Graphene

4. AdS/CFT and quantum critical transport



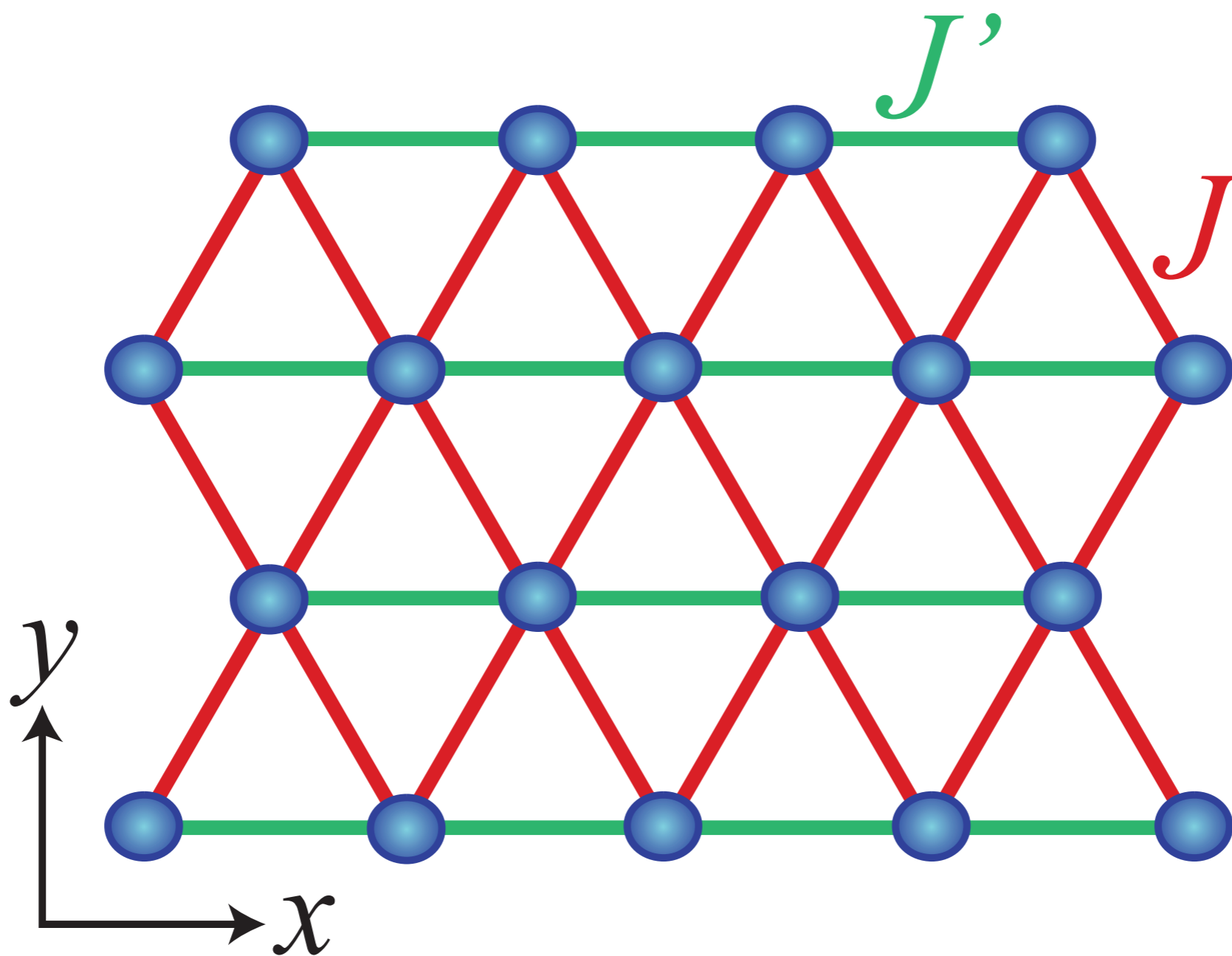
Half-filled band  $\rightarrow$  Mott insulator with spin  $S = 1/2$

Triangular lattice of  $[\text{Pd}(\text{dmit})_2]_2$

$\rightarrow$  frustrated quantum spin system

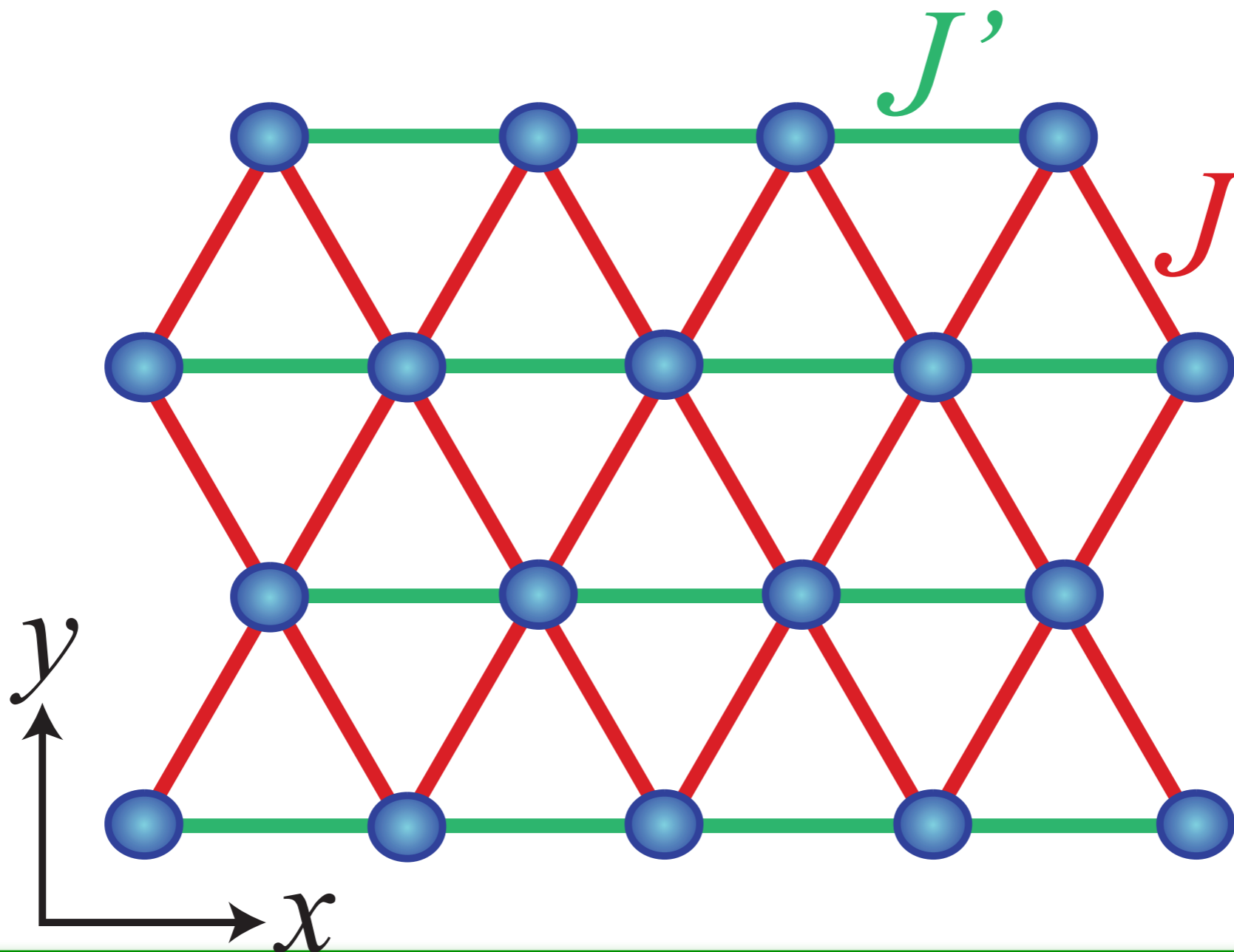
$$H = \sum_{\langle ij \rangle} J_{ij} \vec{S}_i \cdot \vec{S}_j + \dots$$

$\vec{S}_i \Rightarrow$  spin operator with  $S = 1/2$



$$H = \sum_{\langle ij \rangle} J_{ij} \vec{S}_i \cdot \vec{S}_j + \dots$$

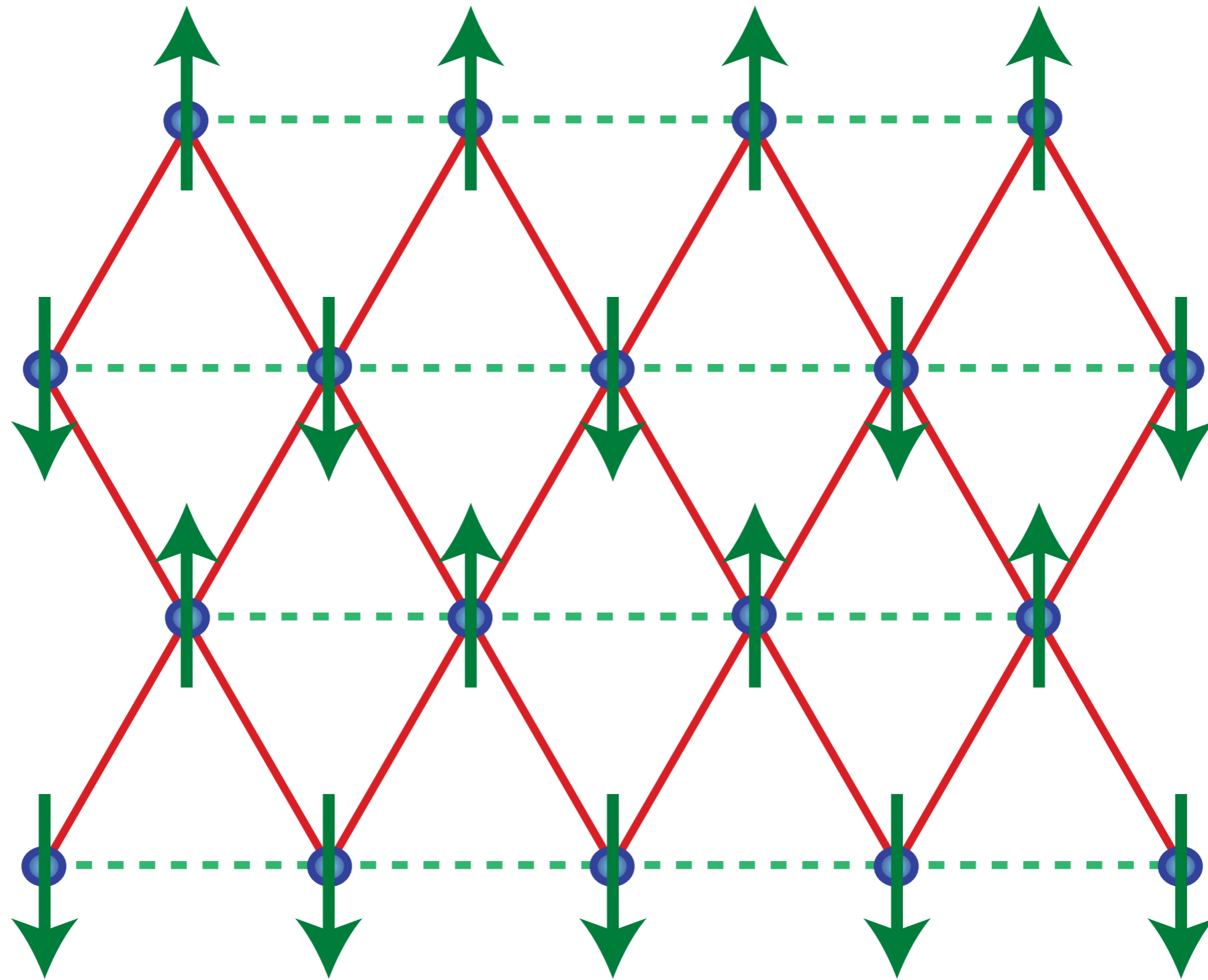
$\vec{S}_i \Rightarrow$  spin operator with  $S = 1/2$



What is the ground state as a function of  $J'/J$  ?

# Anisotropic triangular lattice antiferromagnet

Broken spin rotation symmetry



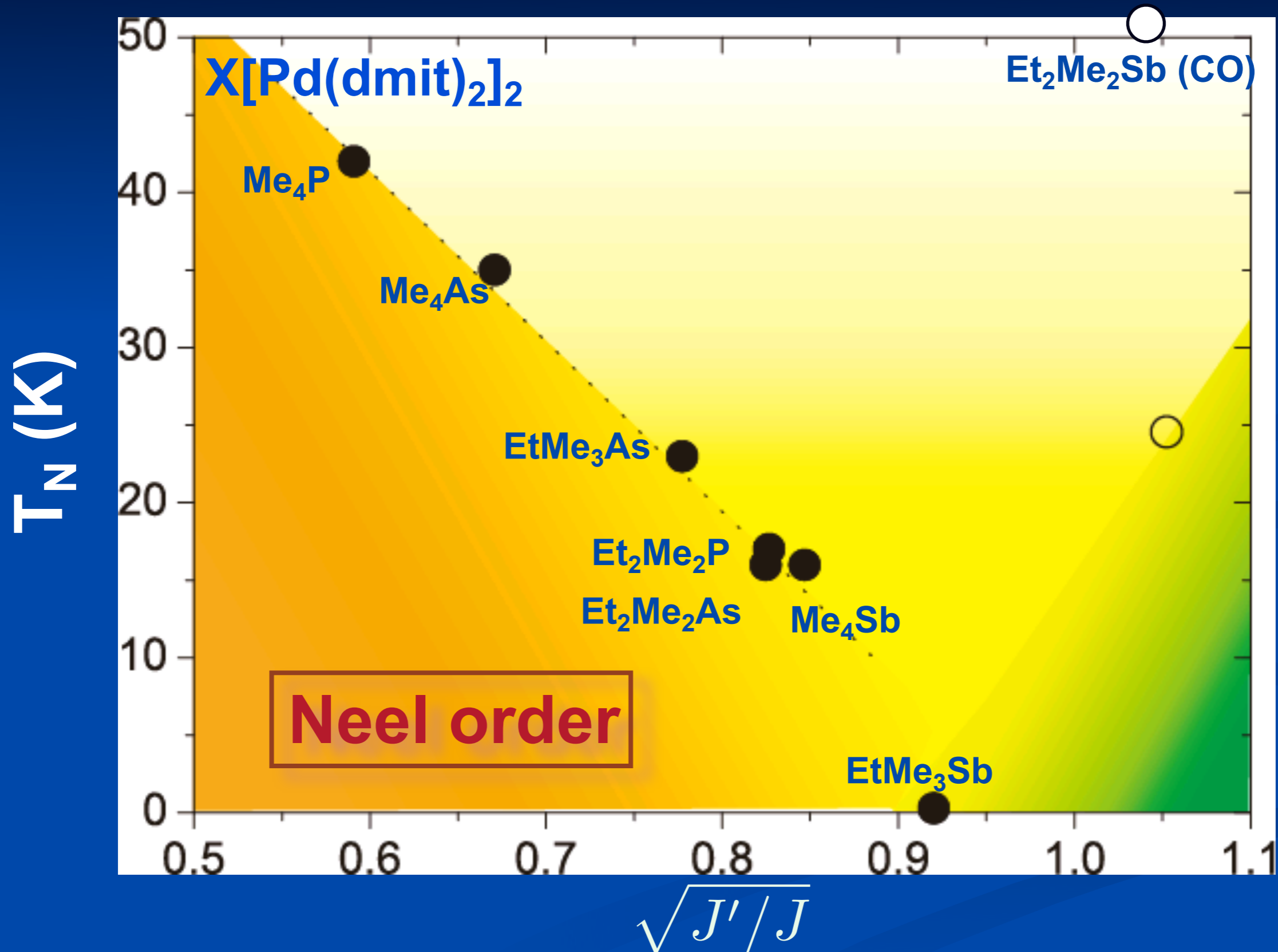
Neel ground state for small  $J'/J$

## Anisotropic triangular lattice antiferromagnet

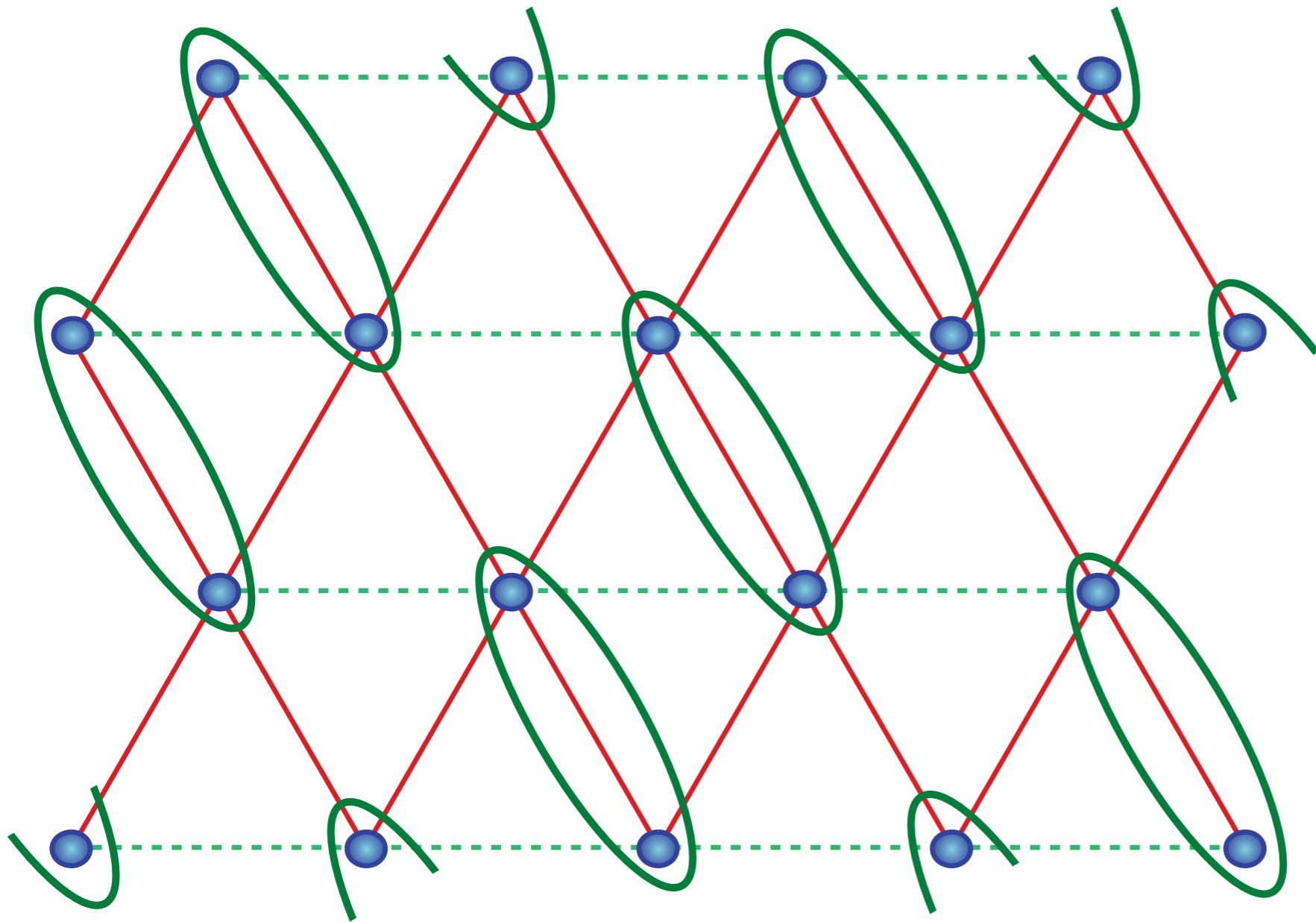
Possible ground states as a function of  $J'/J$

- Néel antiferromagnetic LRO

# Magnetic Criticality



# Anisotropic triangular lattice antiferromagnet

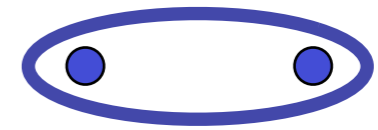
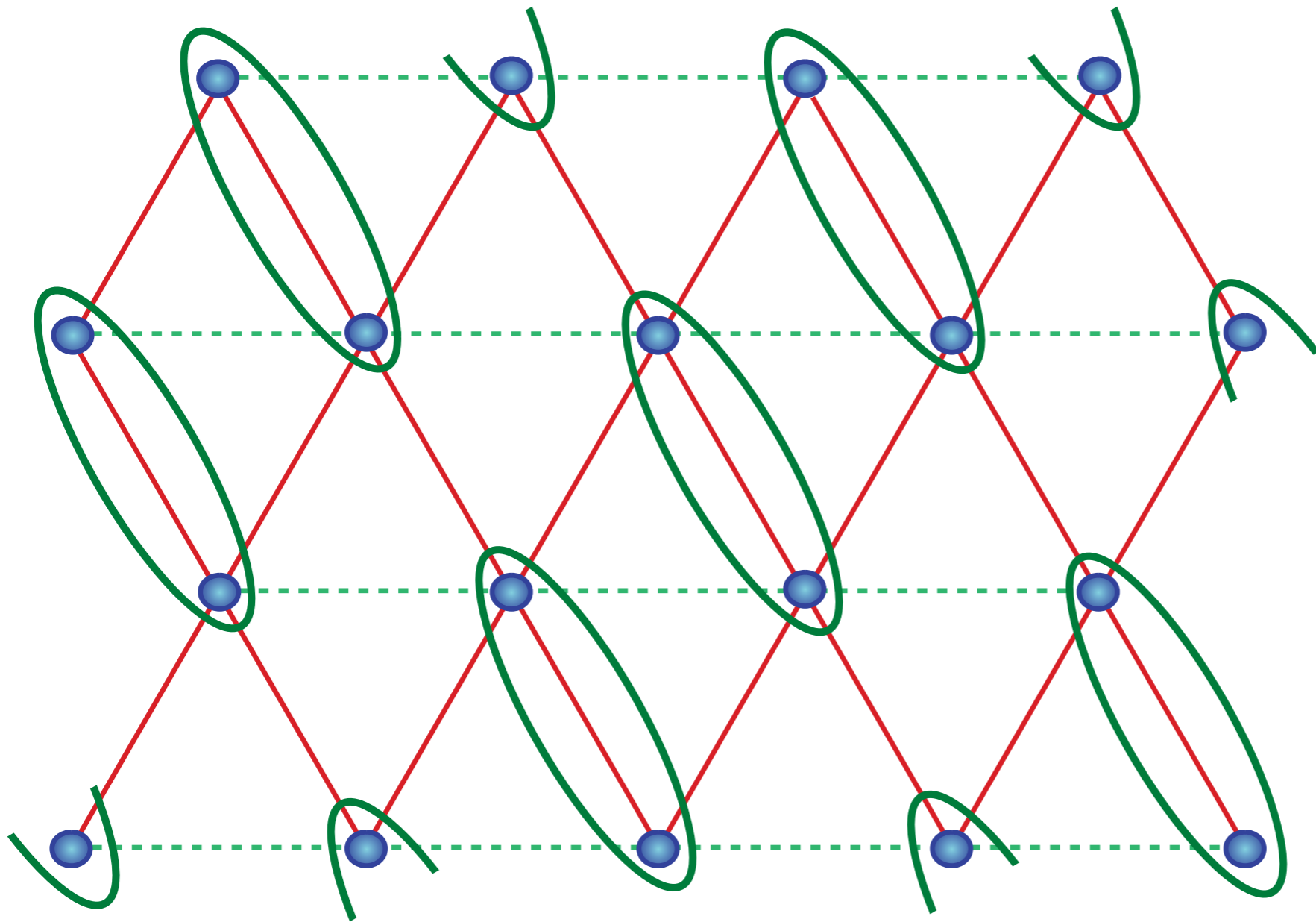


$$\begin{array}{l} \text{Diagram of two spheres in an oval} \\ = \frac{(|\uparrow\downarrow\rangle - |\downarrow\uparrow\rangle)}{\sqrt{2}} \end{array}$$

Possible ground state for intermediate  $J'/J$

# Anisotropic triangular lattice antiferromagnet

Broken lattice space group symmetry



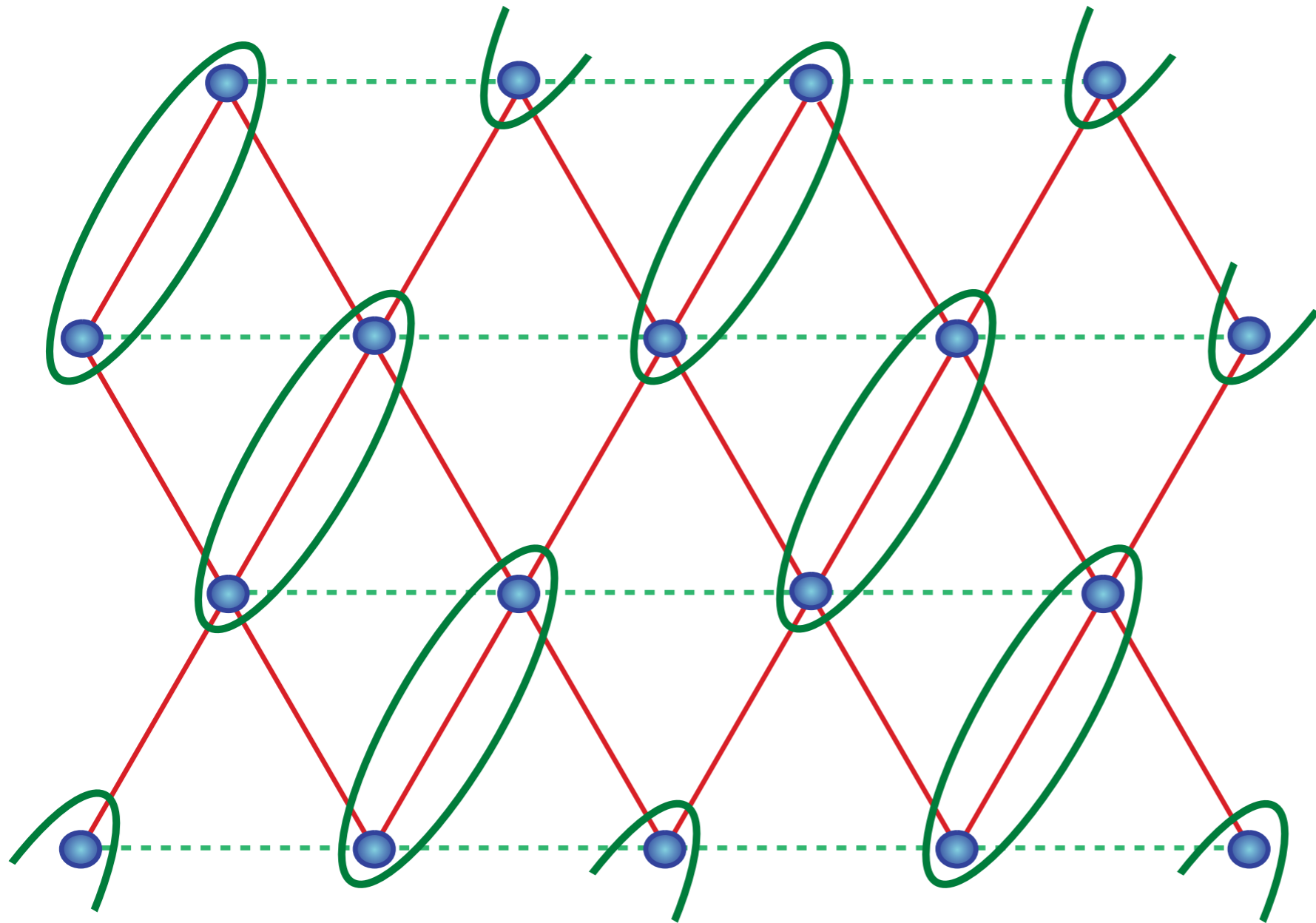
$$= \frac{(|\uparrow\downarrow\rangle - |\downarrow\uparrow\rangle)}{\sqrt{2}}$$

## Valence bond solid (VBS)

Possible ground state for intermediate  $J'/J$

# Anisotropic triangular lattice antiferromagnet

Broken lattice space group symmetry



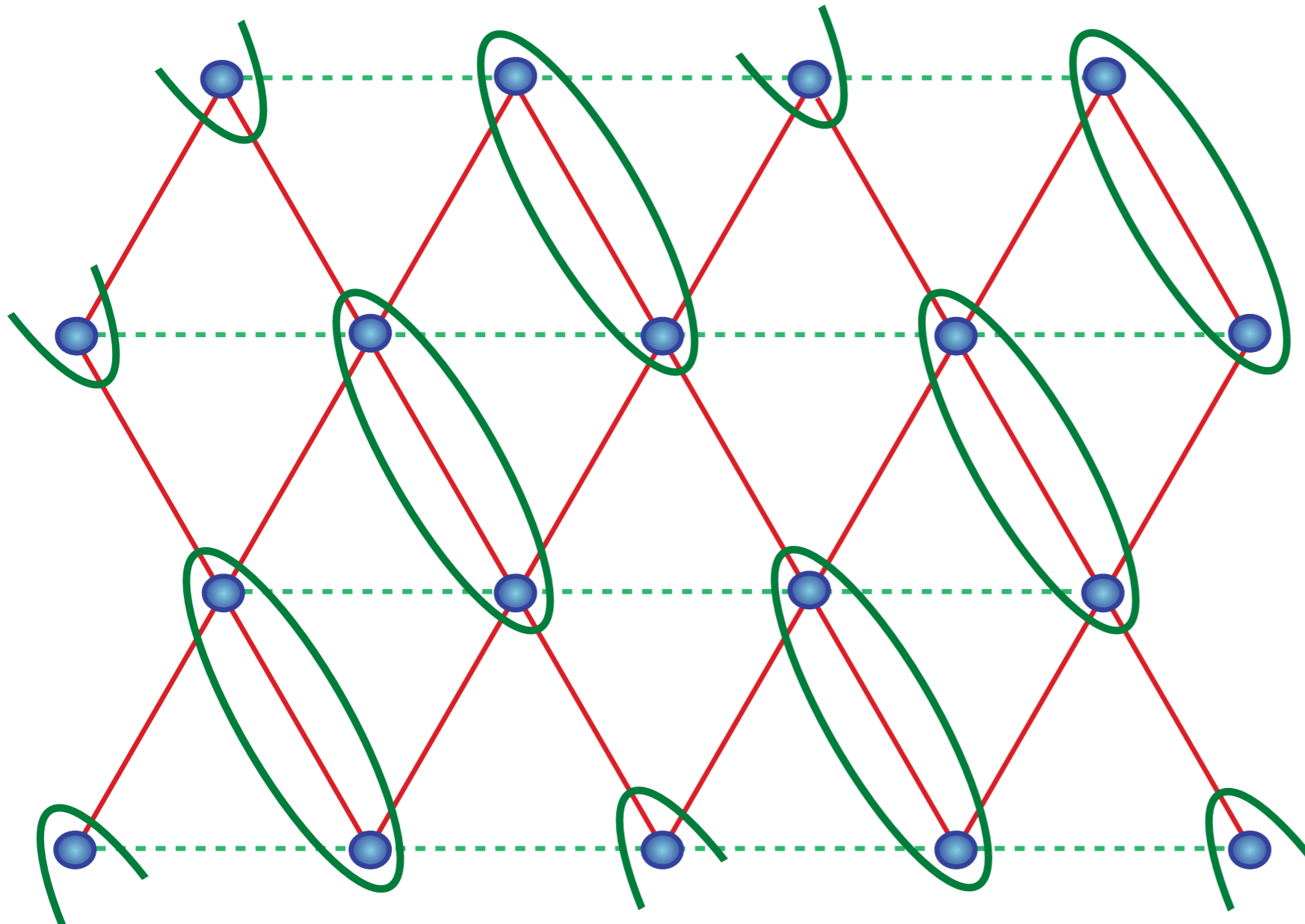
$$= \frac{(|\uparrow\downarrow\rangle - |\downarrow\uparrow\rangle)}{\sqrt{2}}$$

## Valence bond solid (VBS)

Possible ground state for intermediate  $J'/J$

# Anisotropic triangular lattice antiferromagnet

Broken lattice space group symmetry



$$\begin{array}{c} \text{Diagram of two atoms in a dimer} \\ = \frac{(|\uparrow\downarrow\rangle - |\downarrow\uparrow\rangle)}{\sqrt{2}} \end{array}$$

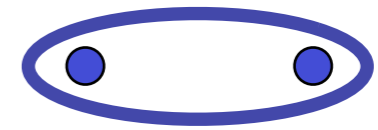
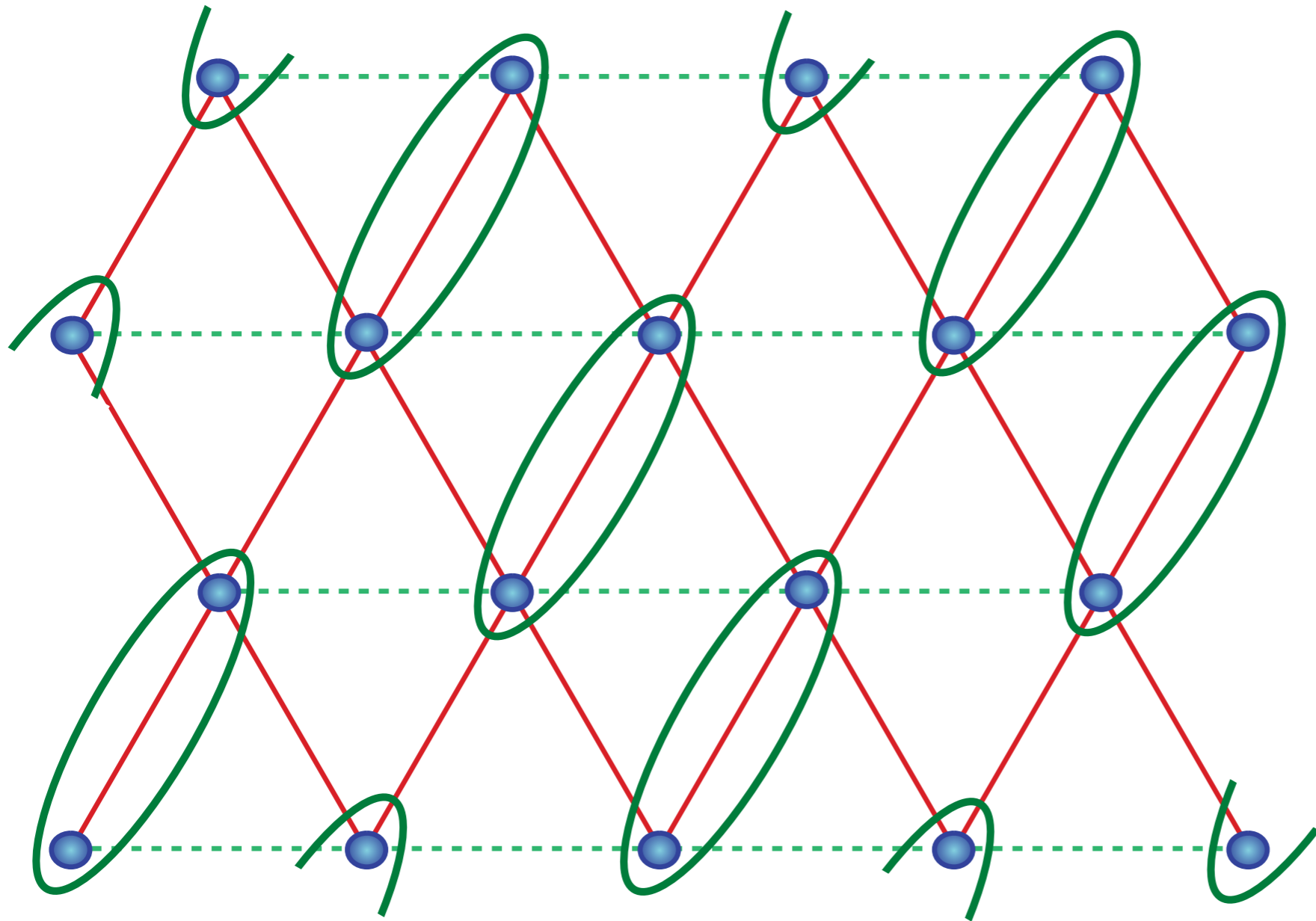


## Valence bond solid (VBS)

Possible ground state for intermediate  $J'/J$

# Anisotropic triangular lattice antiferromagnet

Broken lattice space group symmetry



$$= \frac{(|\uparrow\downarrow\rangle - |\downarrow\uparrow\rangle)}{\sqrt{2}}$$



## Valence bond solid (VBS)

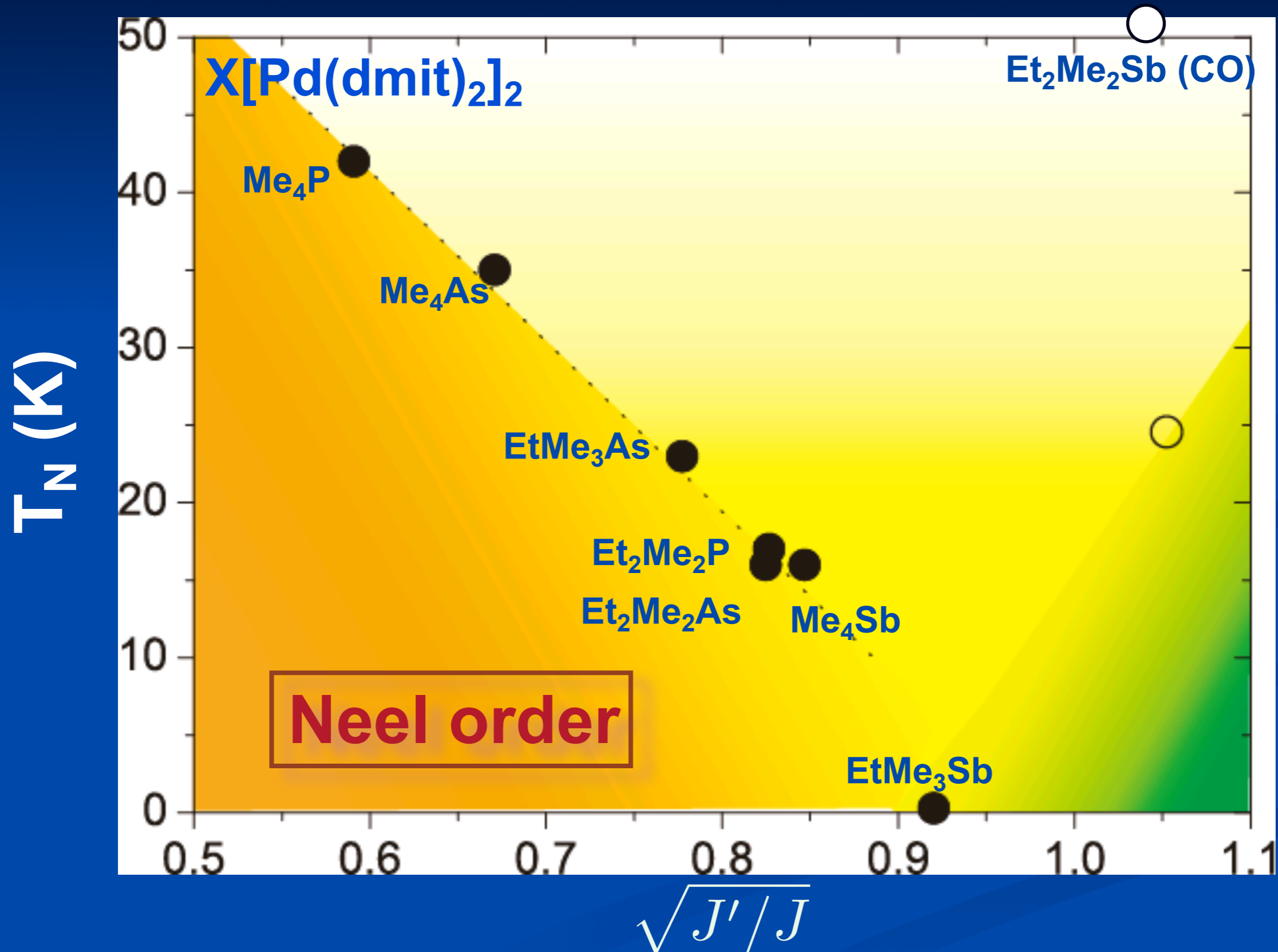
Possible ground state for intermediate  $J'/J$

## Anisotropic triangular lattice antiferromagnet

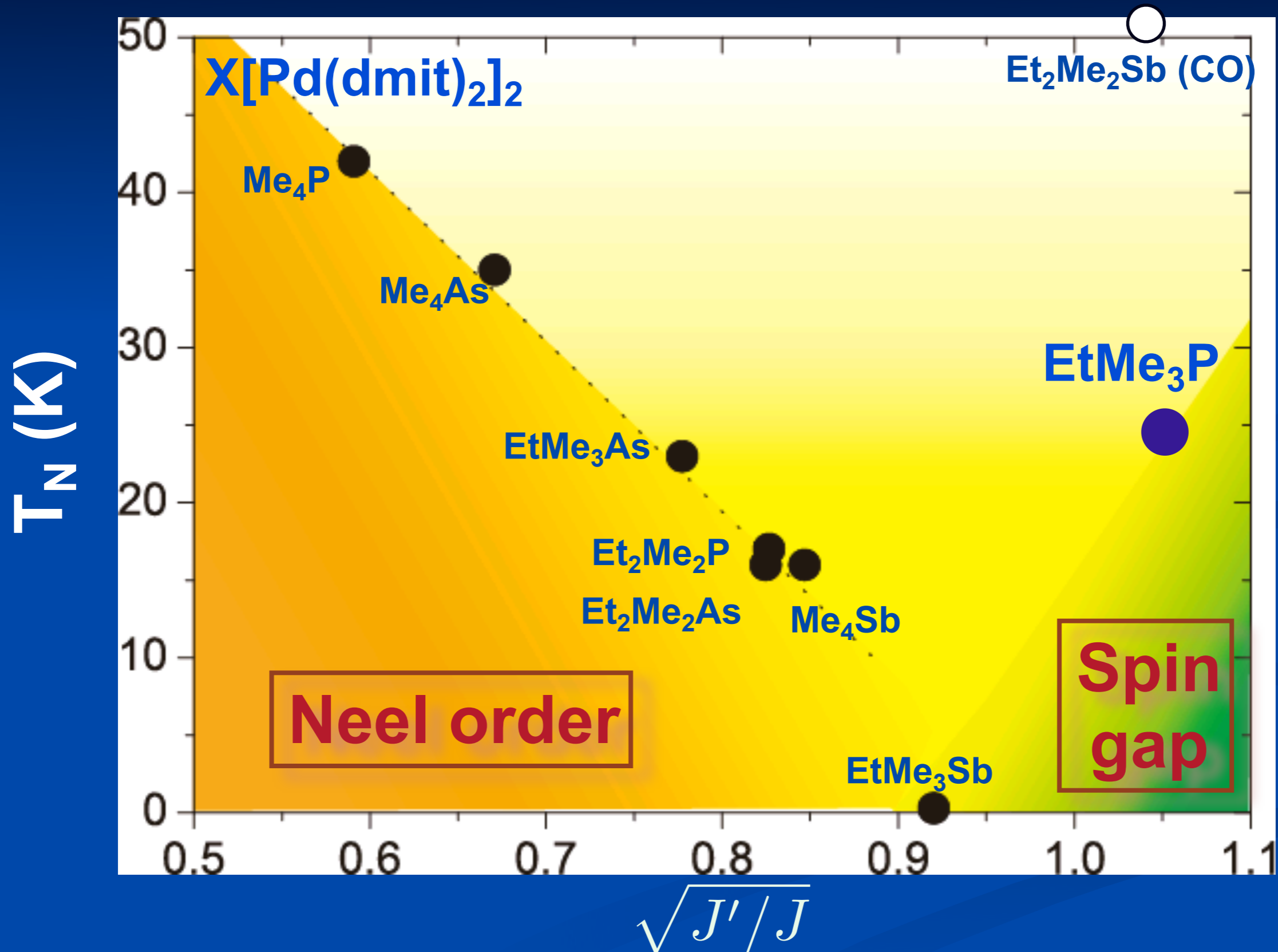
Possible ground states as a function of  $J'/J$

- Néel antiferromagnetic LRO
- Valence bond solid

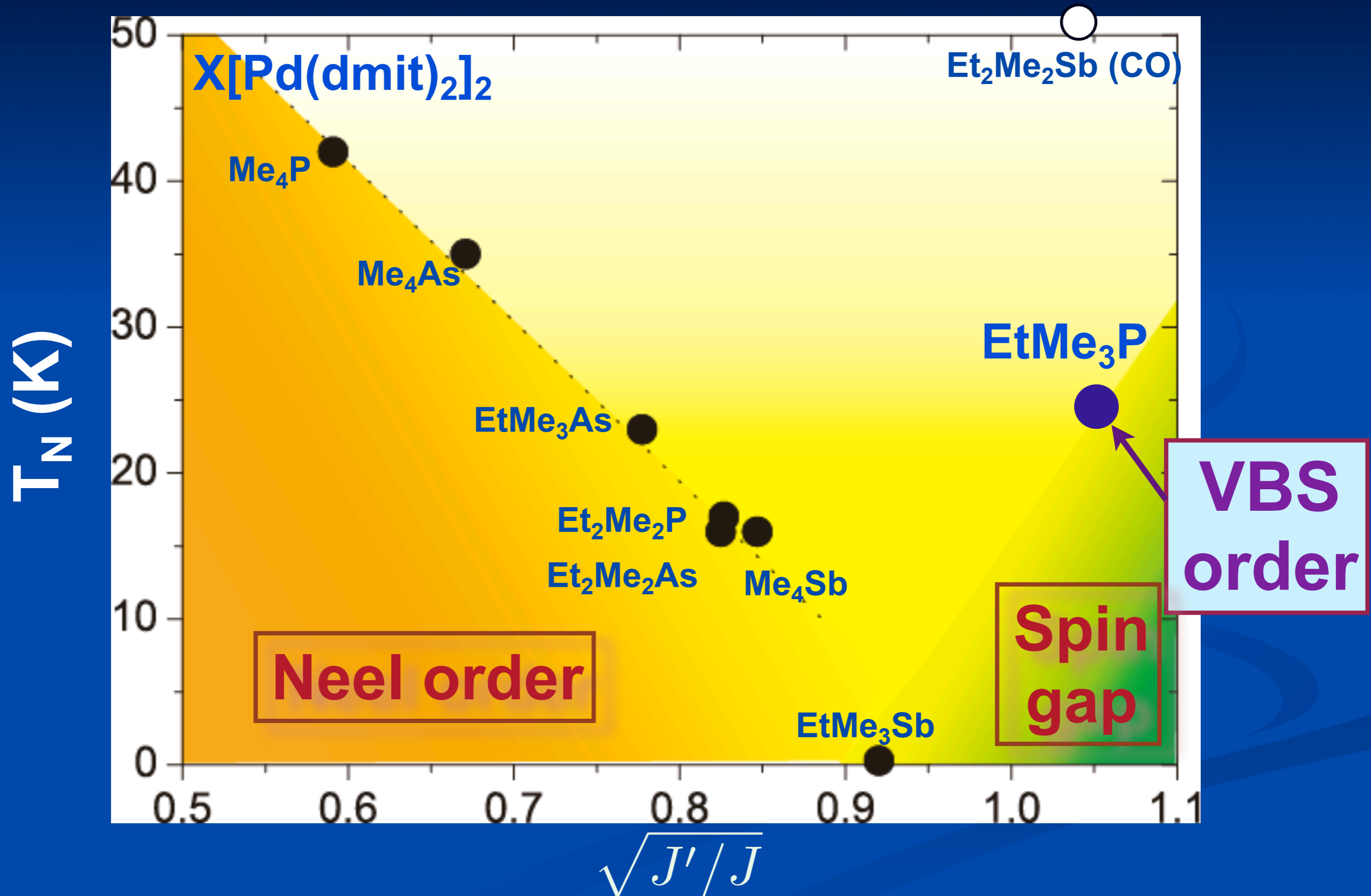
# Magnetic Criticality



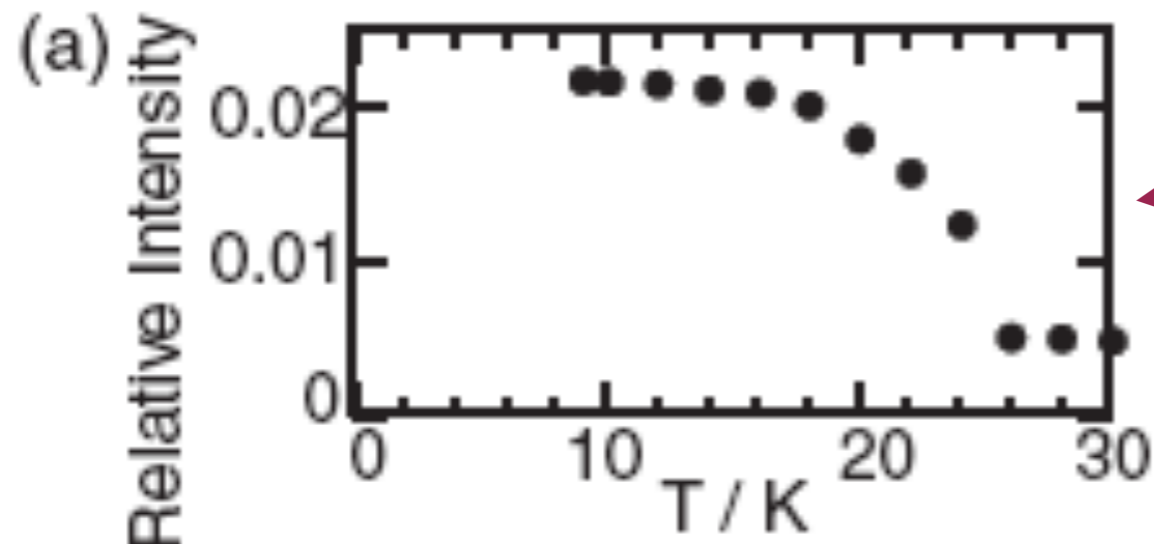
# Magnetic Criticality



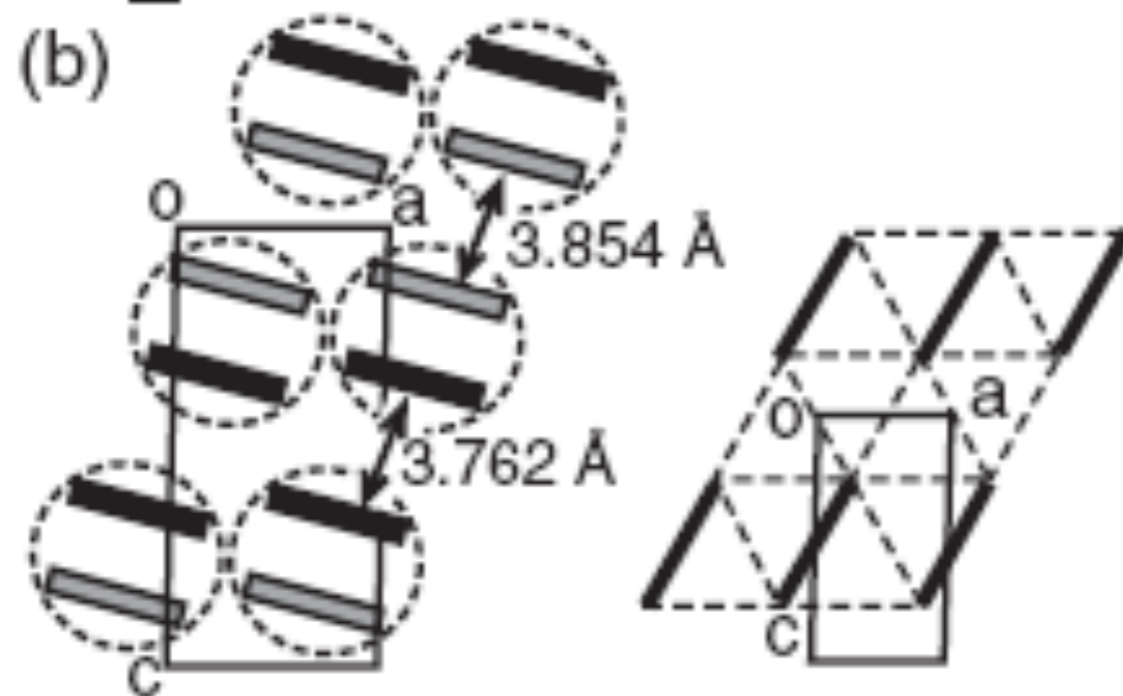
# Magnetic Criticality



# Observation of a valence bond solid (VBS) in $\text{ETMe}_3\text{P}[\text{Pd}(\text{dmit})_2]_2$



X-ray scattering

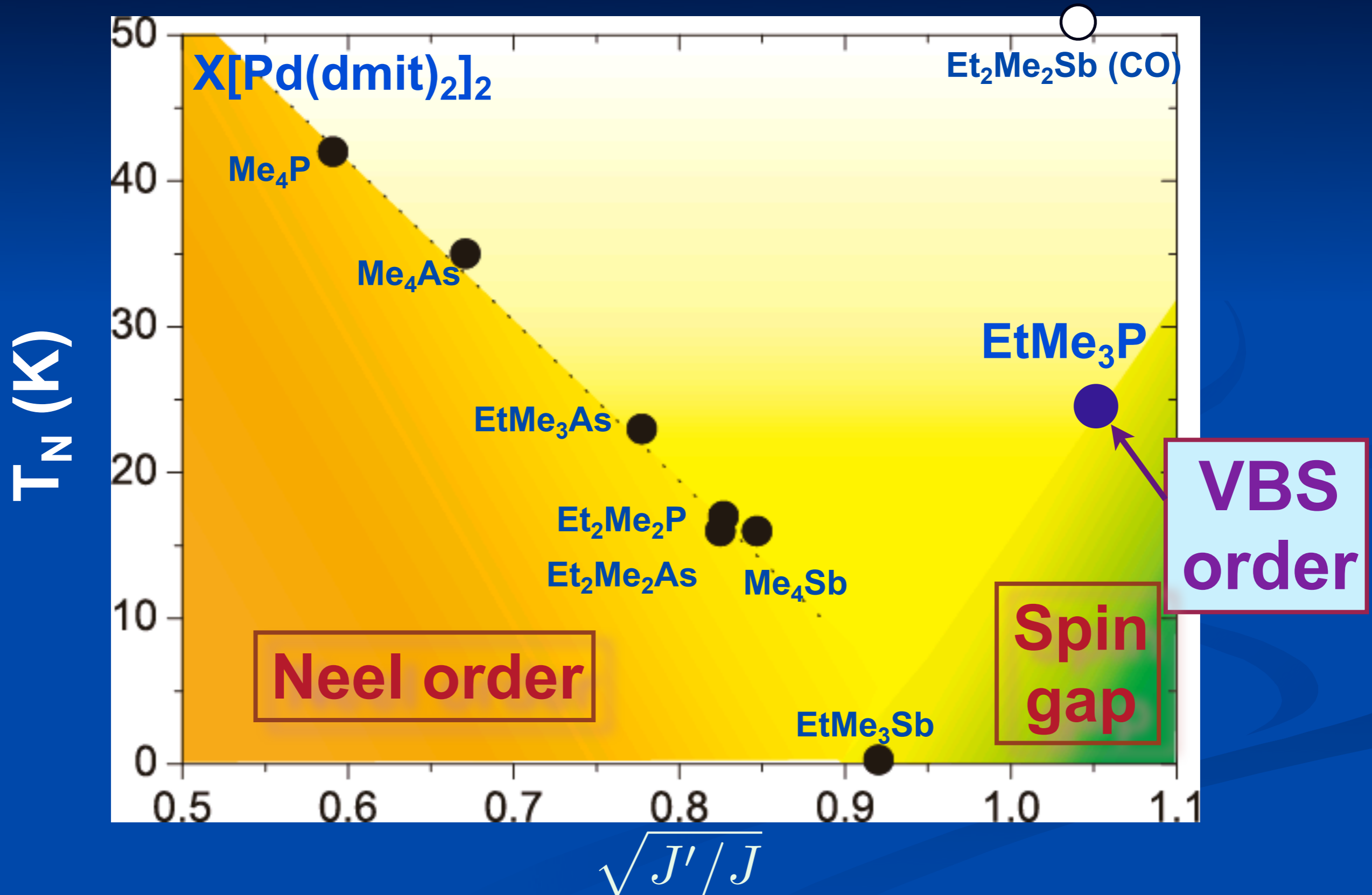


Spin gap  $\sim 40$  K  
 $J \sim 250$  K

M. Tamura, A. Nakao and R. Kato, *J. Phys. Soc. Japan* **75**, 093701 (2006)

Y. Shimizu, H. Akimoto, H. Tsujii, A. Tajima, and R. Kato, *Phys. Rev. Lett.* **99**, 256403 (2007)

# Magnetic Criticality

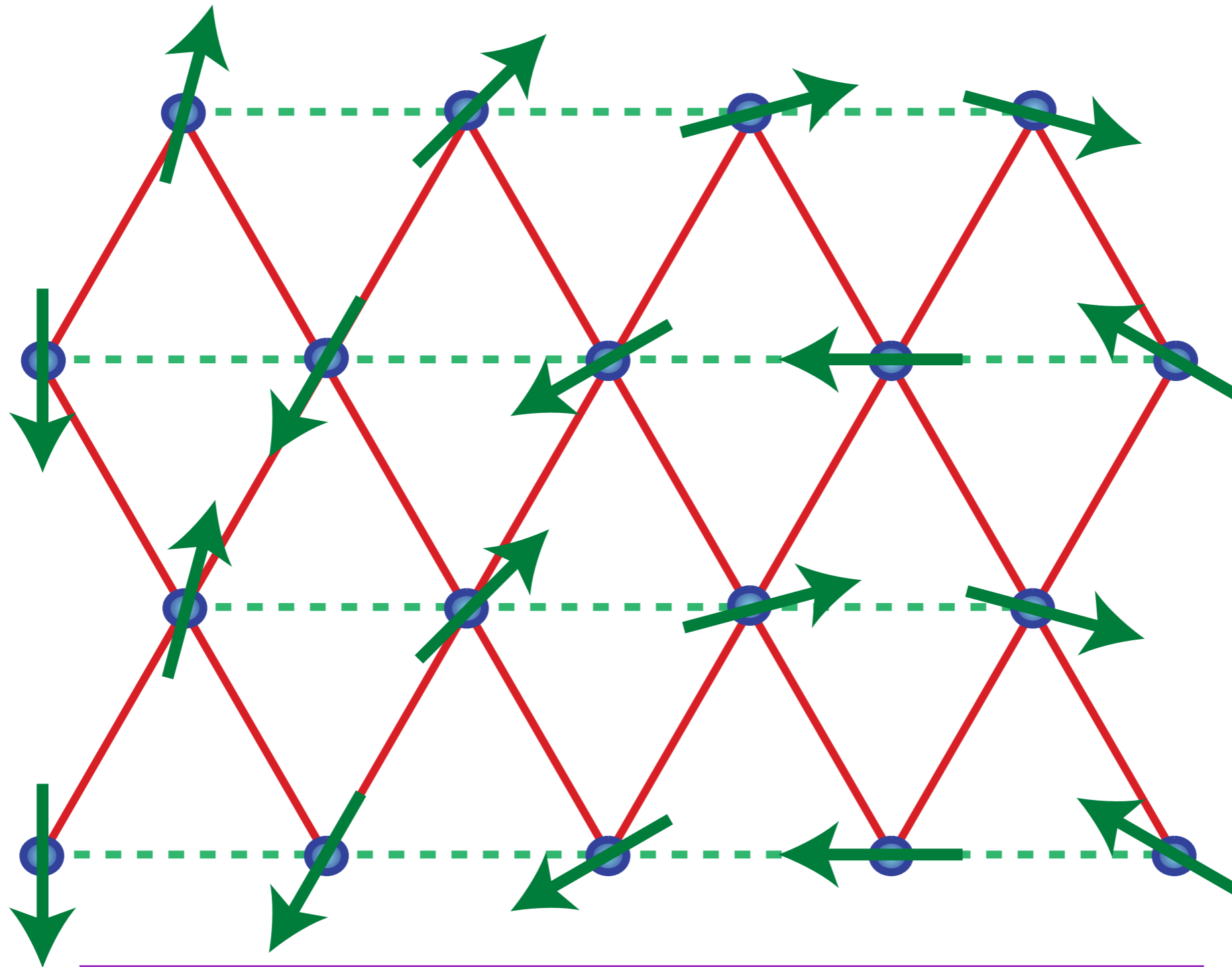


## Anisotropic triangular lattice antiferromagnet

Possible ground states as a function of  $J'/J$

- Néel antiferromagnetic LRO
- Valence bond solid

# Anisotropic triangular lattice antiferromagnet



Classical ground state for large  $J'/J$

Found in  $\text{Cs}_2\text{CuCl}_4$

## Anisotropic triangular lattice antiferromagnet

Possible ground states as a function of  $J'/J$

- Néel antiferromagnetic LRO
- Valence bond solid
- Spiral LRO

## Anisotropic triangular lattice antiferromagnet

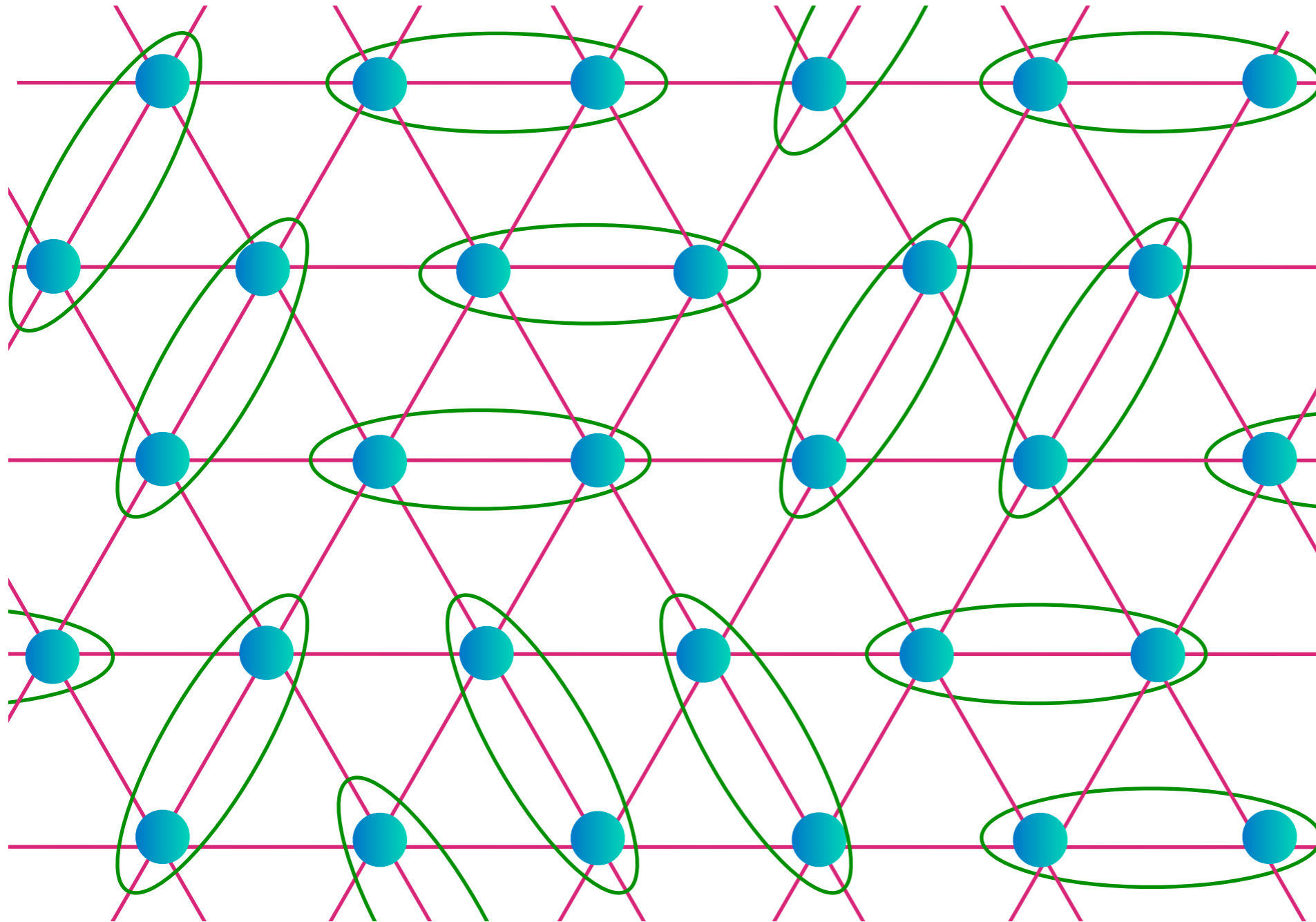
### Possible ground states as a function of $J'/J$

- Néel antiferromagnetic LRO
- Valence bond solid
- Spiral LRO
- $Z_2$  spin liquid: preserves all symmetries of Hamiltonian

# Triangular lattice antiferromagnet

Spin liquid obtained in a generalized spin model with  $S=1/2$  per unit cell

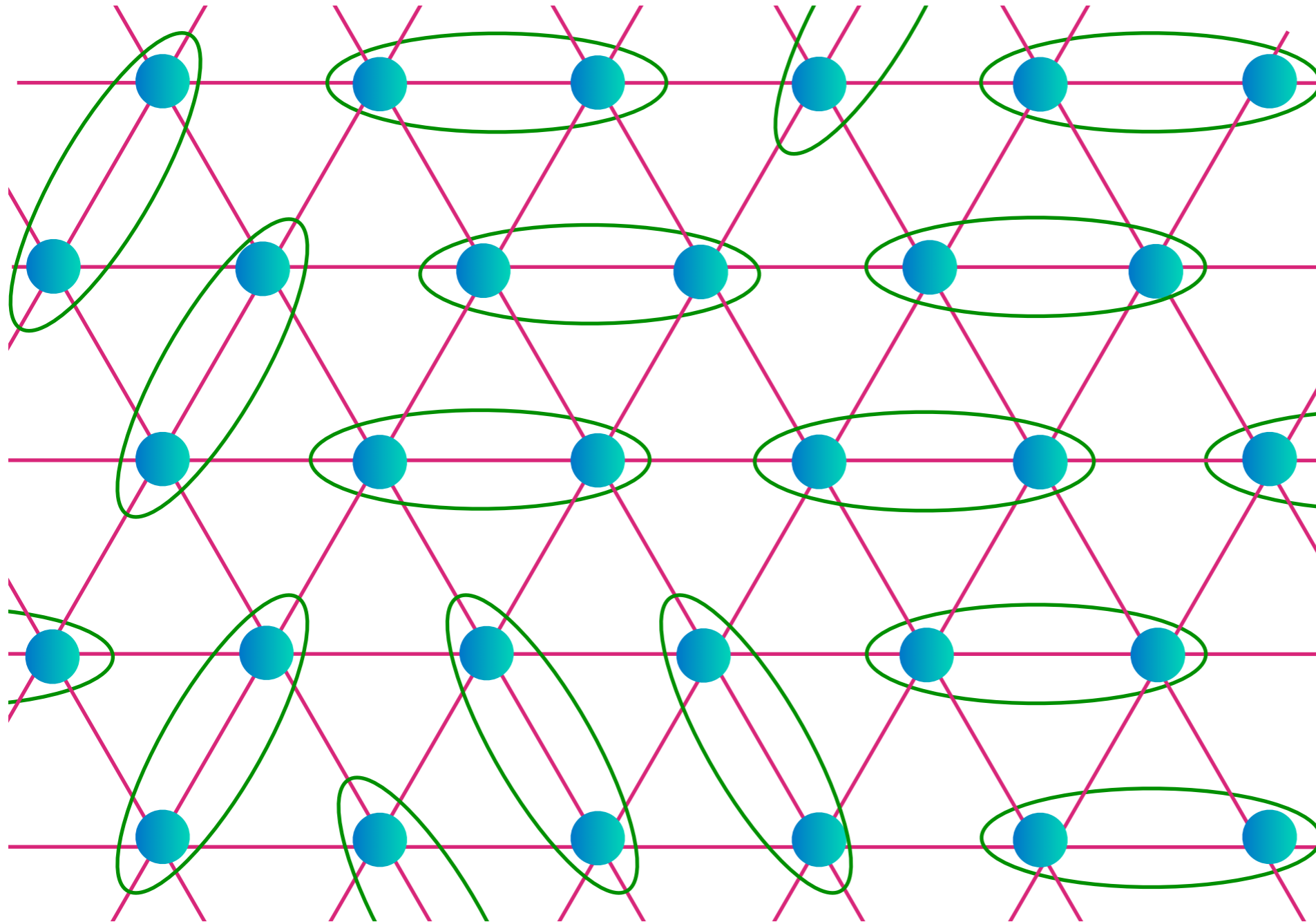
$$\begin{array}{c} \text{---} \circ \text{---} \circ \text{---} \\ \text{---} \end{array} = \frac{1}{\sqrt{2}} (|\uparrow\downarrow\rangle - |\downarrow\uparrow\rangle)$$



# Triangular lattice antiferromagnet

Spin liquid obtained in a generalized spin model with  $S=1/2$  per unit cell

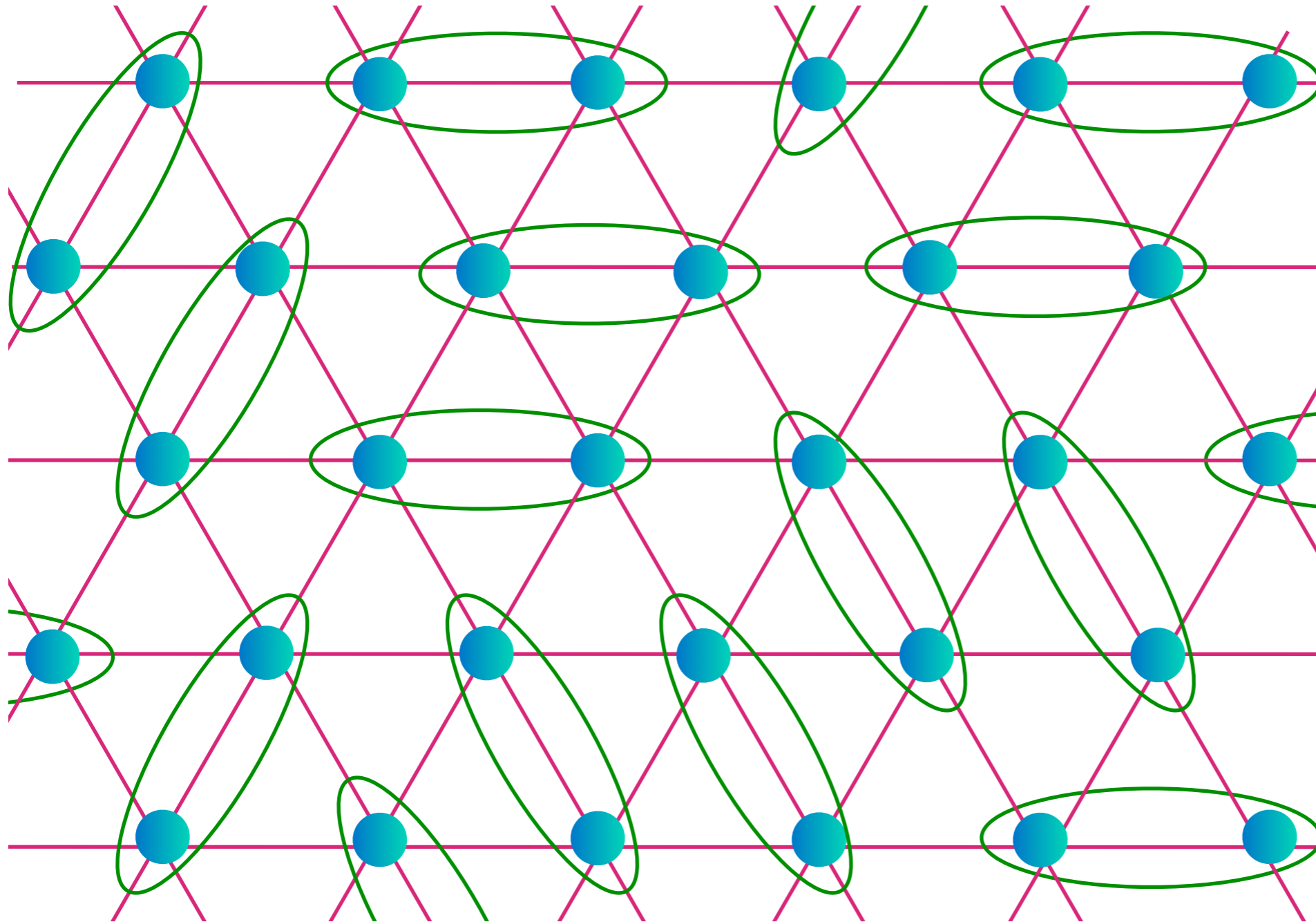
$$\begin{array}{c} \text{---} \circ \text{---} \circ \text{---} \\ \text{---} \end{array} = \frac{1}{\sqrt{2}} (|\uparrow\downarrow\rangle - |\downarrow\uparrow\rangle)$$



# Triangular lattice antiferromagnet

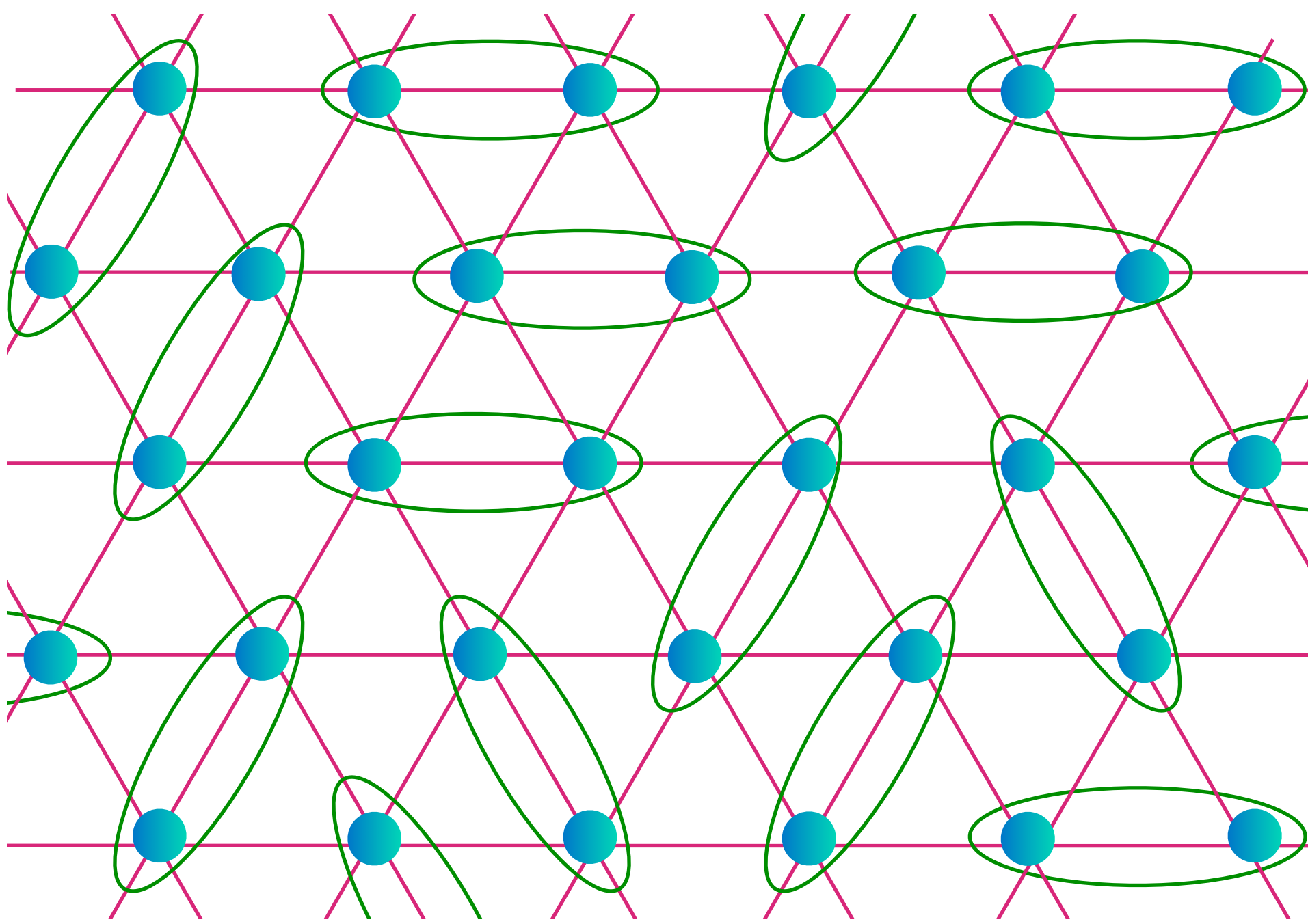
Spin liquid obtained in a generalized spin model with  $S=1/2$  per unit cell

$$\begin{array}{c} \text{---} \circ \text{---} \circ \text{---} \\ \text{---} \end{array} = \frac{1}{\sqrt{2}} (|\uparrow\downarrow\rangle - |\downarrow\uparrow\rangle)$$



# Triangular lattice antiferromagnet

Spin liquid obtained in a generalized spin model with  $S=1/2$  per unit cell



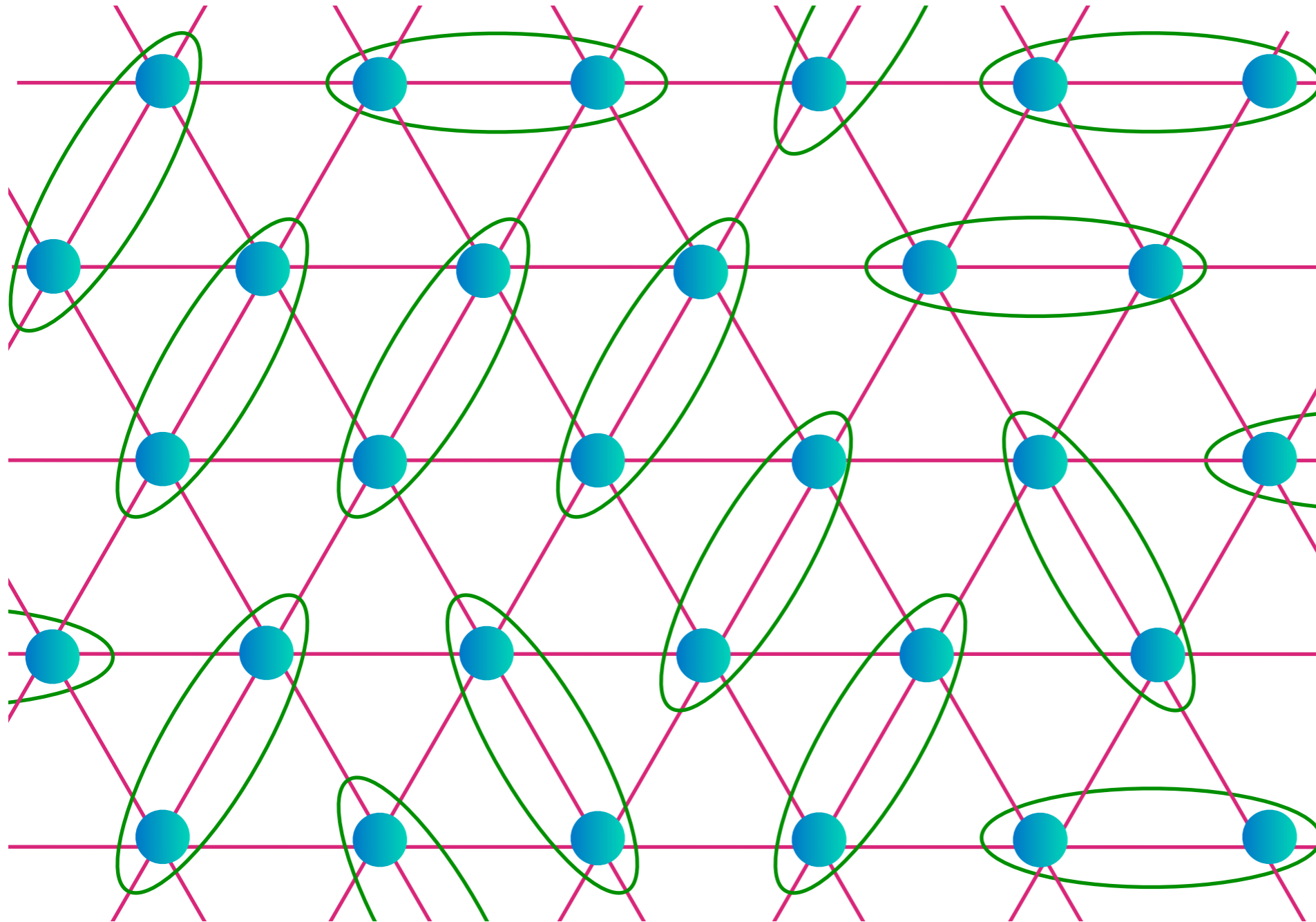
The diagram shows a triangular lattice of blue spheres (sites) connected by magenta lines. Green ovals are drawn around pairs of sites, illustrating the spin liquid state. The ovals are arranged in a pattern that covers the lattice, with some overlapping and some not. The ovals are oriented in various directions, showing the non-trivial nature of the spin liquid state.

$$= \frac{1}{\sqrt{2}} (|\uparrow\downarrow\rangle - |\downarrow\uparrow\rangle)$$

# Triangular lattice antiferromagnet

Spin liquid obtained in a generalized spin model with  $S=1/2$  per unit cell

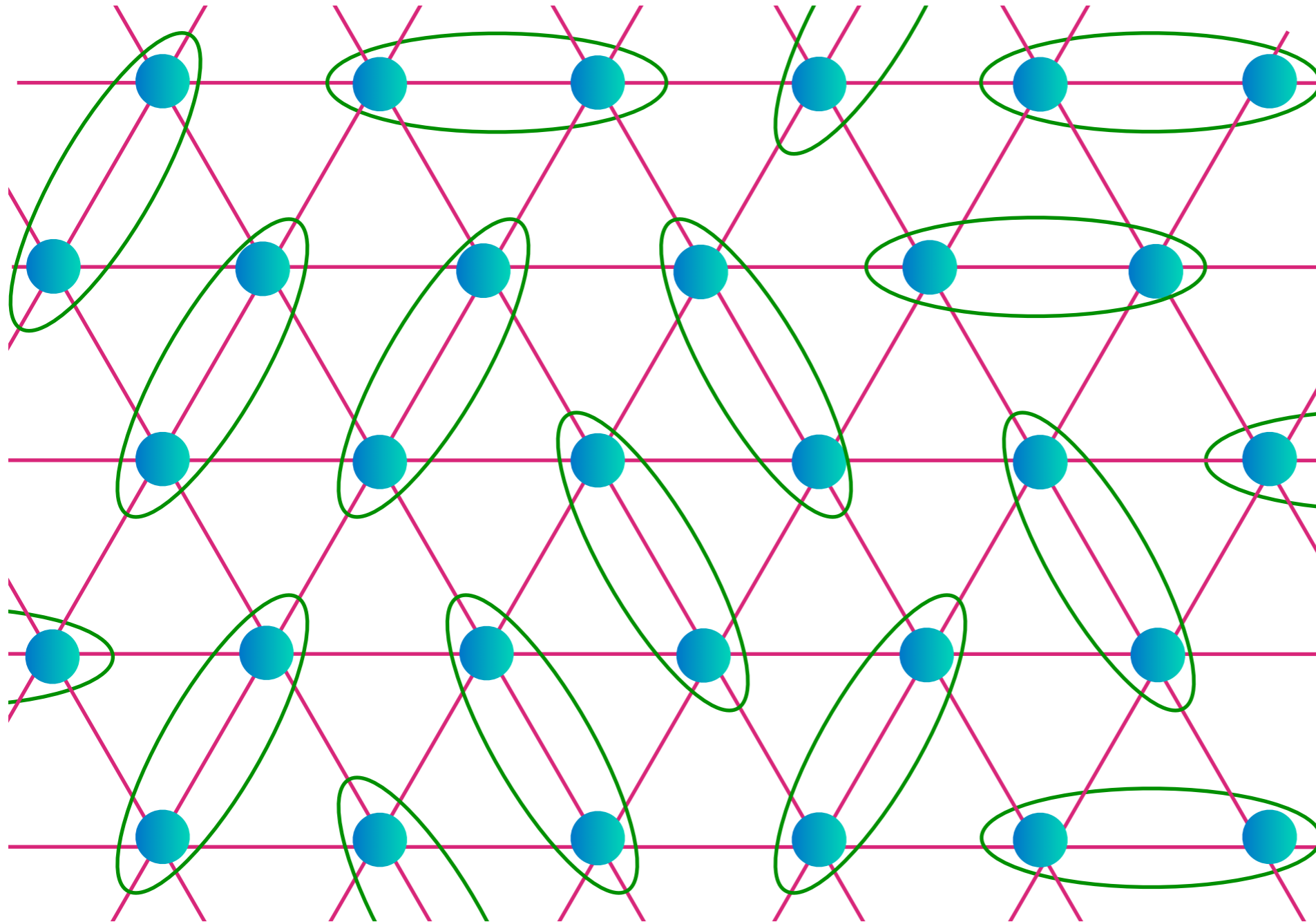
$$\begin{array}{c} \text{---} \circ \text{---} \circ \text{---} \\ \text{---} \end{array} = \frac{1}{\sqrt{2}} (|\uparrow\downarrow\rangle - |\downarrow\uparrow\rangle)$$



# Triangular lattice antiferromagnet

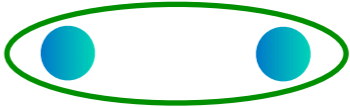
Spin liquid obtained in a generalized spin model with  $S=1/2$  per unit cell

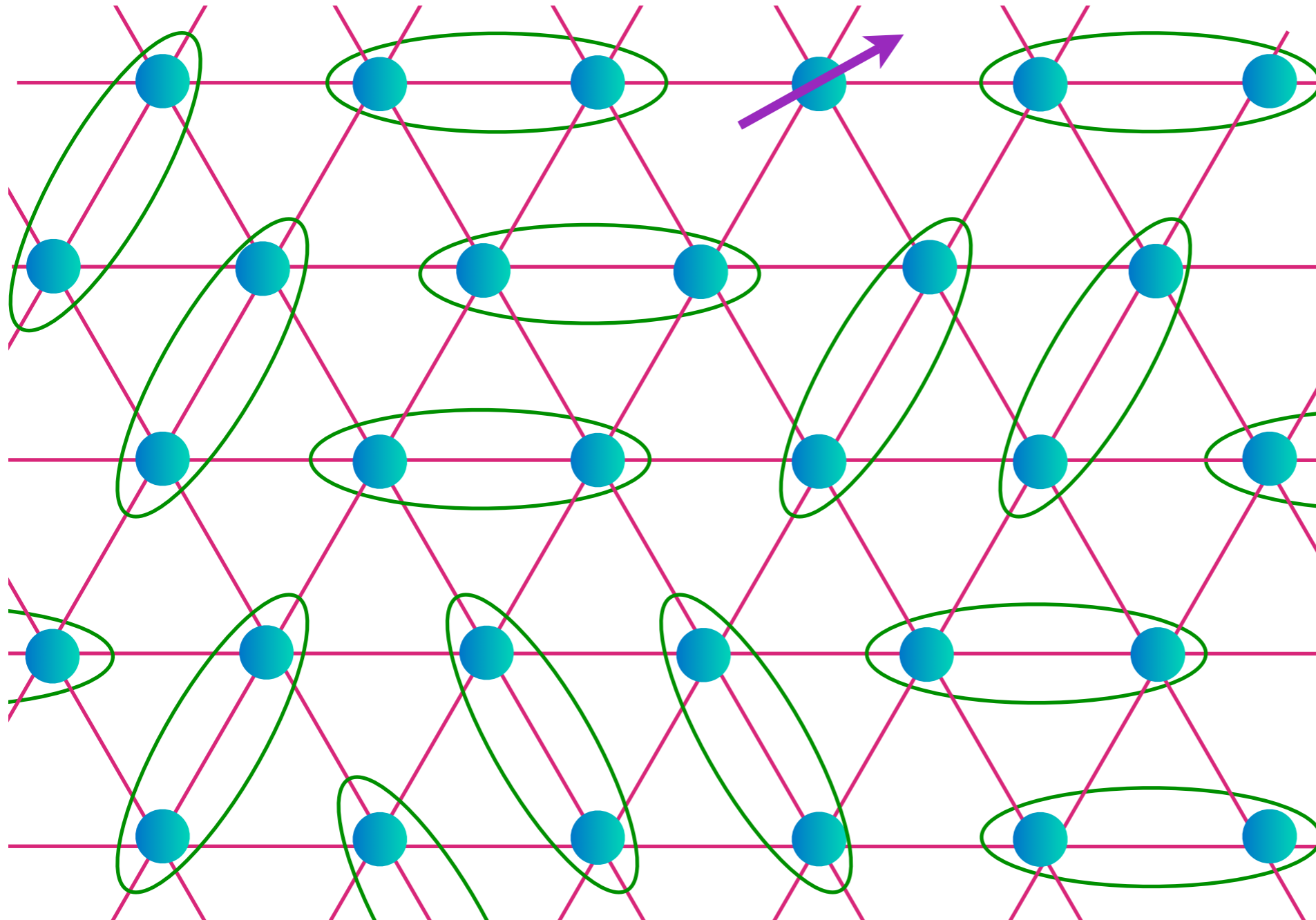
$$\begin{array}{c} \text{---} \text{---} \\ \text{---} \text{---} \\ \text{---} \text{---} \\ \text{---} \text{---} \\ \text{---} \text{---} \end{array} = \frac{1}{\sqrt{2}} (|\uparrow\downarrow\rangle - |\downarrow\uparrow\rangle)$$



# Excitations of the $Z_2$ Spin liquid


A spinon

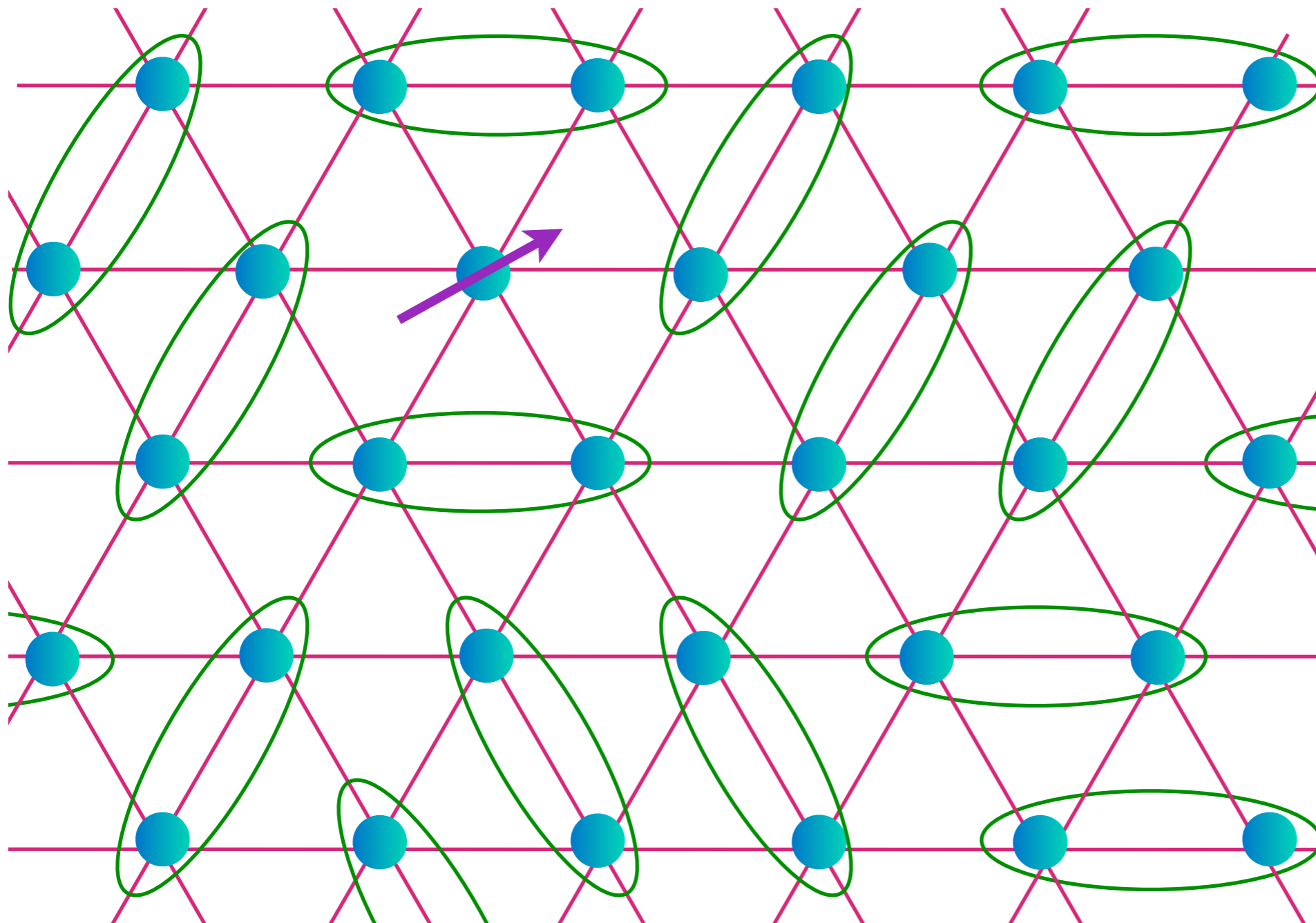

$$= \frac{1}{\sqrt{2}} (|\uparrow\downarrow\rangle - |\downarrow\uparrow\rangle)$$



# Excitations of the $Z_2$ Spin liquid

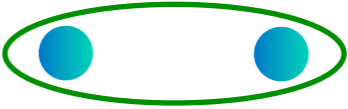
A spinon

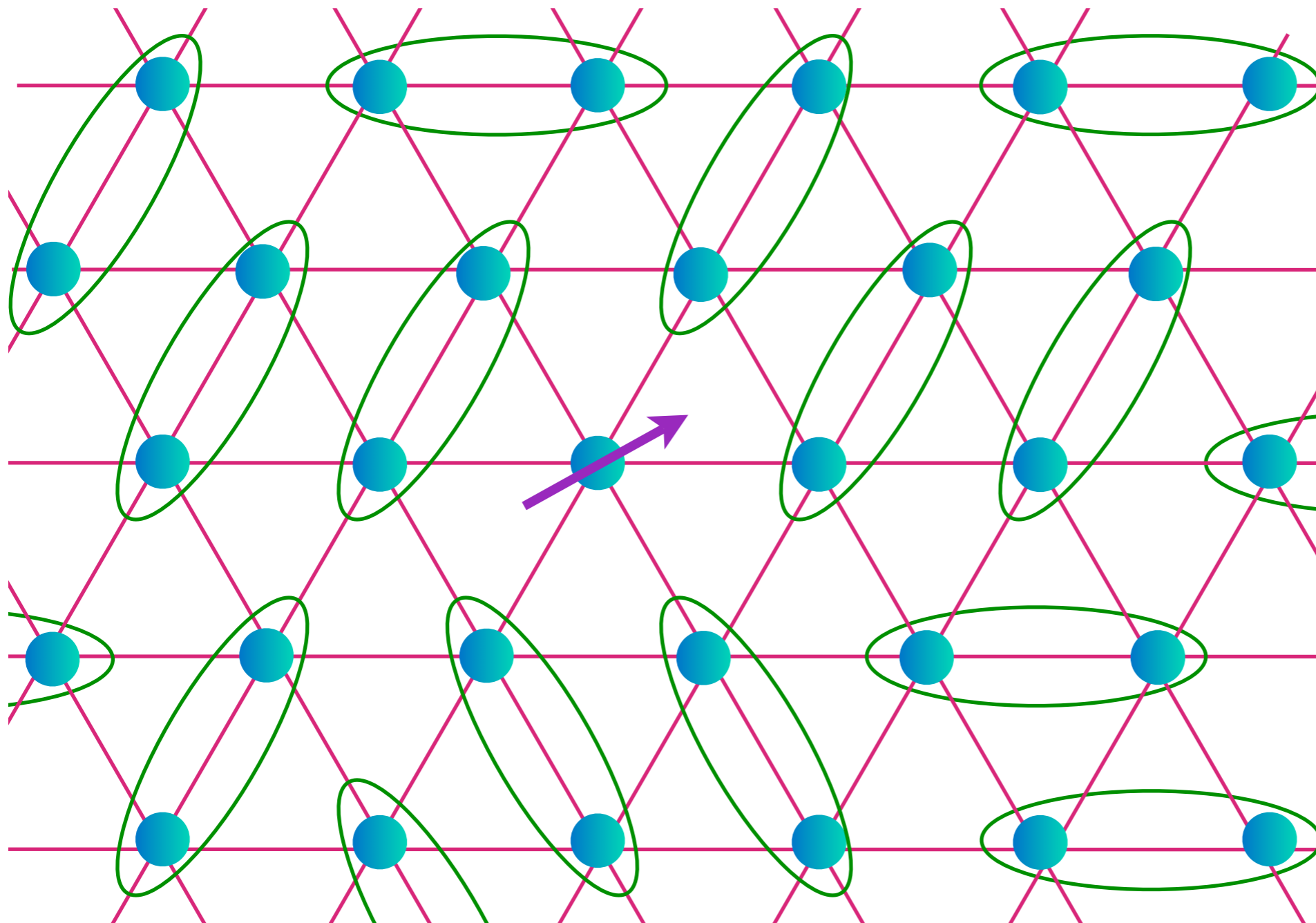

$$= \frac{1}{\sqrt{2}} (|\uparrow\downarrow\rangle - |\downarrow\uparrow\rangle)$$



# Excitations of the $Z_2$ Spin liquid

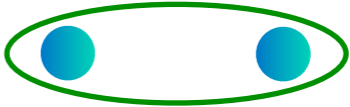
A spinon

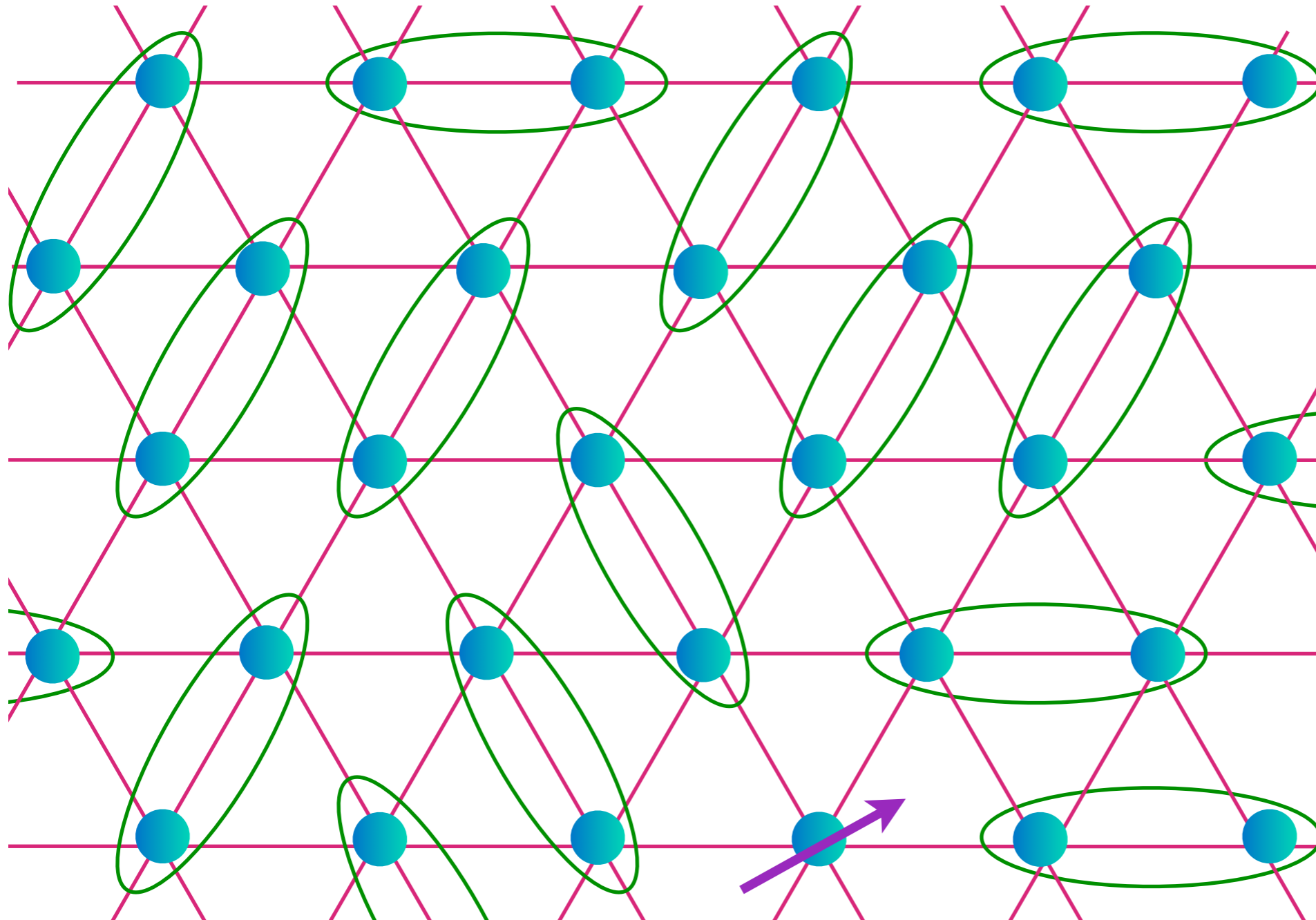

$$= \frac{1}{\sqrt{2}} (|\uparrow\downarrow\rangle - |\downarrow\uparrow\rangle)$$



# Excitations of the $Z_2$ Spin liquid

A spinon


$$= \frac{1}{\sqrt{2}} (|\uparrow\downarrow\rangle - |\downarrow\uparrow\rangle)$$



# Excitations of the $Z_2$ Spin liquid

## A spinon

The spinon annihilation operator is a spinor  $z_\alpha$ , where  $\alpha = \uparrow, \downarrow$ .

The Néel order parameter,  $\vec{\varphi}$  is a composite of the spinons:

$$\vec{\varphi} = z_{i\alpha}^\dagger \vec{\sigma}_{\alpha\beta} z_{i\beta}$$

where  $\vec{\sigma}$  are Pauli matrices

# Excitations of the $Z_2$ Spin liquid

## A spinon

The spinon annihilation operator is a spinor  $z_\alpha$ , where  $\alpha = \uparrow, \downarrow$ .

The Néel order parameter,  $\vec{\varphi}$  is a composite of the spinons:

$$\vec{\varphi} = z_{i\alpha}^\dagger \vec{\sigma}_{\alpha\beta} z_{i\beta}$$

where  $\vec{\sigma}$  are Pauli matrices

The theory for quantum phase transitions is expressed in terms of fluctuations of  $z_\alpha$ , and *not* the order parameter  $\vec{\varphi}$ .

Effective theory for  $z_\alpha$  must be invariant under the U(1) gauge transformation

$$z_{i\alpha} \rightarrow e^{i\theta} z_{i\alpha}$$

# Excitations of the $Z_2$ Spin liquid

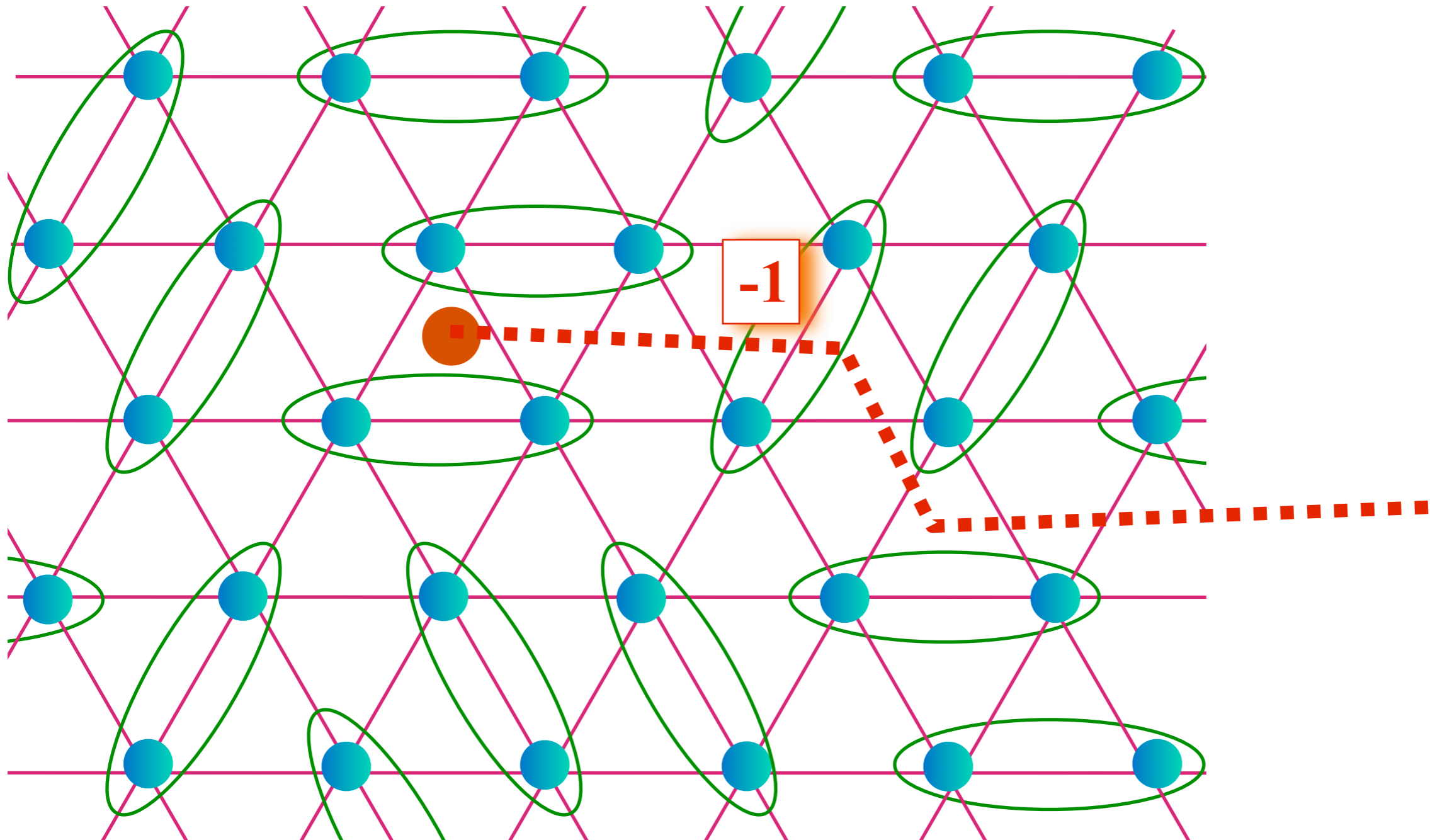
## A vison

- A characteristic property of a  $Z_2$  spin liquid is the presence of a spinon pair condensate
- A vison is an Abrikosov vortex in the pair condensate of spinons
- Visions are the dark matter of spin liquids: they likely carry most of the energy, but are very hard to detect because they do not carry charge or spin.

# Excitations of the $Z_2$ Spin liquid


A vison

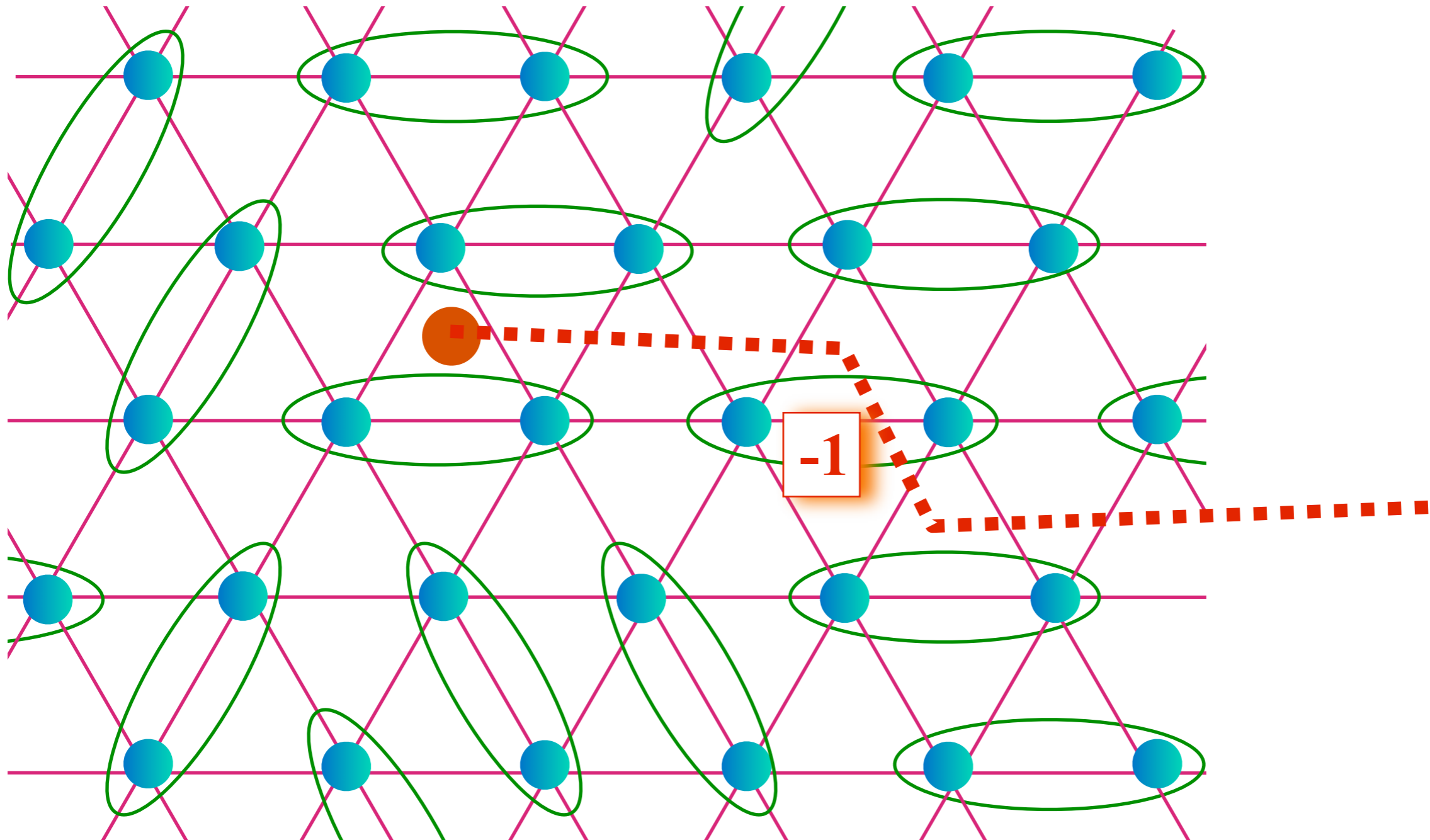
$$\begin{array}{c} \text{---} \circ \text{---} \circ \text{---} \\ \text{---} \end{array} = \frac{1}{\sqrt{2}} (|\uparrow\downarrow\rangle - |\downarrow\uparrow\rangle)$$



# Excitations of the $Z_2$ Spin liquid

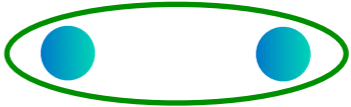
A vison

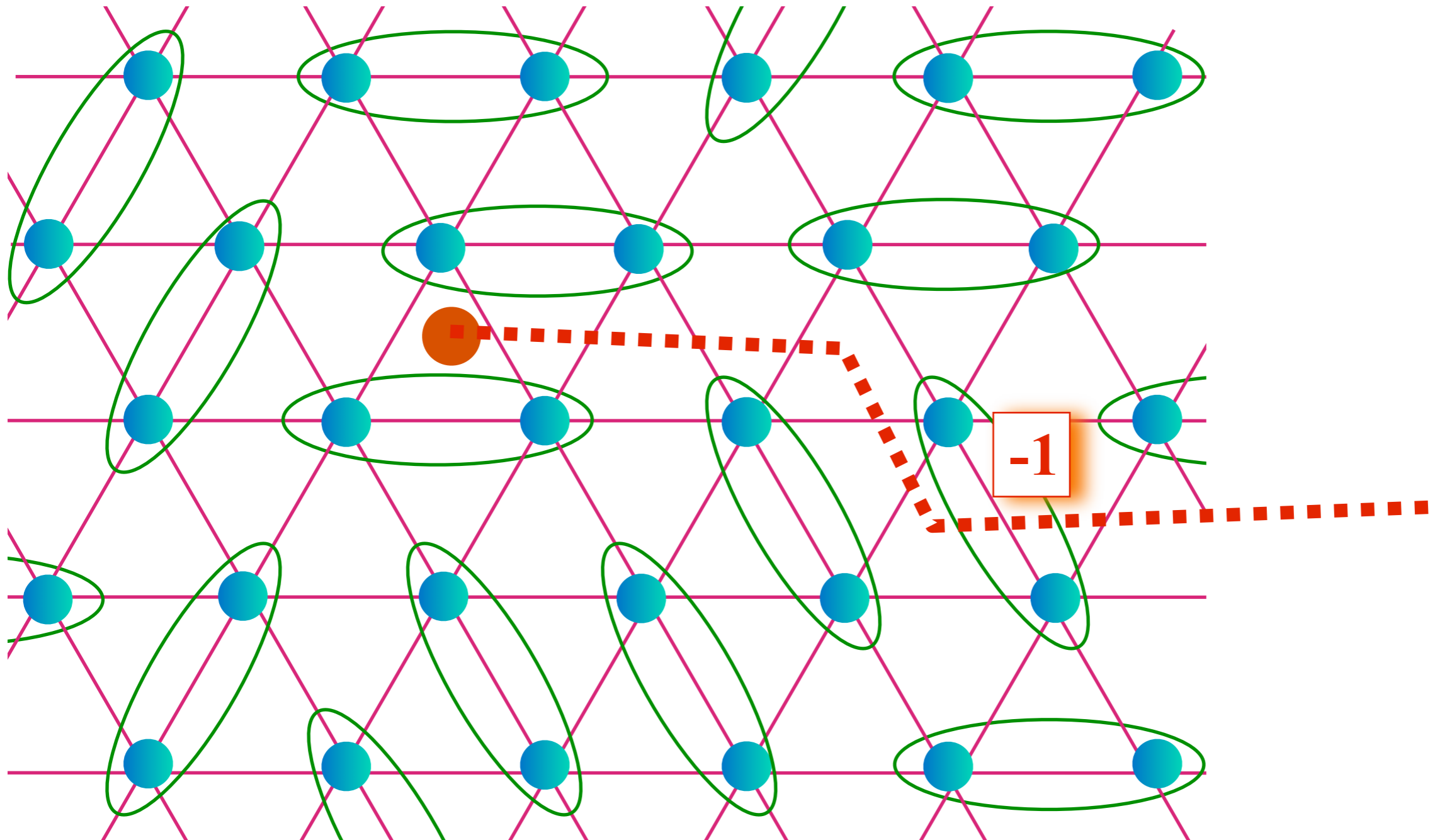

$$= \frac{1}{\sqrt{2}} (|\uparrow\downarrow\rangle - |\downarrow\uparrow\rangle)$$



# Excitations of the $Z_2$ Spin liquid

A vison

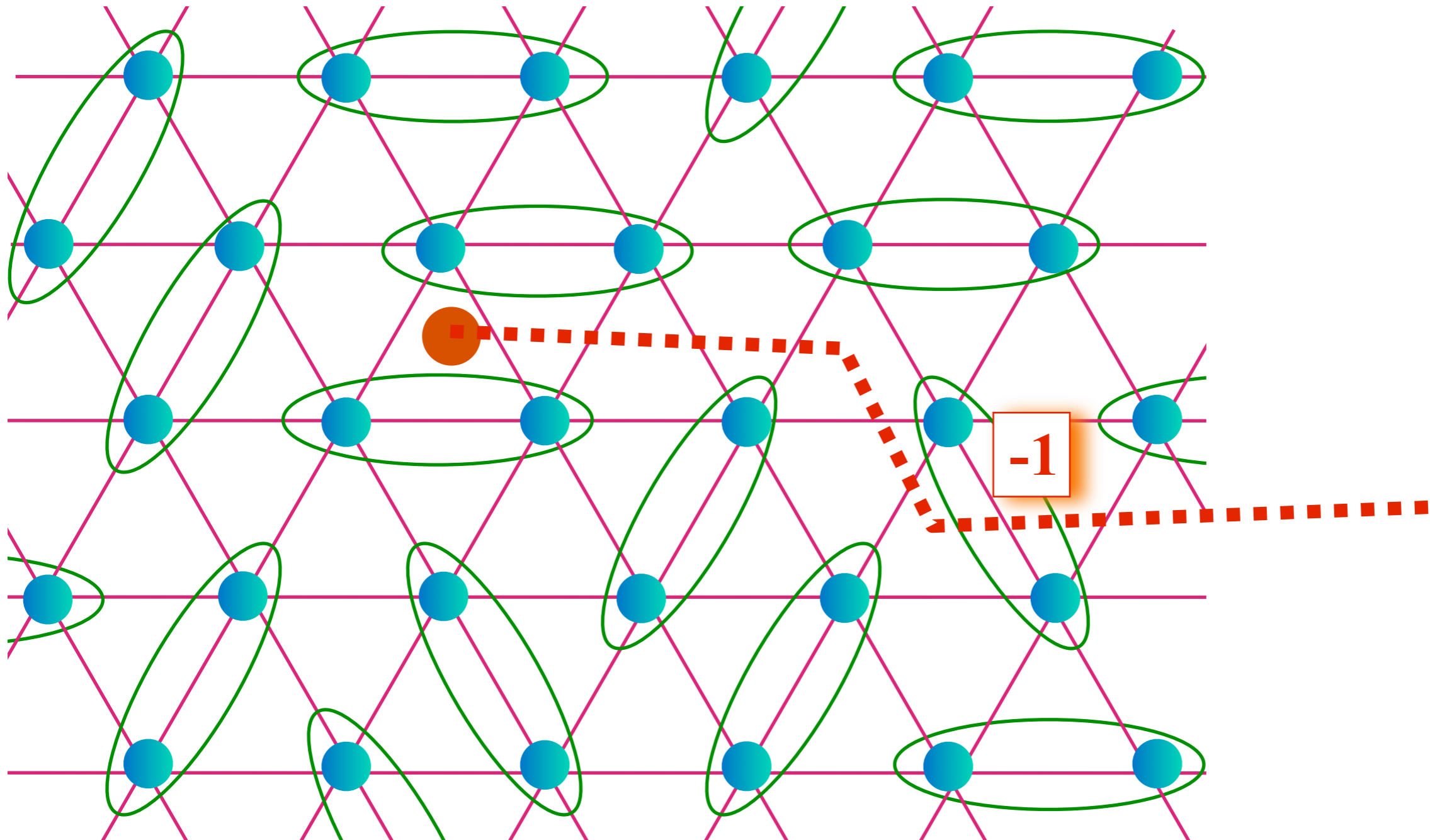

$$= \frac{1}{\sqrt{2}} (|\uparrow\downarrow\rangle - |\downarrow\uparrow\rangle)$$



# Excitations of the $Z_2$ Spin liquid

A vison

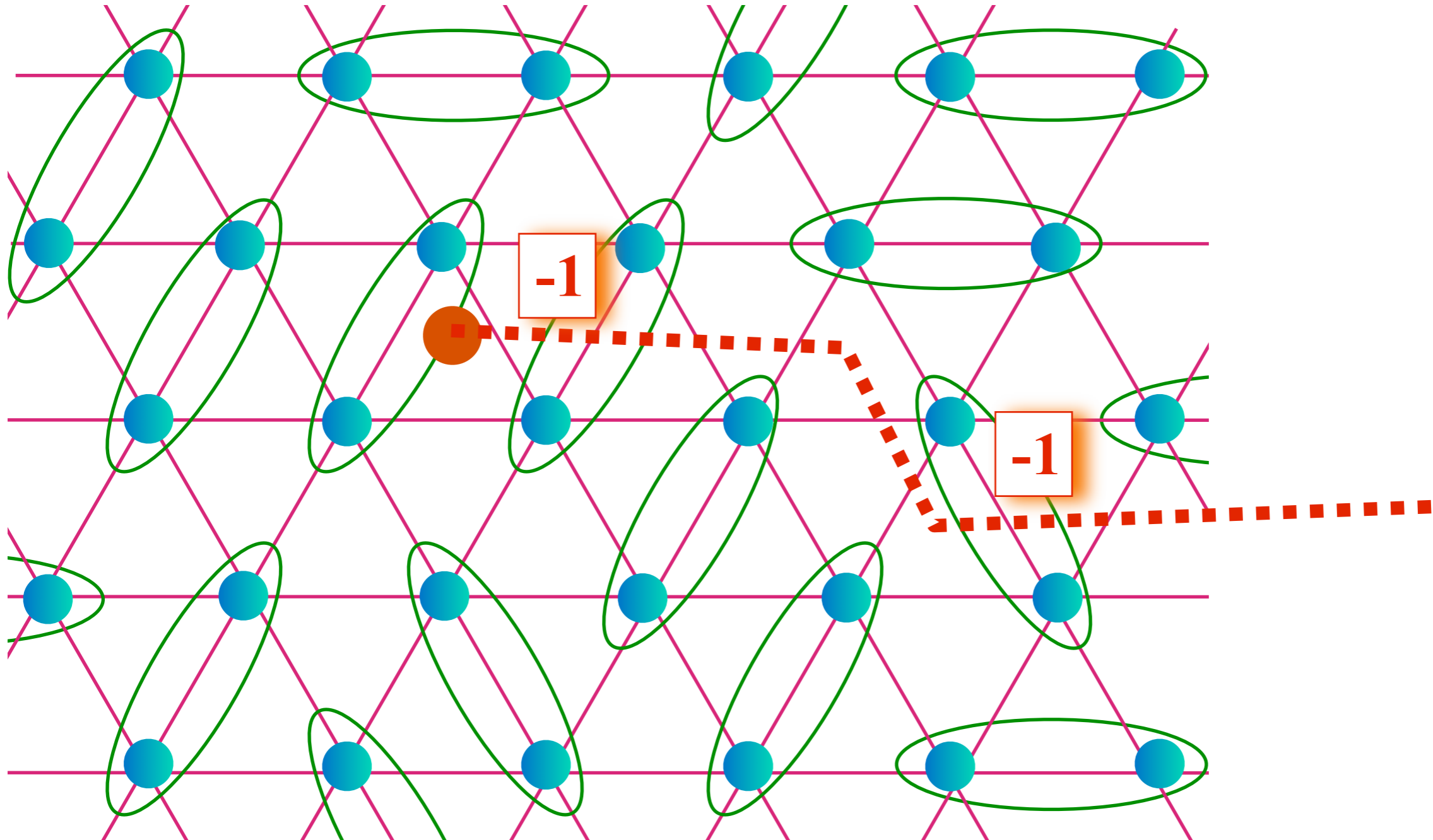
$$\begin{array}{c} \text{---} \circ \text{---} \circ \text{---} \\ \text{---} \end{array} = \frac{1}{\sqrt{2}} (|\uparrow\downarrow\rangle - |\downarrow\uparrow\rangle)$$



# Excitations of the $Z_2$ Spin liquid

A vison

$$\begin{array}{c} \text{---} \circ \text{---} \circ \text{---} \\ \text{---} \end{array} = \frac{1}{\sqrt{2}} (|\uparrow\downarrow\rangle - |\downarrow\uparrow\rangle)$$



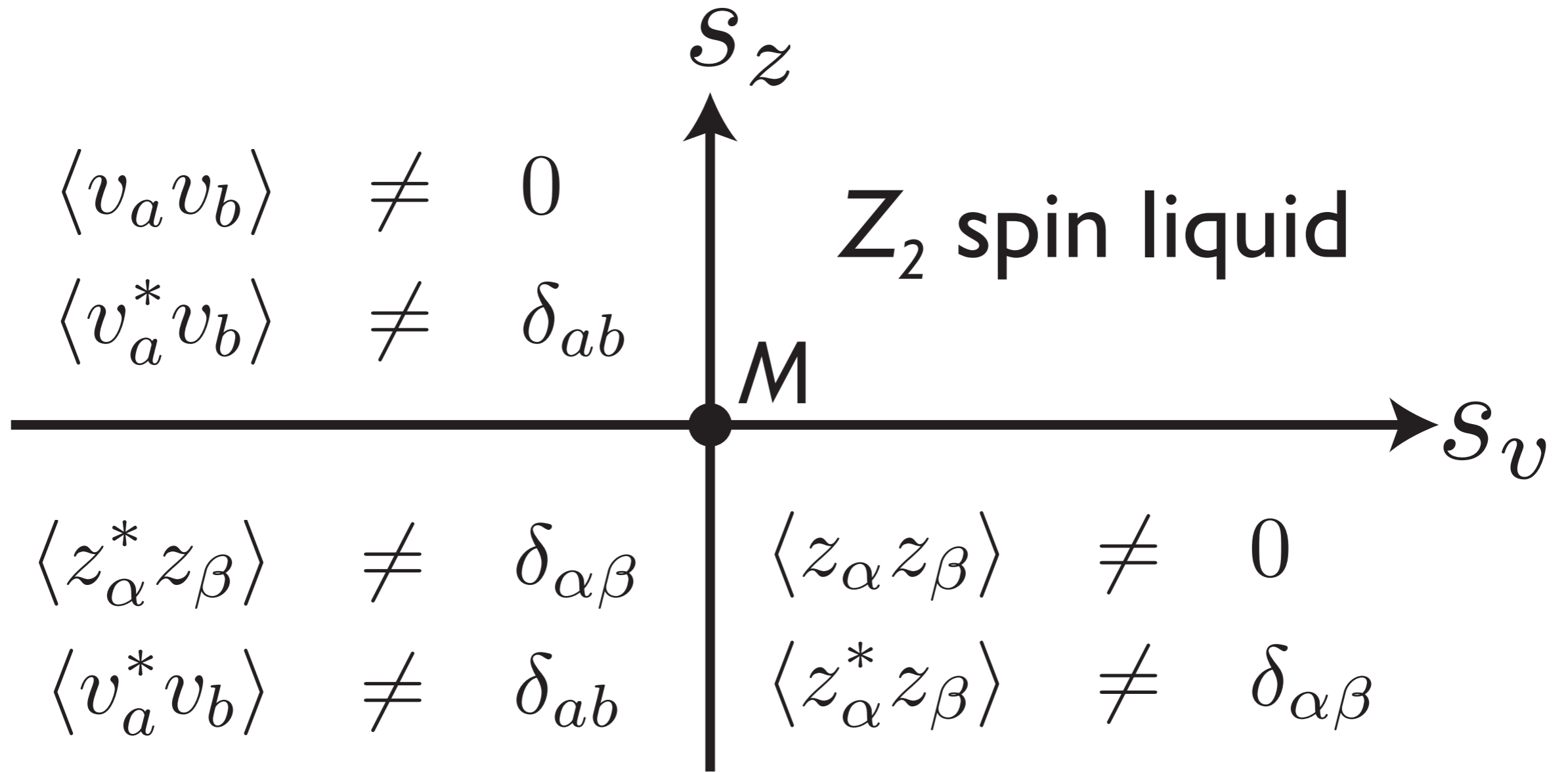


# Mutual Chern-Simons Theory

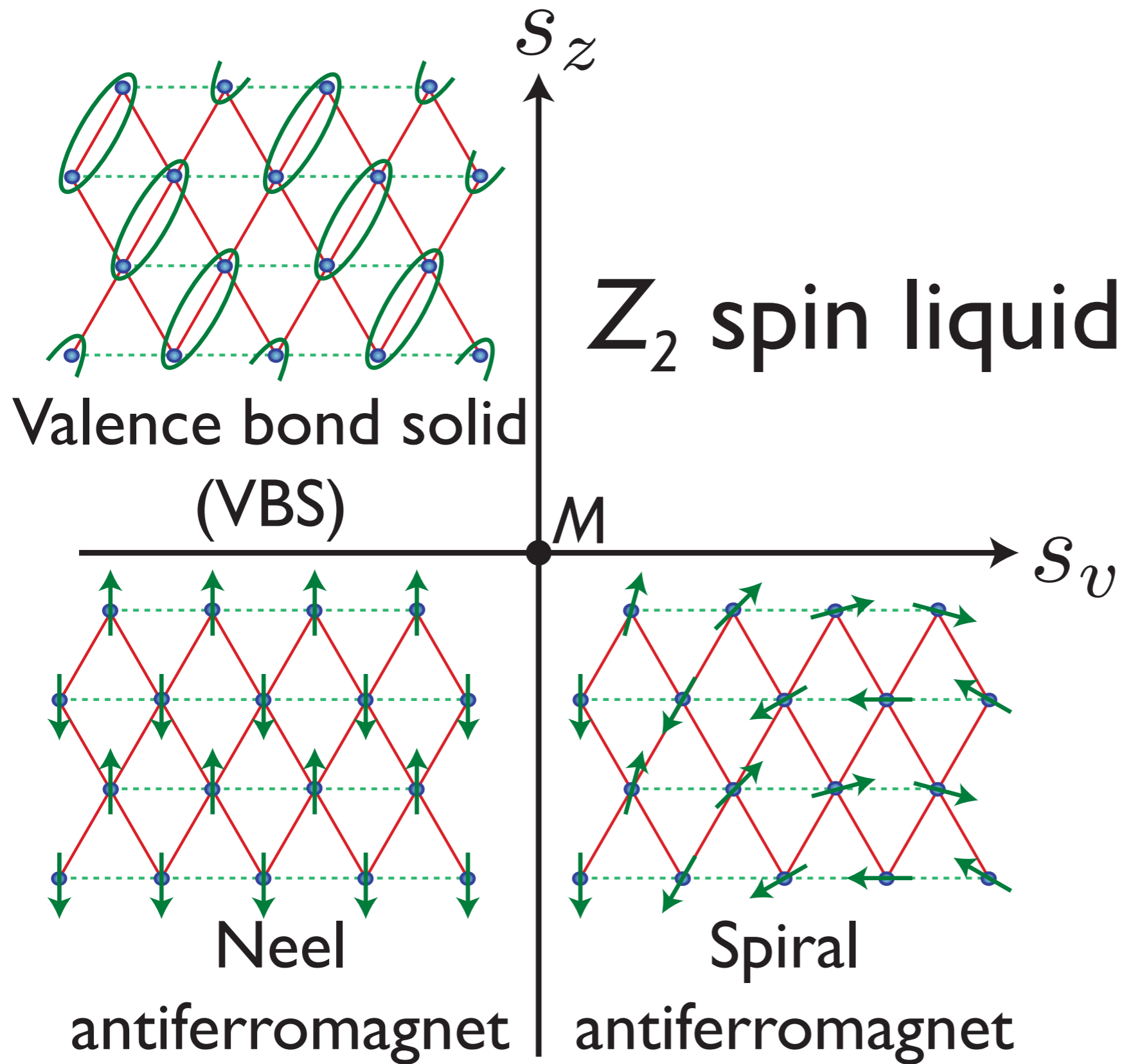
Express theory in terms of the physical excitations of the  $Z_2$  spin liquid: the spinons,  $z_\alpha$ , and the visons. After accounting for Berry phase effects, the visons can be described by complex fields  $v_a$ , which transforms non-trivially under the square lattice space group operations.

A related Berry phase is the phase of  $-1$  acquired by a spinon encircling a vortex. This is implemented in the following “mutual Chern-Simons” theory at  $k = 2$ :

$$\begin{aligned} \mathcal{L} &= \sum_{\alpha=1}^2 \left\{ |(\partial_\mu - ia_\mu)z_\alpha|^2 + s_z |z_\alpha|^2 + u_z (|z_\alpha|^2)^2 \right\} \\ &+ \sum_{a=1}^{N_v} \left\{ |(\partial_\mu - ib_\mu)v_a|^2 + s_v |v_a|^2 + u_v (|v_a|^2)^2 \right\} \\ &+ \frac{ik}{2\pi} \epsilon_{\mu\nu\lambda} a_\mu \partial_\nu b_\lambda + \dots \end{aligned}$$



# Theoretical global phase diagram

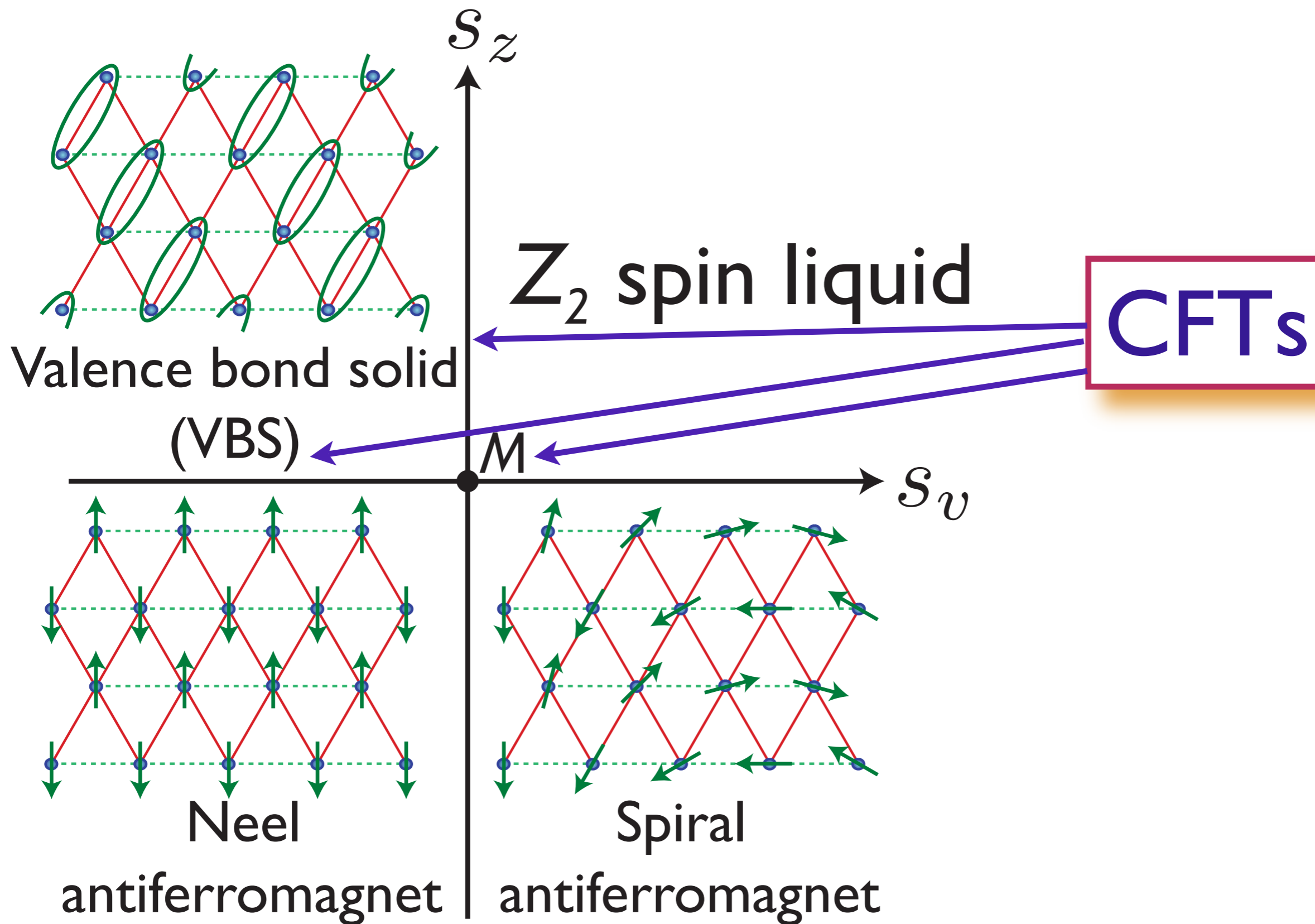


N. Read and S. Sachdev, *Phys. Rev. Lett.* **66**, 1773 (1991)

T. Senthil, A. Vishwanath, L. Balents, S. Sachdev and M.P.A. Fisher, *Science* **303**, 1490 (2004).

Cenke Xu and S. Sachdev, arXiv:0811.1220

# Theoretical global phase diagram



N. Read and S. Sachdev, *Phys. Rev. Lett.* **66**, 1773 (1991)

T. Senthil, A. Vishwanath, L. Balents, S. Sachdev and M.P.A. Fisher, *Science* **303**, 1490 (2004).

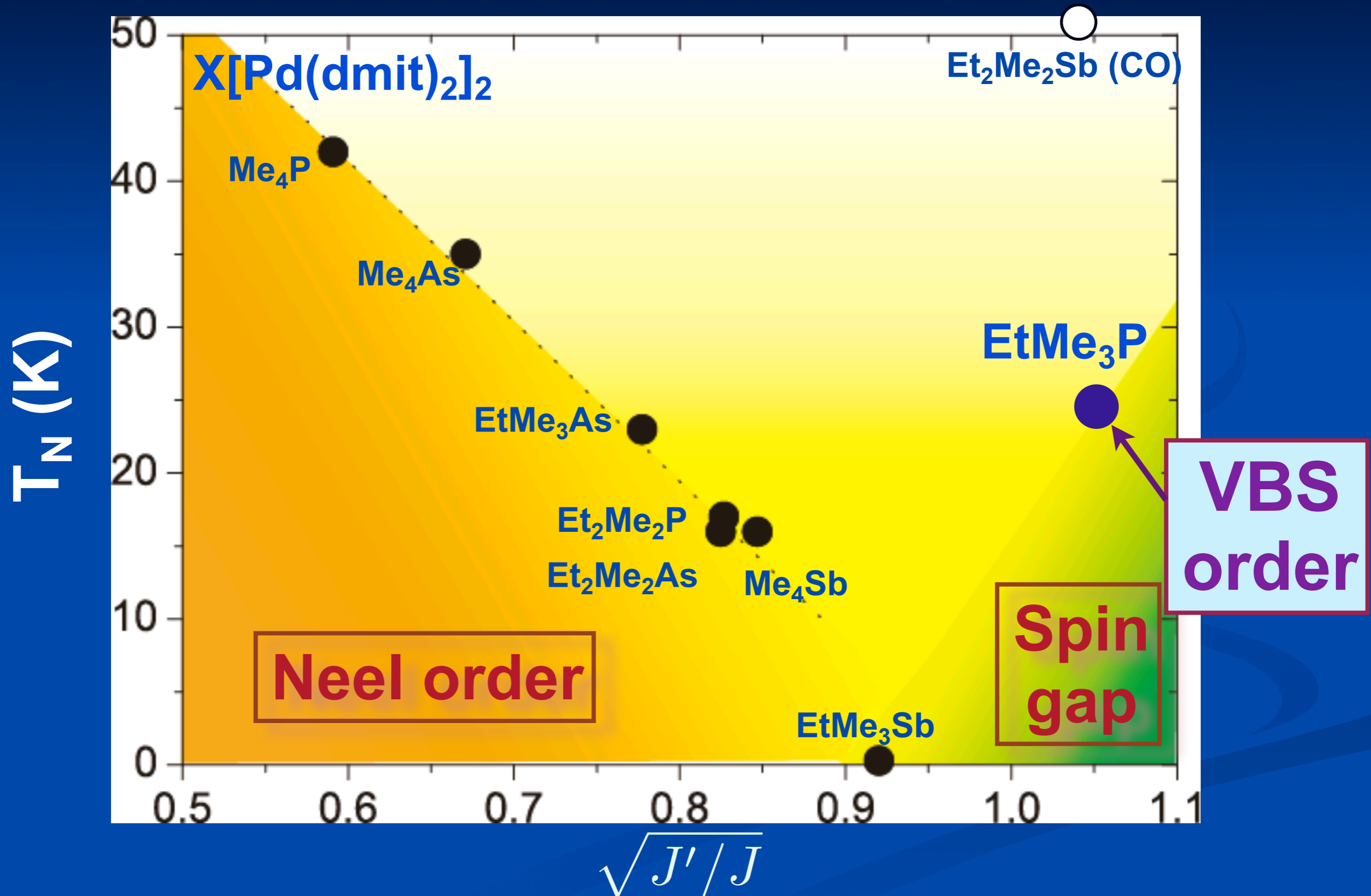
Cenke Xu and S. Sachdev, arXiv:0811.1220

## From quantum antiferromagnets to string theory

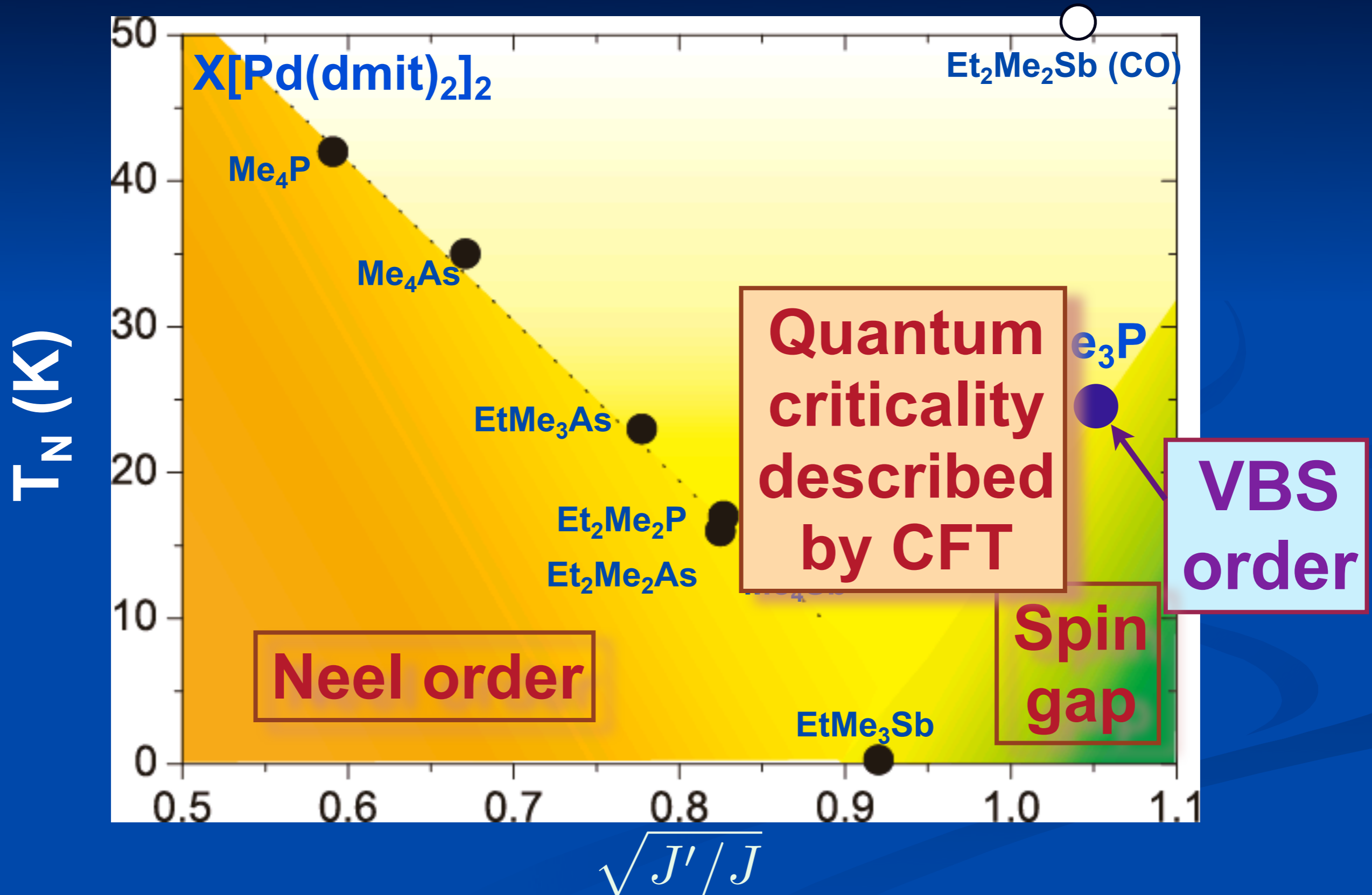
A direct generalization of the CFT of the multicritical point M ( $s_z = s_v = 0$ ) to  $\mathcal{N} = 4$  supersymmetry and the  $U(N)$  gauge group was shown by O. Aharony, O. Bergman, D. L. Jafferis, J. Maldacena, JHEP **0810**, 091 (2008) to be dual to a theory of quantum gravity (M theory) on  $AdS_4 \times S_7 / Z_k$ .

$$\begin{aligned} \mathcal{L} &= \sum_{\alpha=1}^2 \left\{ |(\partial_\mu - ia_\mu)z_\alpha|^2 + s_z |z_\alpha|^2 + u_z (|z_\alpha|^2)^2 \right\} \\ &+ \sum_{a=1}^{N_v} \left\{ |(\partial_\mu - ib_\mu)v_a|^2 + s_v |v_a|^2 + u_v (|v_a|^2)^2 \right\} \\ &+ \frac{ik}{2\pi} \epsilon_{\mu\nu\lambda} a_\mu \partial_\nu b_\lambda + \dots \end{aligned}$$

# Magnetic Criticality



# Magnetic Criticality



## Outline

# A. “Relativistic” field theories of quantum phase transitions

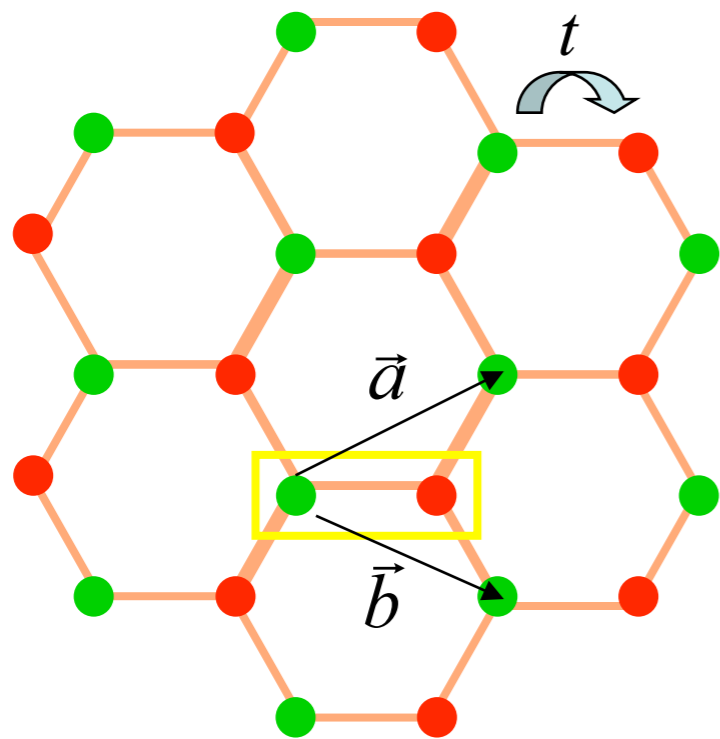
1. Coupled dimer antiferromagnets
2. Triangular lattice antiferromagnets
3. Graphene
4. AdS/CFT and quantum critical transport

## Outline

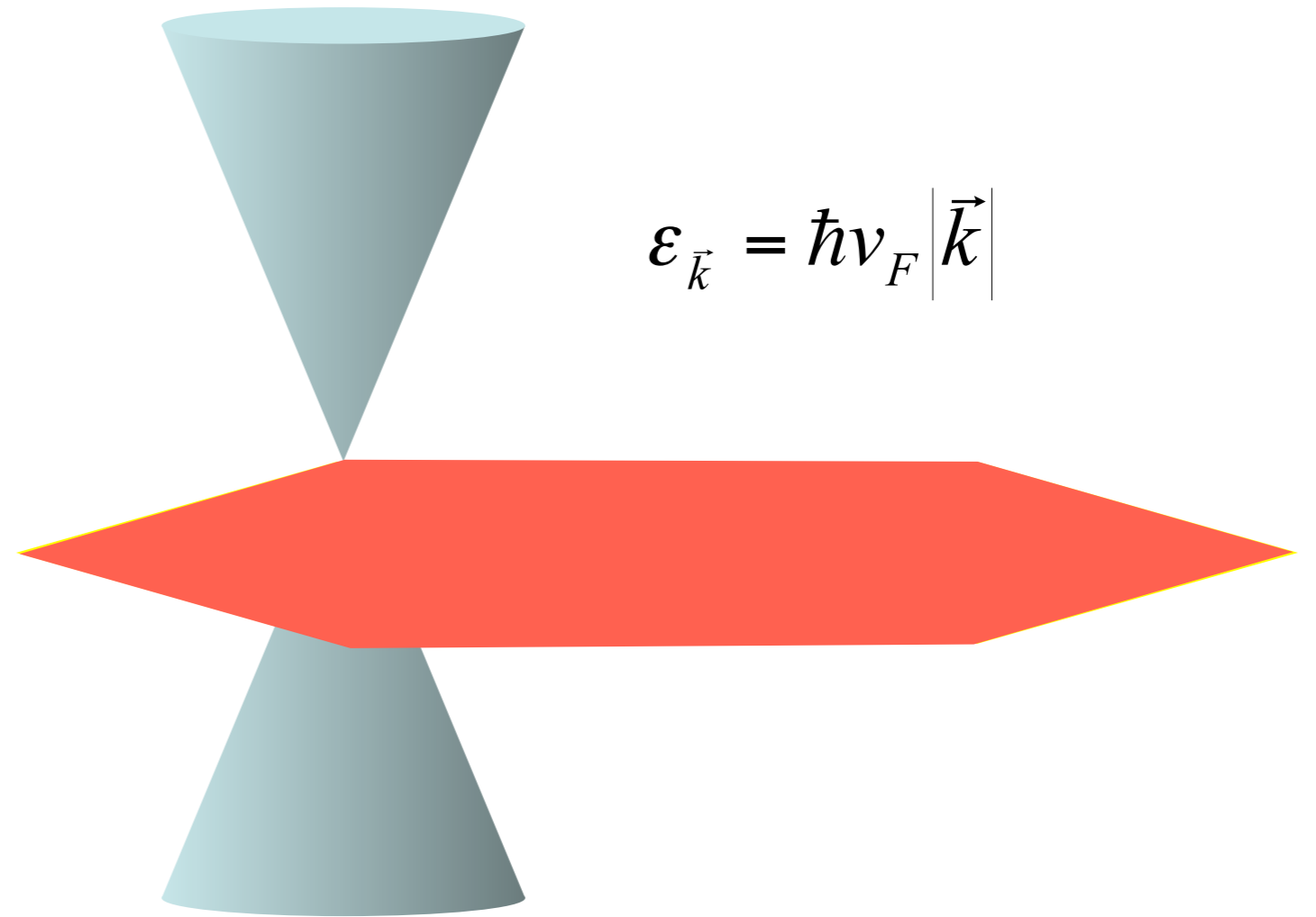
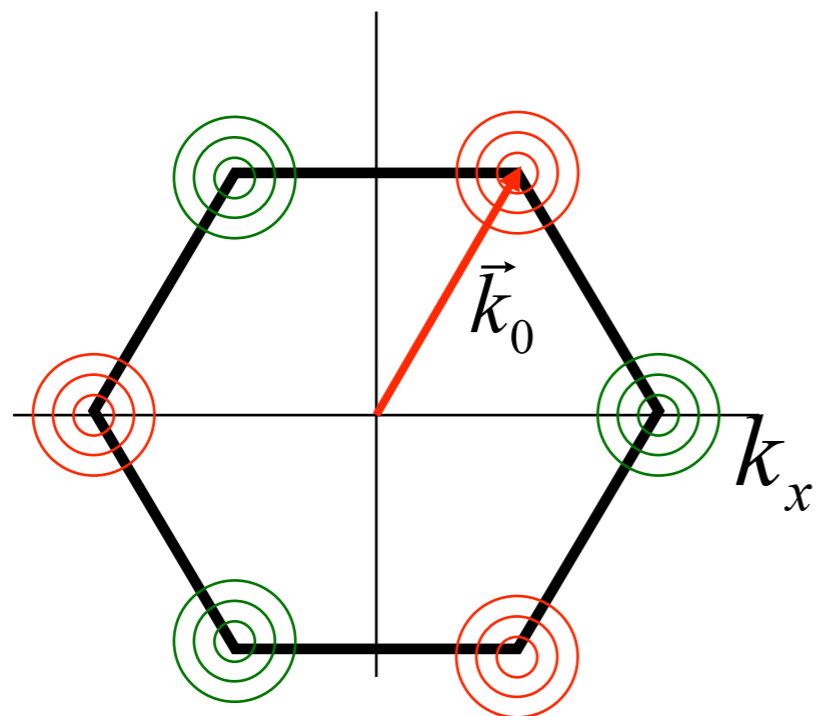
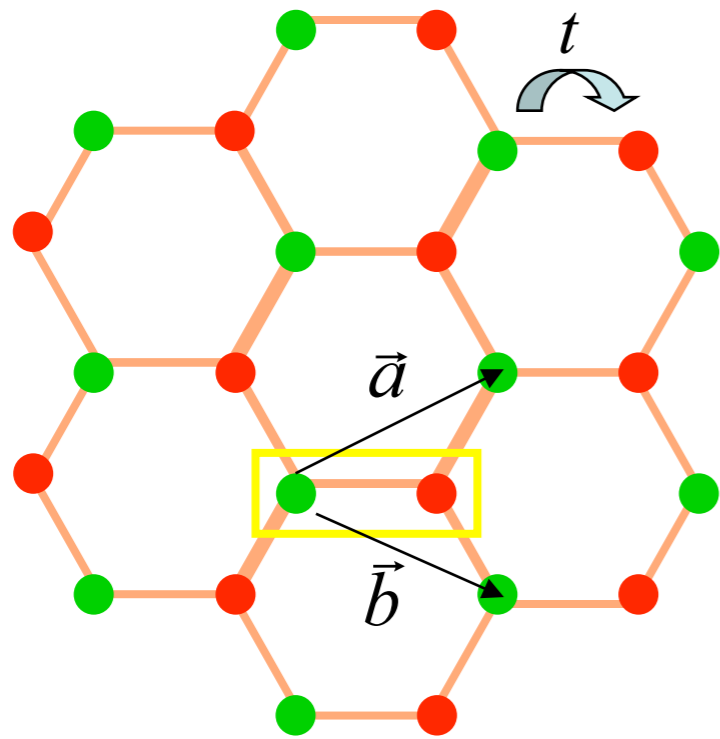
# A. “Relativistic” field theories of quantum phase transitions

1. Coupled dimer antiferromagnets
2. Triangular lattice antiferromagnets
3. Graphene
4. AdS/CFT and quantum critical transport

# Graphene

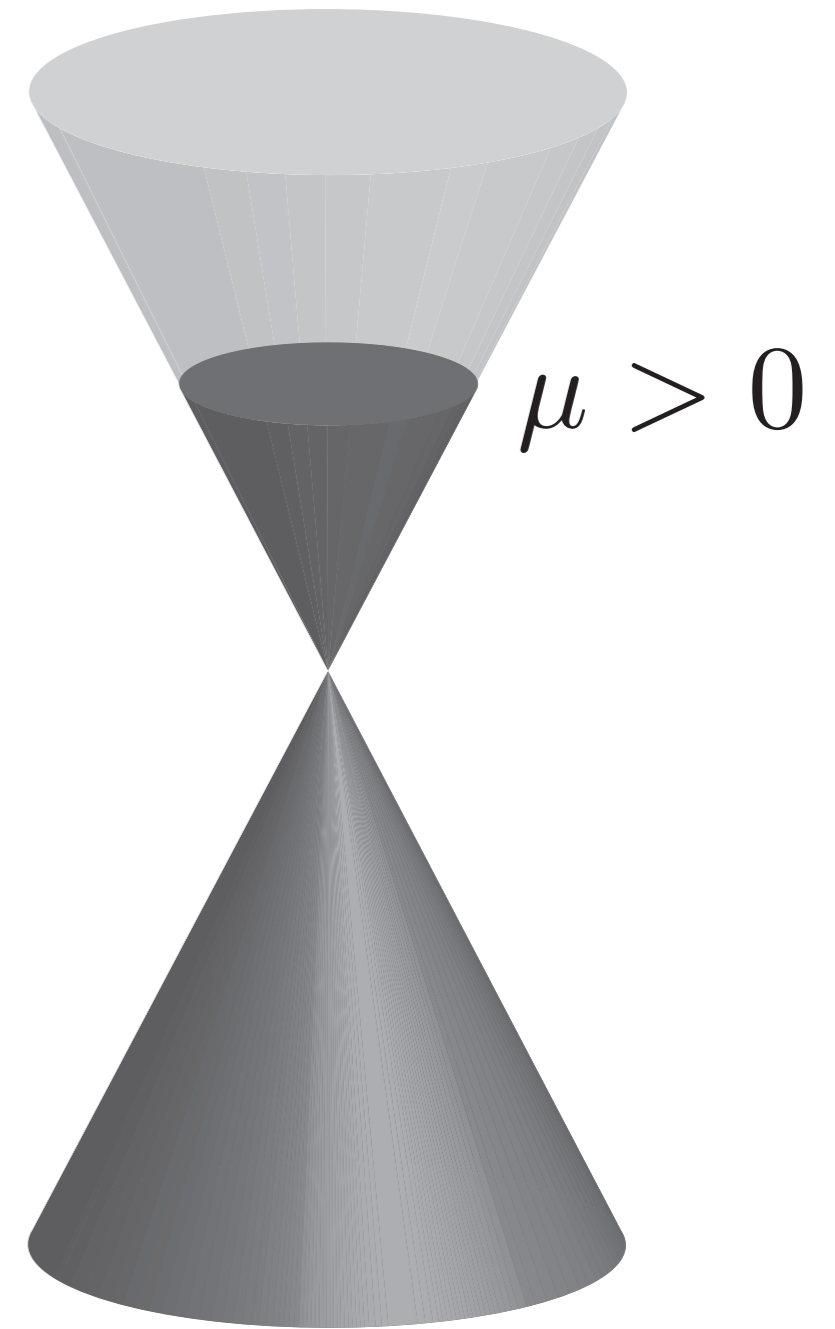


# Graphene



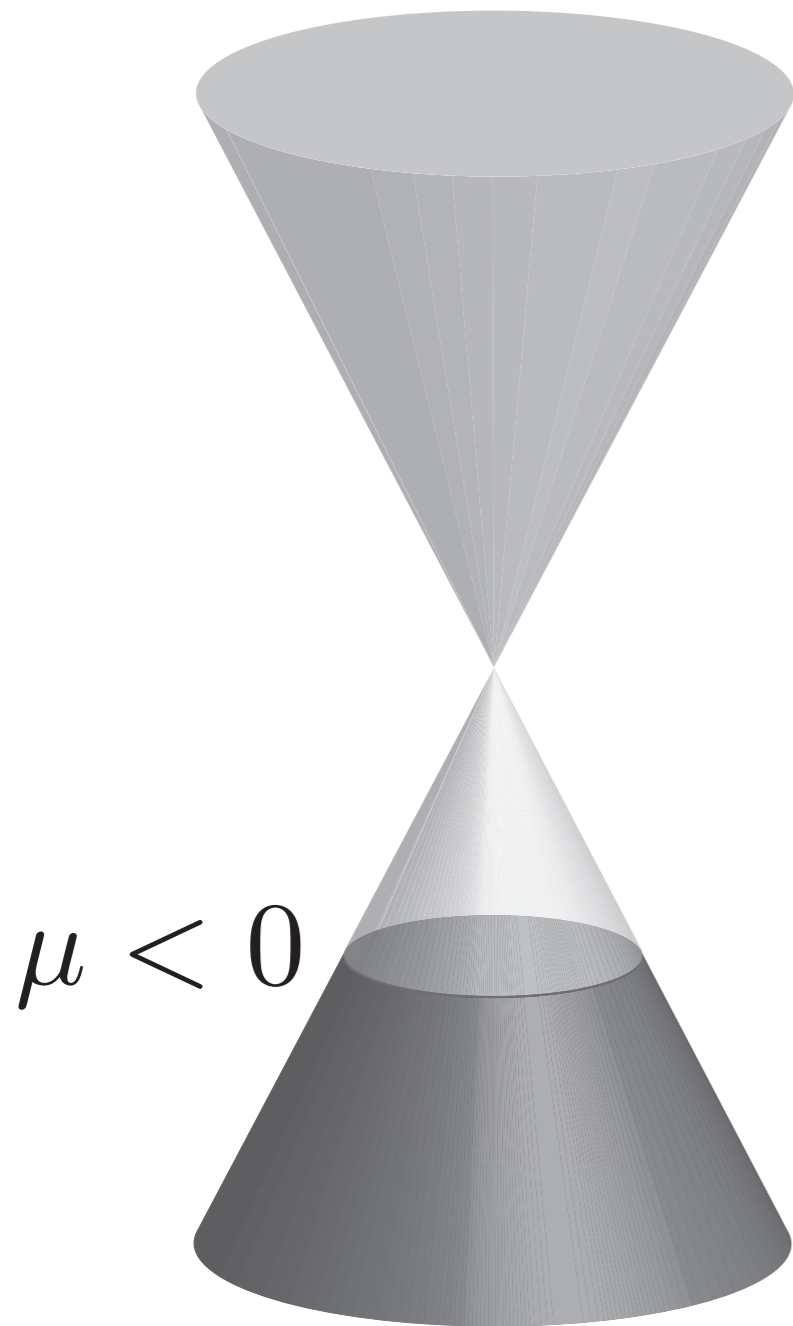
**Conical Dirac dispersion**

# Quantum phase transition in graphene tuned by a bias voltage

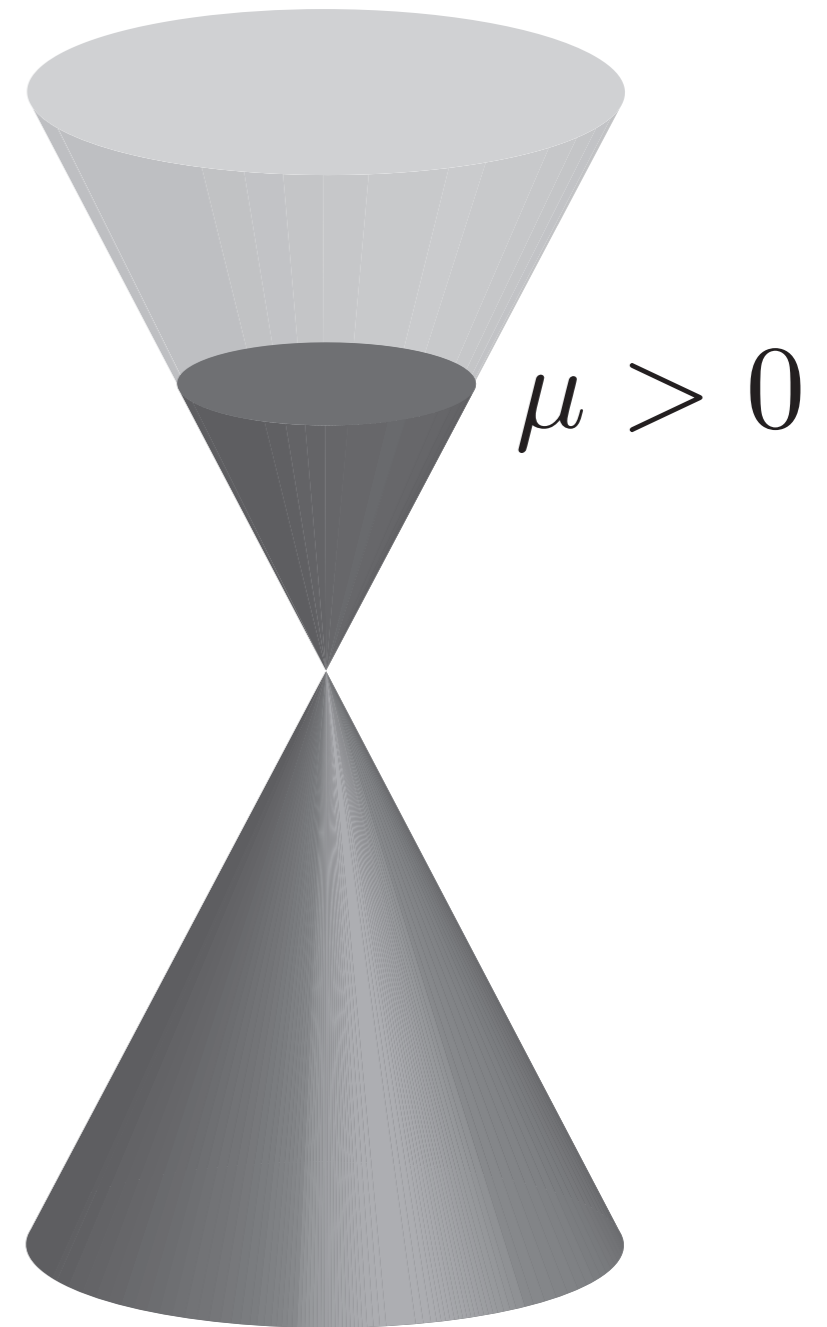


**Electron  
Fermi surface**

Quantum phase transition in graphene  
tuned by a bias voltage



**Hole  
Fermi surface**



**Electron  
Fermi surface**

# Quantum phase transition in graphene tuned by a bias voltage

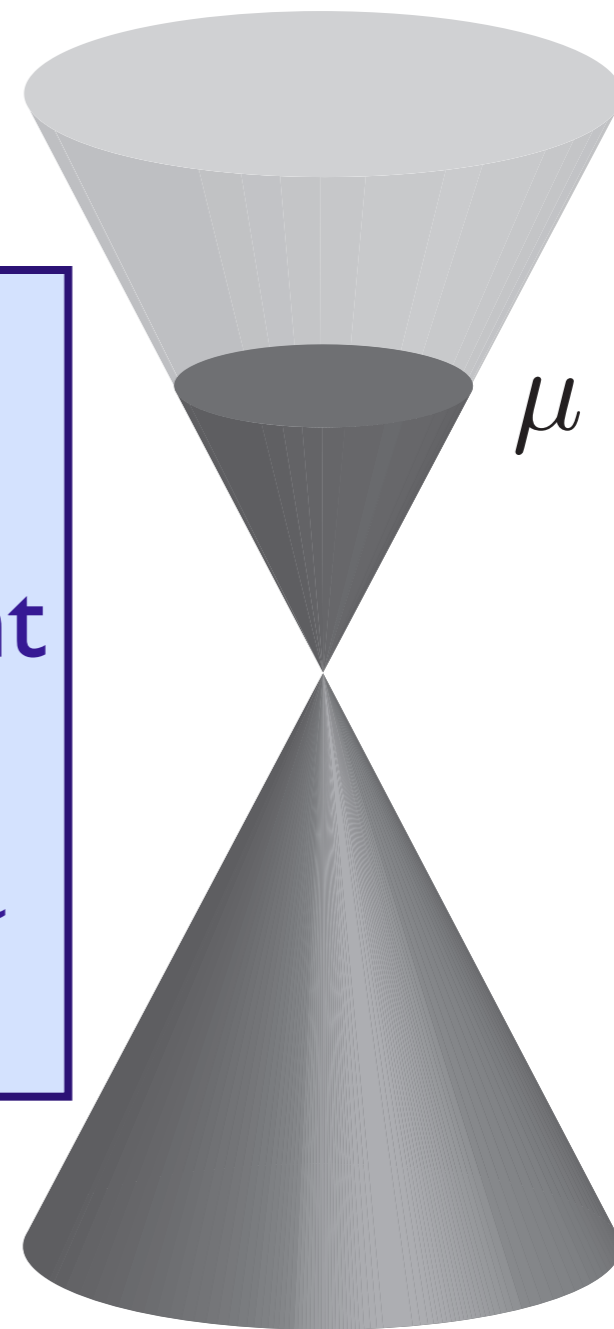
There must be an  
intermediate  
quantum critical point  
where the Fermi  
surfaces reduce to a  
Dirac point

$$\mu < 0$$



**Hole  
Fermi surface**

$$\mu > 0$$



**Electron  
Fermi surface**

# Quantum critical graphene

Low energy theory has 4 two-component Dirac fermions,  $\psi_\sigma$ ,  $\sigma = 1 \dots 4$ , interacting with a  $1/r$  Coulomb interaction

$$\mathcal{S} = \int d^2r d\tau \psi_\sigma^\dagger \left( \partial_\tau - i v_F \vec{\sigma} \cdot \vec{\nabla} \right) \psi_\sigma + \frac{e^2}{2} \int d^2r d^2r' d\tau \psi_\sigma^\dagger \psi_\sigma(r) \frac{1}{|r - r'|} \psi_{\sigma'}^\dagger \psi_{\sigma'}(r')$$

# Quantum critical graphene

Low energy theory has 4 two-component Dirac fermions,  $\psi_\sigma$ ,  $\sigma = 1 \dots 4$ , interacting with a  $1/r$  Coulomb interaction

$$\mathcal{S} = \int d^2r d\tau \psi_\sigma^\dagger \left( \partial_\tau - i v_F \vec{\sigma} \cdot \vec{\nabla} \right) \psi_\sigma + \frac{e^2}{2} \int d^2r d^2r' d\tau \psi_\sigma^\dagger \psi_\sigma(r) \frac{1}{|r - r'|} \psi_{\sigma'}^\dagger \psi_{\sigma'}(r')$$

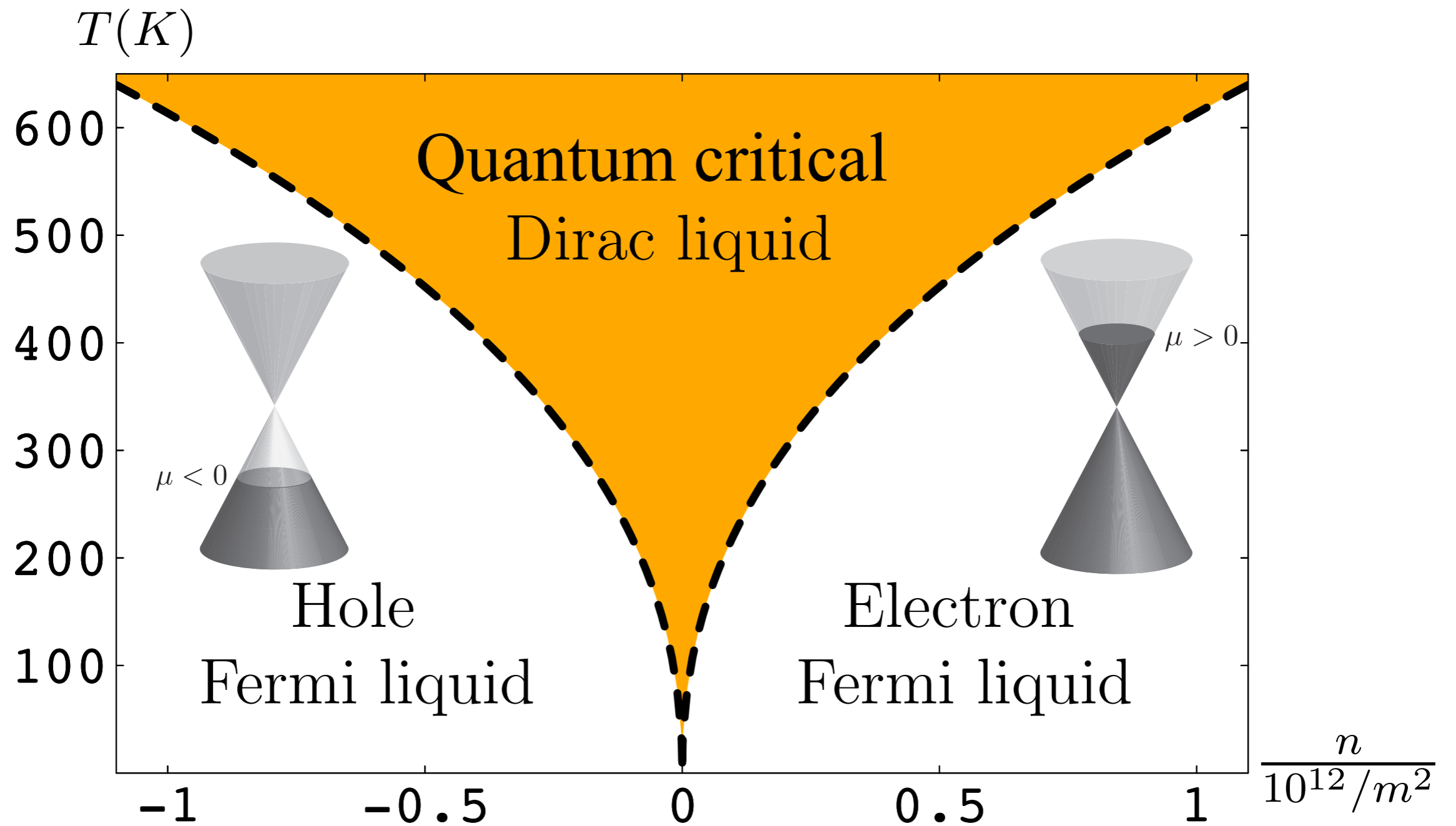
Dimensionless “fine-structure” constant  $\alpha = e^2 / (\hbar v_F)$ .

RG flow of  $\alpha$ :

$$\frac{d\alpha}{d\ell} = -\alpha^2 + \dots$$

**Behavior is similar to a conformal field theory (CFT) in 2+1 dimensions with  $\alpha \sim 1 / \ln(\text{scale})$**

# Quantum phase transition in graphene



## Outline

# A. “Relativistic” field theories of quantum phase transitions

1. Coupled dimer antiferromagnets
2. Triangular lattice antiferromagnets
3. Graphene
4. AdS/CFT and quantum critical transport

## Outline

# A. “Relativistic” field theories of quantum phase transitions

1. Coupled dimer antiferromagnets
2. Triangular lattice antiferromagnets
3. Graphene
4. AdS/CFT and quantum critical transport

# Quantum critical transport

Quantum “*perfect fluid*”  
with shortest possible  
relaxation time,  $\tau_R$

$$\tau_R \gtrsim \frac{\hbar}{k_B T}$$

# Quantum critical transport

Transport co-efficients not determined  
by collision rate, but by  
universal constants of nature

## Electrical conductivity

$$\sigma = \frac{e^2}{h} \times [\text{Universal constant } \mathcal{O}(1)]$$

# Quantum critical transport

Transport co-efficients not determined  
by collision rate, but by  
universal constants of nature

## Momentum transport

$$\frac{\eta}{s} \equiv \frac{\text{viscosity}}{\text{entropy density}}$$
$$= \frac{\hbar}{k_B} \times [\text{Universal constant } \mathcal{O}(1) ]$$

## Density correlations in CFTs at $T > 0$

Two-point density correlator,  $\chi(k, \omega)$

Kubo formula for conductivity  $\sigma(\omega) = \lim_{k \rightarrow 0} \frac{-i\omega}{k^2} \chi(k, \omega)$

For *all* CFT2s, at all  $\hbar\omega/k_B T$

$$\chi(k, \omega) = \frac{4e^2}{h} K \frac{vk^2}{v^2k^2 - \omega^2} \quad ; \quad \sigma(\omega) = \frac{4e^2}{h} \frac{Kv}{-i\omega}$$

where  $K$  is a universal number characterizing the CFT2 (the level number), and  $v$  is the velocity of “light”.

This follows from the conformal mapping of the plane to the cylinder, which relates correlators at  $T = 0$  to those at  $T > 0$ .

## Density correlations in CFTs at $T > 0$

Two-point density correlator,  $\chi(k, \omega)$

Kubo formula for conductivity  $\sigma(\omega) = \lim_{k \rightarrow 0} \frac{-i\omega}{k^2} \chi(k, \omega)$

For *all* CFT2s, at all  $\hbar\omega/k_B T$

$$\chi(k, \omega) = \frac{4e^2}{h} K \frac{vk^2}{v^2k^2 - \omega^2} \quad ; \quad \sigma(\omega) = \frac{4e^2}{h} \frac{Kv}{-i\omega}$$

where  $K$  is a universal number characterizing the CFT2 (the level number), and  $v$  is the velocity of “light”.

This follows from the conformal mapping of the plane to the cylinder, which relates correlators at  $T = 0$  to those at  $T > 0$ .

**No hydrodynamics in CFT2s.**

## Density correlations in CFTs at $T > 0$

Two-point density correlator,  $\chi(k, \omega)$

Kubo formula for conductivity  $\sigma(\omega) = \lim_{k \rightarrow 0} \frac{-i\omega}{k^2} \chi(k, \omega)$

For *all* CFT3s, at  $\hbar\omega \gg k_B T$

$$\chi(k, \omega) = \frac{4e^2}{h} K \frac{k^2}{\sqrt{v^2 k^2 - \omega^2}} ; \quad \sigma(\omega) = \frac{4e^2}{h} K$$

where  $K$  is a universal number characterizing the CFT3, and  $v$  is the velocity of “light”.

## Density correlations in CFTs at $T > 0$

Two-point density correlator,  $\chi(k, \omega)$

Kubo formula for conductivity  $\sigma(\omega) = \lim_{k \rightarrow 0} \frac{-i\omega}{k^2} \chi(k, \omega)$

**However**, for *all* CFT3s, at  $\hbar\omega \ll k_B T$ , we have the Einstein relation

$$\chi(k, \omega) = 4e^2 \chi_c \frac{Dk^2}{Dk^2 - i\omega} \quad ; \quad \sigma(\omega) = 4e^2 D \chi_c = \frac{4e^2}{h} \Theta_1 \Theta_2$$

where the **compressibility**,  $\chi_c$ , and the **diffusion constant**  $D$  obey

$$\chi = \frac{k_B T}{(h\nu)^2} \Theta_1 \quad ; \quad D = \frac{h\nu^2}{k_B T} \Theta_2$$

with  $\Theta_1$  and  $\Theta_2$  universal numbers characteristic of the CFT3

## Density correlations in CFTs at $T > 0$

In CFTs collisions are “phase” randomizing, and lead to relaxation to local thermodynamic equilibrium. So there is a crossover from collisionless behavior for  $\hbar\omega \gg k_B T$ , to hydrodynamic behavior for  $\hbar\omega \ll k_B T$ .

$$\sigma(\omega) = \begin{cases} \frac{4e^2}{h} K & , \quad \hbar\omega \gg k_B T \\ \frac{4e^2}{h} \Theta_1 \Theta_2 \equiv \sigma_Q & , \quad \hbar\omega \ll k_B T \end{cases}$$

and in general we expect  $K \neq \Theta_1 \Theta_2$  (verified for Wilson-Fisher fixed point).

## SU( $N$ ) SYM3 with $\mathcal{N} = 8$ supersymmetry

- Has a single dimensionful coupling constant,  $e_0$ , which flows to a strong-coupling fixed point  $e_0 = e_0^*$  in the infrared.
- The CFT3 describing this fixed point resembles “critical spin liquid” theories.
- This CFT3 is the low energy limit of string theory on an M2 brane. The AdS/CFT correspondence provides a dual description using 11-dimensional supergravity on  $\text{AdS}_4 \times S_7$ .
- The CFT3 has a global  $\text{SO}(8)$  R symmetry, and correlators of the  $\text{SO}(8)$  charge density can be computed exactly in the large  $N$  limit, even at  $T > 0$ .

## SU( $N$ ) SYM3 with $\mathcal{N} = 8$ supersymmetry

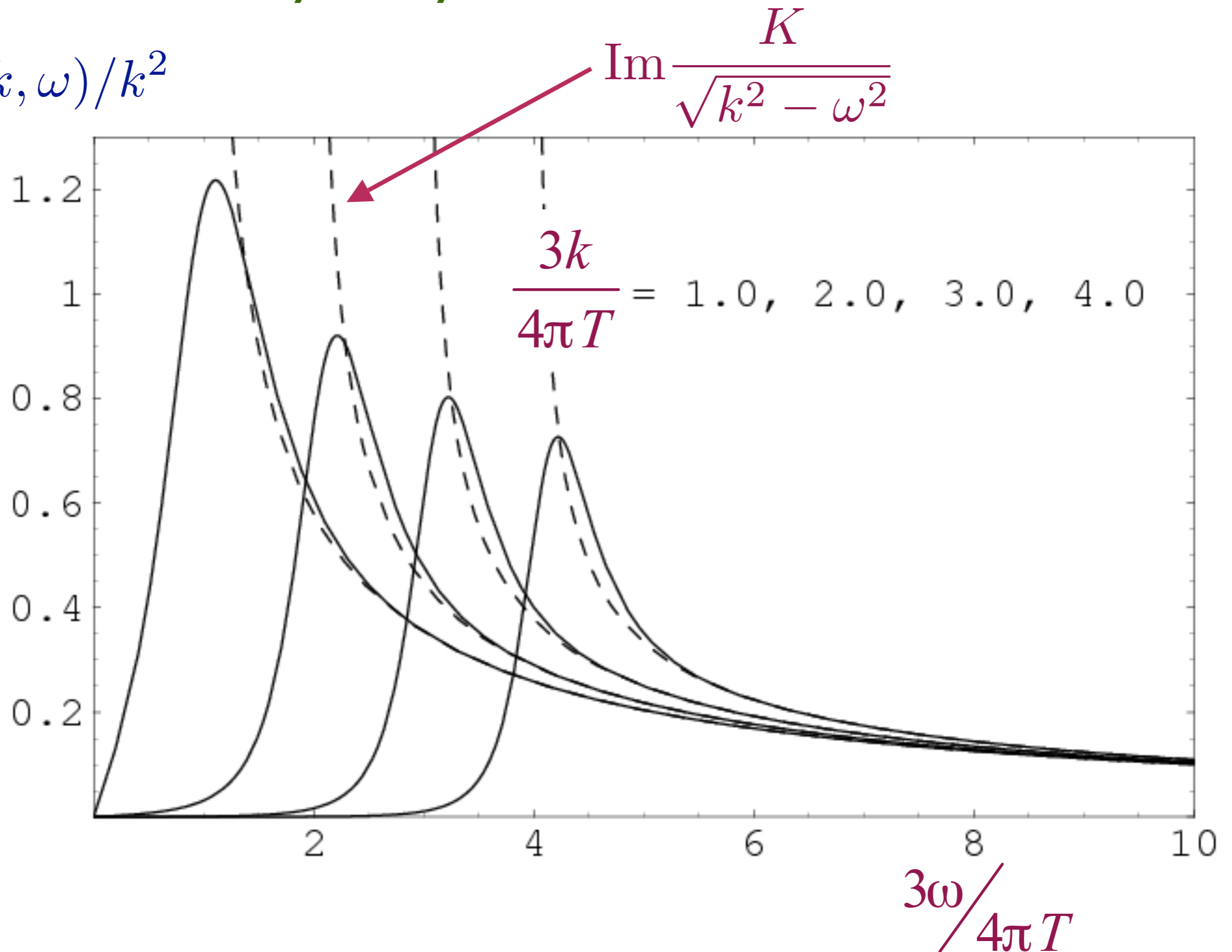
- The SO(8) charge correlators of the CFT3 are given by the usual AdS/CFT prescription applied to the following gauge theory on AdS4:

$$\mathcal{S} = -\frac{1}{4g_{4D}^2} \int d^4x \sqrt{-g} g^{MA} g^{NB} F_{MN}^a F_{AB}^a$$

where  $a = 1 \dots 28$  labels the generators of SO(8). Note that in large  $N$  theory, this looks like 28 copies of an Abelian gauge theory.

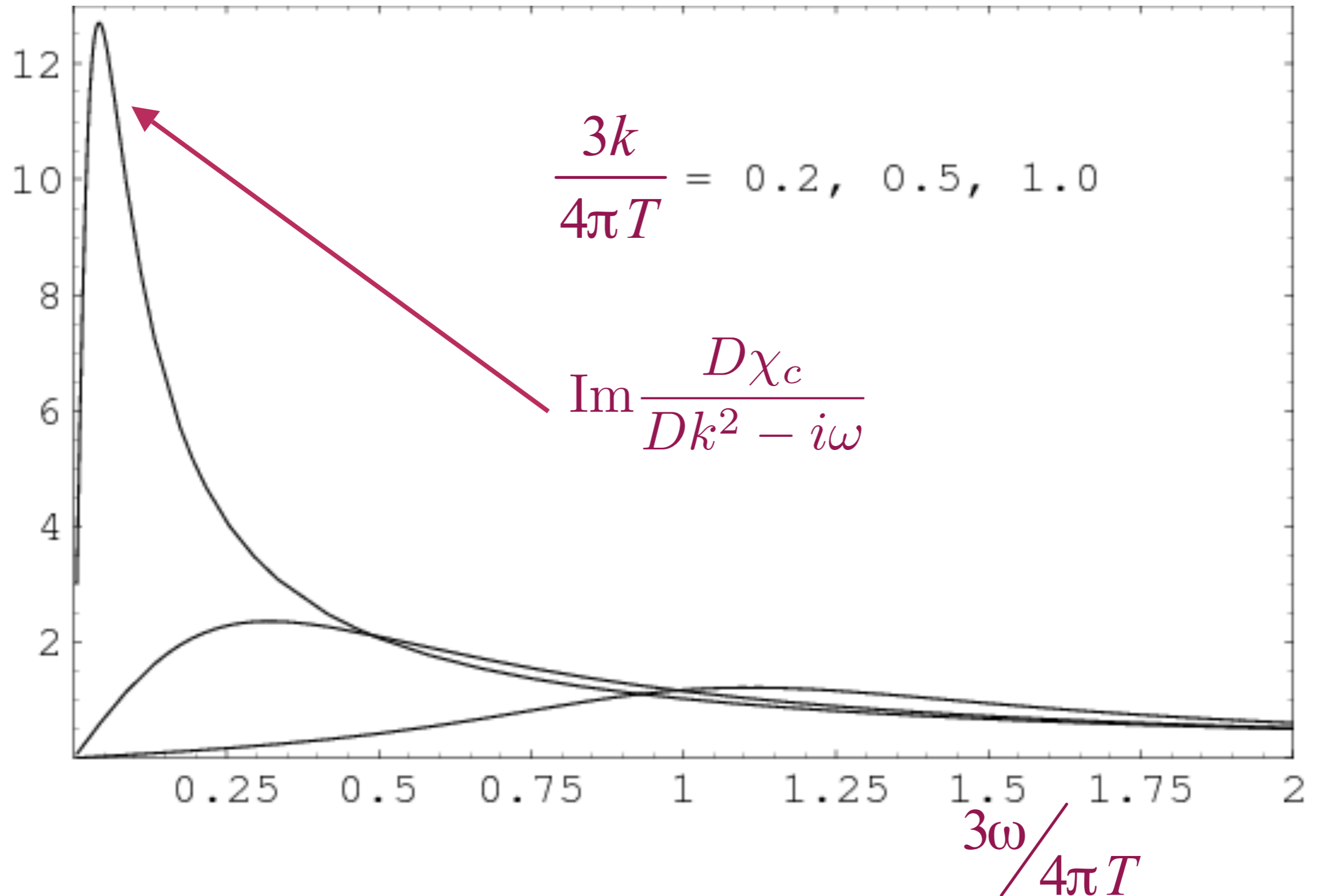
# Collisionless to hydrodynamic crossover of SYM3

$$\text{Im}\chi(k, \omega)/k^2$$



# Collisionless to hydrodynamic crossover of SYM3

$\text{Im}\chi(k, \omega)/k^2$



# Universal constants of SYM3

$$\chi_c = \frac{k_B T}{(h\nu)^2} \Theta_1$$
$$D = \frac{h\nu^2}{k_B T} \Theta_2$$
$$\sigma(\omega) = \begin{cases} \frac{4e^2}{h} K & , \quad \hbar\omega \gg k_B T \\ \frac{4e^2}{h} \Theta_1 \Theta_2 & , \quad \hbar\omega \ll k_B T \end{cases}$$

$$K = \frac{\sqrt{2} N^{3/2}}{3}$$

$$\Theta_1 = \frac{8\pi^2 \sqrt{2} N^{3/2}}{9}$$

$$\Theta_2 = \frac{3}{8\pi^2}$$

C. Herzog, JHEP **0212**, 026 (2002)

P. Kovtun, C. Herzog, S. Sachdev, and D.T. Son, Phys. Rev. D **75**, 085020 (2007)

# Electromagnetic self-duality

- Unexpected result,  $K = \Theta_1 \Theta_2$ . Actually, a stronger result holds:  $\sigma(\omega)$  is independent of  $\omega$  for all  $\hbar\omega/(k_B T)$ .

# Electromagnetic self-duality

- Unexpected result,  $K = \Theta_1 \Theta_2$ . Actually, a stronger result holds:  $\sigma(\omega)$  is independent of  $\omega$  for all  $\hbar\omega/(k_B T)$ .
- This is traced to a *four*-dimensional electromagnetic self-duality of the theory on  $\text{AdS}_4$ . In the large  $N$  limit, the  $\text{SO}(8)$  currents decouple into 28  $\text{U}(1)$  currents with a Maxwell action for the  $\text{U}(1)$  gauge fields on  $\text{AdS}_4$ .

# Electromagnetic self-duality

- Unexpected result,  $K = \Theta_1 \Theta_2$ . Actually, a stronger result holds:  $\sigma(\omega)$  is independent of  $\omega$  for all  $\hbar\omega/(k_B T)$ .
- This is traced to a *four*-dimensional electromagnetic self-duality of the theory on  $\text{AdS}_4$ . In the large  $N$  limit, the  $\text{SO}(8)$  currents decouple into 28  $\text{U}(1)$  currents with a Maxwell action for the  $\text{U}(1)$  gauge fields on  $\text{AdS}_4$ .
- **Special properties of CFT3s with gravity duals:**  $\sigma(\omega)$  is  $\omega$ -independent and equal to the self-dual value. These results are the analog of  $\eta/s = \hbar/(4k_B\pi)$ .

# Electromagnetic self-duality

- Unexpected result,  $K = \Theta_1 \Theta_2$ . Actually, a stronger result holds:  $\sigma(\omega)$  is independent of  $\omega$  for all  $\hbar\omega/(k_B T)$ .
- This is traced to a *four*-dimensional electromagnetic self-duality of the theory on  $\text{AdS}_4$ . In the large  $N$  limit, the  $\text{SO}(8)$  currents decouple into 28  $\text{U}(1)$  currents with a Maxwell action for the  $\text{U}(1)$  gauge fields on  $\text{AdS}_4$ .
- **Special properties of CFT3s with gravity duals:**  $\sigma(\omega)$  is  $\omega$ -independent and equal to the self-dual value. These results are the analog of  $\eta/s = \hbar/(4k_B\pi)$ .
- **Curious fact:** Experimental studies show a quantum critical  $\sigma$  close to the self-dual value.

# Resistivity of Bi films

## Conductivity $\sigma$

$$\sigma_{\text{Superconductor}}(T \rightarrow 0) = \infty$$

$$\sigma_{\text{Insulator}}(T \rightarrow 0) = 0$$

$$\sigma_{\text{Quantum critical point}}(T \rightarrow 0) \approx \frac{4e^2}{h}$$

D. B. Haviland, Y. Liu, and A. M. Goldman,  
*Phys. Rev. Lett.* **62**, 2180 (1989)

M. P. A. Fisher, *Phys. Rev. Lett.* **65**, 923 (1990)

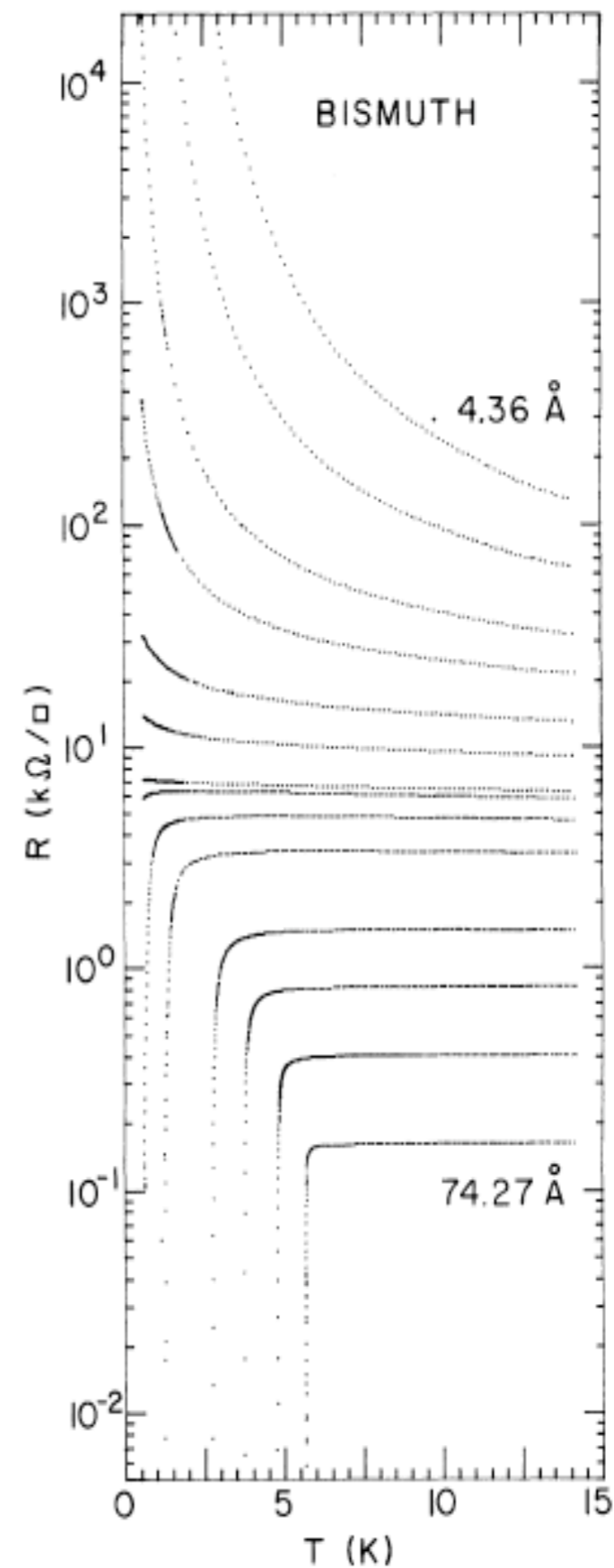


FIG. 1. Evolution of the temperature dependence of the sheet resistance  $R(T)$  with thickness for a Bi film deposited onto Ge. Fewer than half of the traces actually acquired are shown. Film thicknesses shown range from 4.36 to 74.27 Å.

# Quantum critical transport in graphene

$$\sigma(\omega) = \begin{cases} \frac{e^2}{h} \left[ \frac{\pi}{2} + \mathcal{O} \left( \frac{1}{\ln(\Lambda/\omega)} \right) \right] & , \quad \hbar\omega \gg k_B T \\ \frac{e^2}{h\alpha^2(T)} \left[ 0.760 + \mathcal{O} \left( \frac{1}{|\ln(\alpha(T))|} \right) \right] & , \quad \hbar\omega \ll k_B T \alpha^2(T) \end{cases}$$

$$\frac{\eta}{s} = \frac{\hbar}{k_B \alpha^2(T)} \times 0.130$$

where the “fine structure constant” is

$$\alpha(T) = \frac{\alpha}{1 + (\alpha/4) \ln(\Lambda/T)} \stackrel{T \rightarrow 0}{\sim} \frac{4}{\ln(\Lambda/T)}$$

L. Fritz, J. Schmalian, M. Müller and S. Sachdev, *Physical Review B* **78**, 085416 (2008)

M. Müller, J. Schmalian, and L. Fritz, *Physical Review Letters* **103**, 025301 (2009)